INVESTIGATION OF THE CATALYTIC AND REGULATORY DOMAINS OF CYSTATHIONINE β-SYNTHASE

By

Edgar Abouassaf, B.Sc.

A thesis submitted to

the Faculty of Graduate and Postdoctoral Affairs

in partial fulfillment of

the requirements for the degree of

Doctor of Philosophy, in Science

Department of Biology

Ottawa-Carleton Institute of Biology

Carleton University

Ottawa, Ontario

February, 2015

ABSTRACT

Cysthationine β-Synthase (CBS) is a pyridoxal 5'-phosphate (PLP)-dependent enzyme that catalyzes the condensation of serine and homocysteine to form cysthathionine. Human CBS (hCBS) is a modular enzyme that contains an N-terminal domain that binds heme, a catalytic domain that binds the PLP cofactor and a regulatory domain that binds *S*-adenosyl-methionine (SAM). The interaction between the catalytic and regulatory regions is limited to a linker region that forms the main communication between these two domains. Deficiency in CBS activity is the leading cause for the disorder homocystinuria in humans. The focus of the studies described in this thesis is to investigate the mechanism of homocystinuria-associated mutations in the active site of yeast CBS, the potential of native tryptophan residues as probes of conformational change and the binding of SAM to the regulatory domain.

Site-directed replacement variants of 9 residues located in the active-site of the truncated form of yeast CBS (residues 1-353) were characterized. The results suggest that the hydrogen bonding network comprising residues K112, E111, K327, E244 and T326 is a determinant of active-site architecture and dynamics. Residues G245, I246 and G247, situated adjacent to the cofactor, play a role in maintaining PLP in a catalytically productive orientation.

With the goal of developing probes of conformational change within the catatlytic domain and of communication between the catalytic and regulatory domain of CBS, single and triple-substitution, site-directed variants of the four tryptophan residues of yeast CBS (W132, W263, W333 and W340) were characterized in the truncated and full-length enzyme forms. Residues W132 and W263 are located in the active site, while

W333 and W340 are located in the linker region that connects the catalytic and regulatory domains. The results demonstrate that residue W263 is the main contributor for fluorescence resonance energy transfer to the PLP cofactor. Substitution of W333 and W340 causes a change in the degree of solvent exposure in the microenvironment of these residues. This is due to the presence of the regulatory domain in the full-length enzyme.

Binding of SAM to the regulatory domain of human CBS leads to enzyme activation. In contrast, the *Drosophila melanogaster* and yeast CBS enzymes are not activated by SAM. The binding of SAM to the regulatory domains of yeast and human CBS was investigated via fluorescence spectroscopy and mass spectrometry. The results indicate that the full-length yeast enzyme does not bind to SAM, suggesting that, similar to the drosophila enzyme, yeast CBS may locked in a conformation that does not allow SAM-binding to its regulatory domain.

PREFACE

This thesis follows the integrated thesis format and, as such, the main chapters represent work that will be submitted for publication in a peer-reviewed journal (chapters 3-5).

Statement of contributions

My contributions to the research described in this thesis include:

1. development of the research questions and experimental design, in partnership with Dr. S.M. Aitken,
2. responsibility for the collection and analysis of data,
3. the co-supervision, in collaboration with Dr. S.M. Aitken, of 3 undergraduate students:

   Sherwin Habibi participated in the construction, purification and steady-state characterization of site-directed variants for chapters 3 and 4. Augustina Esedebe participated in stability studies for site-directed variants for chapter 3. Nicholas Humphries participated in construction of the site-directed variants described in chapters 5.
4. the preparation of drafts of this thesis, which was edited under the guidance of Dr. S.M. Aitken.

I formally acknowledge the contributions of the co-authors of the manuscripts that comprise the research chapters of my thesis. My supervisor, Dr. S.M. Aitken contributed her expertise by guiding me in the formulation of the research questions and experimental design and by assisting with the analysis and interpretation of data and guidance in the writing of my thesis. Dominique Morneau (Ph.D. 2014) constructed, purified and performed the preliminary characterization of 4 of the site-directed variants described in chapter 4. The mass spectrometry data analysis described in chapter 5 was performed in

collaboration with Dr. Jeff Smith (Department of Chemistry, Carleton University). The contributions of former and current undergraduate students are described above.

I have obtained permission from each of my co-authors to use collaborative works in this thesis.

ACKNOWLEDGEMENTS

It is really hard to sum up an experience of six years with a few words, but being surrounded by a great group of people who are willing to provide advice and guidance through the ups and downs, has helped me become a better scientist and a more mature person.

I would like to thank my supervisor Dr. Susan M. Aitken for being a great mentor, a role model and a constant source of inspiration. None of this would have been possible without her trust and guidance. Apart from providing advice for my career, she always made sure I was on the right track when faced with hard times. I am very grateful for the valuable opportunity to work in her laboratory and especially for her patience throughout the years. I am sure that I will continue to learn from her as I move forward in life.

I would also like to extend my deepest thanks to my committee members, Dr. Amanda MacFarlane and Dr. Ken Storey for the helpful feedback and comments I received throughout my committee meetings and qualifying exam.

Completing this Ph.D. thesis would not have been possible without the help of the undergraduate students, whom I had the privilege to work with throughout my degree; I would like to thank, Roger Habashi, Adrienne Manders, Sherwin Habibi, Mohammad Ahmed, Augustina Esedebe and Nicholas Humphries. These students were really smart, fast learners, dedicated and always eager to work. I will never forget all the help they provided. To all the undergraduate students that I had the pleasure to TA for BIOL2200 and BIOL2104, thank you so much! Getting nominated and winning several TA awards would not have been possible without your trust in me and I'm forever grateful for this

experience! My fellow graduate students, Pratik Lodha, Nikita Rayne, Jennifer Skanes, Emily Hopwood, Sorin Gustin and Victoria Samaki were always willing to help and provided guidance when I needed it the most.

Special thanks to my amazing friends, Allison Jaworski, Dominique Morneau and Duale Ahmed. I will always remember the great memories we shared throughout graduate school. To Ally, thank you so much! It was an honor working with you in the laboratory; you are a hard worker and a knowledgeable individual. You always know what to say and how to make bad situations turn into a positive ones! You are a good listener, a special person and I will always value our friendship and the UFC fights we watched together. To DQ, I was happy we became friends, thank you for all the enjoyable/funny moments you provided throughout the years. I will always remember our French conversations, which always brought joy to my heart. Never a dull moment! To Duale, thank you for being a great friend! For all the support and help you provided, I'm very grateful. I will always cherish all the sports discussions we had over the years, the scientific conferences and the good taste in music. To my fellow friends from Carleton University, Mohsen Hooshyar, William Hughes, Magdalena Bugno, Bahram Samanfar, Katayoun Omidi, Christie Childers, Dan Burnside and Kristina Shostak, you have made my time here an experience I will not forget.

Last but not least, this thesis would not have been accomplished without the support of my entire family. To my parents, Kalim Abouassaf and Nawal Atallah, thank you for all the unconditional love, unsolicited advice, financial help and guidance. To my sister, Eliane Abouassaf, thank you for believing in me, for all the laughs we shared and for always reminding me that hard work pays off.

DEDICATION

To **MOM** and **DAD**

TABLE OF CONTENTS

LIST OF TABLES

Page

LIST OF FIGURES

Page

ABBREVIATIONS

ADP	Adenosine diphospahte
AMP	Adenosine monophosphate
AMPK	Adenosine monophosphate kinase
ATP	Adenosine triphosphate
BHMT	Betaine-homocysteine methyltransferase
CBL	Cystathionine β-lyase
CBS	Cystathionine β-synthase
CBS1 (2)	Cystathionine β-synthase regulatory domain 1 (or 2)
CGL	Cystathionine γ-lyase
C_m	Urea-induced unfolding transition mid-point
CO	Carbon monoxide
CooA	Bacterial transcription factor
dCBS	*Drosophila melanogaster* cystathionine β-synthase
DTNB	5,5'-Dithiobis-(2-nitrobenzoic acid)
E-AA	Aminoacrylate intermediate
eCBL	*Escherichia coli* cystathionine β-lyase
EDTA	Ethylenediaminetetraacetic acid

E-L-Cth	External aldimine of cystathionine
E-L-Ser	External aldimine of serine
$Fe^{III+ (II+)}$	Ferric (Ferrous) iron state
FixL	Heme protein kinase
FRET	Förster resonance energy transfer
GD	Germinal diamine
GSH	Glutathione
hCBS	Human Cystathionine β-synthase
htCBS	Human Truncated Cystathionine β-synthase (Residues 1-353)
hCBSΔ516-525	Full-length human cystathionine β-synthase lacking loop 516-525
hCBSΔ516-525/E201S	hCBSΔ516-525 with E201S substitution, in complex with SAM
IMPDH	Inosine monophospahte dehydrogenase
IPTG	Isopropyl- β-*D*-thiogalactopyranoside
L-Cth	L-Cystathionine
L-Cys	L-Cysteine
L-Hcys	L-Homocysteine
L-LDH	L-lactate dehydrogenase

L-Met	L-Methionine
L-Ser	L-Serine
MAT	Methionine-adenosyl transferase
MJ0100	C-terminal domain of *Methanococcus Janashii* protein
MS	Methionine synthase
MS/MS	Tandem mass spectrometry
MTA	Methyl-thioadenosine
MTHFR	$N^{5,10}$-methylene-THF reductase
NAD^+(H)	Nicotinamide adenine dinucleotide, oxidized (reduced) form
Ni-NTA	Ni-nitrilo triacetic acid
NO	Nitric oxide
OASS	*O*-acetylserine sulfhydrylase
PLP	Pyridoxal 5'-phosphate
S. cerevisiae	*Saccharomyces cerevisiae*
SAH	*S*-adenosyl-homocysteine
SAHH	SAH hydrolase
SAM	*S*-adenosyl-methionine

SAMS	SAM-synthetase
sCG	soluble Guanylate cyclase
SDS-PAGE	Sodium dodecyl sulfate polyacrylamide gel electrophoresis
tHcys	Total plasma homocysteine
THF	Tetrahydrofolate
TNB	5'-thionitrobenzoic acid
Tris	Tris-[hydroxymethyl]aminomethane
TrpS	Tryptophan synthase
TS	Threonine synthase
wt-yCBS	Wild-type yeast cystathionine β-synthase
yCBS	Yeast cystathionine β-synthase
yfCBS	Yeast full-length cystathionine β-synthase
ytCBS	Truncated yCBS (residues 1-353)

1. INTRODUCTION

1.1. Metabolic disorders: a brief perspective

The more than 1000 hereditary metabolic disorders reported to date continue to be a focal point of medical research studies (Hoffman *et al.,* 2010). Enzyme deficiencies, due to mutation in the encoding gene, are the leading cause of metabolic diseases such as phenylketonuria, homocystinuria, hyperhomocysteineima, and type1 and type2 tyrosinemia (Berg *et al.,* 2001). Most of these metabolic disorders are inherited autosomal recessive conditions, where two defective genes copies are required for clinical symptoms of the disease to manifest (Berg *et al.,* 2001). Treatment for some of these disorders includes modification of the diet or drug therapy, such as a reduced phenylalanine and tyrosine diet in the case of tyrosinemia and supplementation with vitamin B_6, folic acid, betaine and dietary methionine restriction in the case of homocystinuria (Mudd *et al.,* 1995; Grompe, 2001).

Mutation(s) in the gene encoding an enzyme can alter protein structure, diminish activity and/or alter regulation, leading to reduction in product formation or accumulation of a toxic intermediate. This is exemplified by the buildup of homocysteine, resulting from cystathionine β-synthase deficiency, in the case of homocystinuria (Kraus *et al.,* 1999). Cystathionine β-synthase (CBS), the first enzyme in the reverse transsulfuration pathway, plays an essential role in homocysteine metabolism. Its regulation influences the flux of homocysteine between the competing remethylation and the transsulfuration pathways (Selhub, 1999). These pathways are coordinated *via* allosteric regulation by *S*-adenosylmethionine (SAM), the universal methyl donor. *S*-adenosylmethionine activates CBS and inhibits $N^{5,10}$-methylene-THF reductase (MTHFR), such that an increase in the

intracellular concentration of SAM shunts excess homocysteine through the transsulfuration pathway (Kutzbach *et al.,* 1971). In contrast, when the cellular concentration of methionine is low, the SAM pool is reduced and inhibition of MTHFR is released allowing the conservation of homocysteine for methionine synthesis (Figure 1.1) (Stipanuk, 2004).

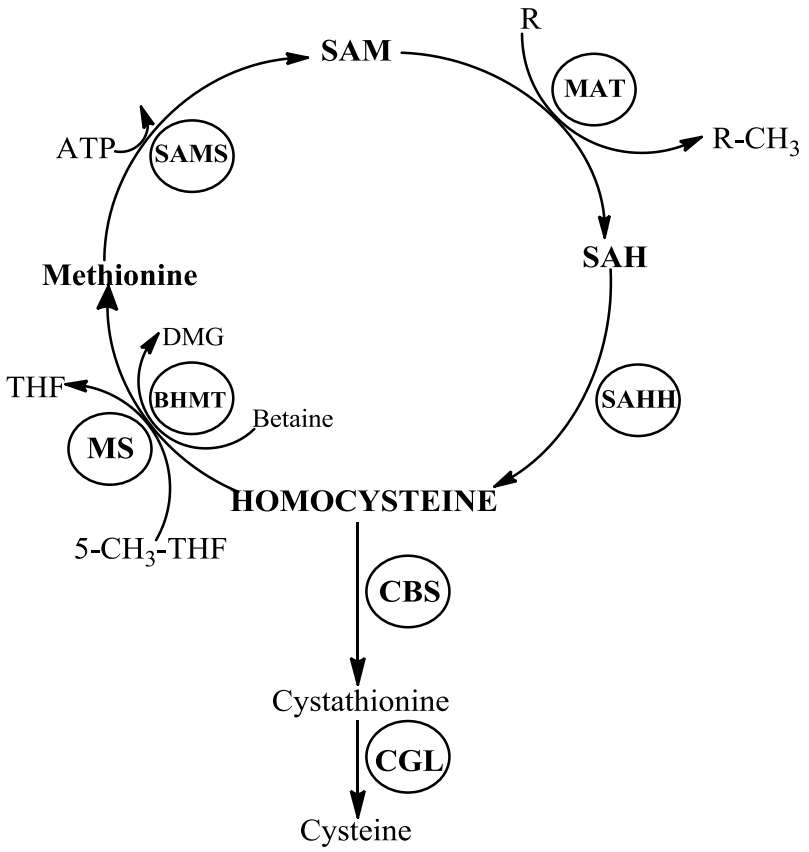

Figure 1.1: Homocysteine is situated at the branch point between the activated methyl cycle and the transsulfuration pathway. Abbreviations: SAM: S-adenosylmethionine, SAMS: SAM-synthetase, SAH: S-adenosylhomocysteine, SAHH: SAH hydrolase, MAT: methionine-adenosyl transferase. MS: methionine synthase, BHMT: betaine-homocysteine methyltransferase, CGL: cystathionine γ-lyase and CBS: cystathionine β-synthase (Caudill *et al.,* 2001).

Mutations in the gene encoding CBS are the leading cause of homocystinuria. Extensive clinical genetic characterization has demonstrated that the majority of CBS mutations are missense mutations in which a single codon is altered, with a resulting amino acid substitution in the protein sequence (Kraus *et al.,* 1999). The mechanism underlying the effect of most homocystinuria-associated mutations on enzyme stability, activity and/or regulation has not yet been investigated. Current treatments of homocystinuria rely primarily on modifying the diet and supplementation with vitamin B_6 or betaine, as gene therapy has yet to be reported for this hereditary disease. Given the >150 distinct homocystinuria-associated mutations of the CBS gene, customization of the B_6 and/or betaine supplementation regime and/or the degree of methionine restriction in the diet involves considerable trial and error. As the effect of homocystinuria manifests in the early childhood years, interfering with developmental processes, acceleration of the optimization of therapeutic regimes may help to limit the severity of the clinical manifestations. Therefore, the study described in chapter 3 aims to increase our understanding of the effect of homocystinuria-associated mutations on CBS stability, activity and the allosteric regulation of CBS, with the goal of refining current treatment regimes, to more efficiently and effectively customize treatment for the specific mutation(s) presented by each patient.

1.2. Hereditary Diseases Associated with CBS: Homocystinuria and Down Syndrome

Homocysteine is a non-protein forming, sulfur-containing amino acid that was discovered by Butz and du Vigneaud in 1932. The total plasma homocysteine (tHcys) refers to the amount of total free and protein-bound homocysteine as well as homocystine and mixed disulfides in plasma (Mudd *et al.,* 2000). The normal concentration of tHcys in human plasma ranges between 5-15 μmol/L (Refsum *et al.,* 1998). Homocysteine is the reduced (sulfhydryl) form, while homocystine is the oxidized (disulfide) form of homocysteine. Reduced homocysteine is reactive and accounts for only 2% of tHcys as homocystine and mixed disulfides, free and protein-bound, account for the remaining 98% (Mudd *et al.,* 2000). Homocysteine was first recognized as a potential risk factor for cardiovascular diseases by pathologist Kilmer McCully in 1969. The autopsy of two children with widespread arterial disease demonstrated a common feature of elevated plasma tHcys. McCully proposed the "homocysteine theory": that elevated levels of homocysteine and homocystine, is the common factor leading to arterial damage. This underlying inborn error of sulfur amino acid metabolism was eventually named homocystinuria.

Numerous experimental studies showed that homocysteine is thrombogenic and causes endothelial damage, suggesting that elevated homocysteine levels are a causal factor in cardiovascular diseases (Welch *et al.,* 1998). However, several studies showed that lowering homocysteine levels, by supplementation with folic acid, vitamin B_6 and B_{12} had no significant effect in reducing the risk of overall stroke or major cardiovascular events in patients with vascular diseases (Lonn *et al.,* 2006; Saposnik *et al.,* 2009; Zhang *et al.,* 2013). Therefore, the role of homocysteine in the vascular damage associated with

homocystinuria remains an open question and exemplifies the complexity of metabolic regulation.

Although the worldwide prevalence of homocystinuria has been reported to be 1:344000 (Mudd *et al.,* 2001), it is as high as 1:65,000 in the population of Celtic heritage in Ireland (Naughten *et al.,* 1998). Studies in Denmark, Germany, Norway and the Czech Republic, based on molecular analysis of CBS mutations, suggest that the frequency of homocystinuria-associated alleles ranges between 1:6,400 to 1:20,500 in European populations (Gaustadnes *et al.,* 1999; Refsum *et al.,* 2004; Janosik *et al.,* 2009). The major clinical symptoms of homocystinuria include ectopia lentis (dislocation of the eye lens), vascular disease with life-threatening thromboembolisms, skeletal deformities, osteoporosis, and mental retardation (Mudd *et al.,* 1995). More than 150 homocystinuria-associated mutations have been identified in the CBS gene (Kraus *et al.,*; http://cbs.lf1.cuni.cz/mutations.php). While these include deletions, insertions and splicing alterations, the majority are missense mutations that result in the substitution of a single amino acid in the CBS enzyme (Kraus *et al.,* 1999). These homocystinuria-associated mutations are distributed widely in the heme-binding, catalytic and regulatory domains of hCBS (Meier *et al.,* 2001; Meier *et al.,* 2003). The two most frequent amino acid substitutions are I278T and G307S. The I278T variant accounts one-fourth of all reported homocystinuric alleles and as much as 50% in specific populations, such as the Netherlands (Kluijtmans *et al.,* 1998). Similarly, the G307S mutation is the leading cause of homocystinuria in Ireland, where it accounts for 71% of identified homocystinuria alleles (Gallagher *et al.,* 1995).

There are two phenotypic variants of this genetic disorder; B_6-responsive and B_6-non-responsive homocystinuria. Approximately one-half of homocystinuria-associated alleles are responsive to high doses of pyridoxine. Patients with vitamin-responsive allele(s) are prescribed supplementation with 100-300 mg of vitamin B_6, in combination with folic acid and vitamin B_{12}. In contrast, a low methionine diet, including a methionine-free cystine-supplemented mixture of amino acids, and supplementation with B_{12} and folic acid is the primary treatment for patients with B_6-non-responsive mutations (Mudd *et al.,* 1995, Yap *et al.,* 2001). Supplementation with folic acid and vitamin B_{12} enhances the remethylation of homocysteine to methionine by ensuring cofactor saturation of the folate cycle and vitamin B_{12}-dependent methionine synthase. As supplementation with folate and B_{12} does not preclude episodic surges in homocysteine following protein ingestion, betaine may also be prescribed (Ubbink *et al.,* 1995; De Baulny *et al.,* 1998). The methyl group from betaine is transferred to homocysteine by betaine-homocysteine methyltransferase (BHMT), regenerating methionine and reducing homocysteine. Following supplementation with 6-9 g of betaine, homocysteine levels were decreased by 74% in homocystinuric patients (Wilcken *et al.,* 1997; Singh *et al.,* 2004). However, betaine treatment requires careful monitoring, as exemplified by the case of a child diagnosed with B_6-non-responsiveness phenotype who developed cerebral edema after methionine levels reached 3 mmol/L during betaine supplementation (Yaghmai *et al.,* 2002; Singh *et al.,* 2004). This illustrates the need for development of an enhanced understanding of the distinct mechanisms by which different homocystinuria mutations affect CBS activity, stability or regulation, with the goal of refining current therapeutic regimes for the range of distinct homocystinuria-associated alleles.

The gene encoding CBS, situated on the 21st chromosome, is also linked to trisomy 21, also known as Down syndrome (DS) and CBS expression is correspondingly increased in the brains of DS individuals during development (Pogribna *et al.,* 2001; Ichinohe *et al.,* 2005). Cystathionine β-synthase is the primary source of H_2S in the brain and the increased expression of this enzyme, due to the presence of a third copy of the 21st chromosome, may impact normal brain development (Shibua *et al.,* 2009). Although H_2S has been proposed to be a neuromodulator and is reported to facilitate the induction of hippocampal long-term potentiation (LTP) by enhancing the activity of N-methyl-D-asparate (NMDA) receptors, it is also a potent neurotoxin (Abe *et al.,* 1996). Therefore, the concentration of H_2S in brain tissue, particularly during development, must be strictly regulated and exploration of CBS regulation is essential in order to understand the role of this enzyme in metabolic diseases.

1.3. Cystathionine β-Synthase

The two pyridoxal 5'-phosphate (PLP)-dependent enzymes of the transsulfuration pathway, CBS and cystathionine γ-lyase (CGL), catalyze the condensation of serine and homocysteine, forming cystathionine, which is hydrolyzed to produce cysteine, α-ketobutyrate and ammonia (Aitken and Kirsch 2005). The cysteine product is the limiting substrate for the production of the major cellular redox-regulatory compound glutathione. Given its position at the head of the transsulfuration pathway, which competes with methionine synthase for homocysteine, CBS is strictly regulated to balance the cellular pools of methionine and cysteine (Figure 1.1) (Selhub *et al.,* 1999).

The position of homocysteine at the metabolic branch point between the activated methyl cycle and glutathione biosynthesis, allows it to be either remethylated, by methionine synthase and BHMT, or converted to cysteine, through the transsulfuration pathway, depending on the methionine status of the cell (Figure 1.1) (Caudill *et al.,* 2001). *S*-adenosylmethionine (SAM) is a key metabolite of the activated methyl cycle as it serves as a methyl donor for a range of cellular methylation reactions, including the synthesis of nucleic acids, phospholipids and neurotransmitters (D'angelo *et al.,* 1997). Following loss of the ε-methyl moiety of SAM, *via* transmethylation, the resulting *S*-adenosylhomocysteine (SAH) is cleaved by SAH-hydrolase to yield homocysteine and adenosine (Figure 1.1). Synthesis of glutathione (GSH), a primary downstream product of transsulfuration, is increased in response to oxidative and chemical stress. When available in excess, cyteine is catabolized to taurine and sulfate rather than conservation as GSH (Bella *et al.,* 1999). Exploration of the structure-function relationships that underlie CBS regulation is required to refine our understanding of the regulation of this key metabolic branchpoint.

1.3.1. CBS Structure

CBS is a homotetrameric, PLP-dependent enzyme. Each 63-kDa subunit contains a N-terminal, heme-binding domain (~70 residues), a highly conserved catalytic core that binds the PLP cofactor (~340 residues) and a C-terminal, regulatory domain (~140 residues) that contains the binding site for the allosteric activator, SAM (Meier *et al.,* 2001; Ereno-Orbea *et al.,* 2014). Enzymes catalyzing transformations of amino acids are typically dependent on the pyridoxal moiety of PLP for catalysis and have been classified

into four structural families, fold types I-IV. The majority of structures available for PLP-dependent enzymes are of fold type I (the aspartate aminotransferase family), including CGL, the second enzyme of the transsulfuration pathway. The homodimeric and homotetrameric proteins of fold type II are evolutionarily and structurally distinct from those of fold-type I (Mehta *et al.,* 2000). These enzymes also differ from those of fold type I in that they often contain additional regulatory domain(s), as exemplified by threonine synthase and cystathionine β-synthase, which are allosterically activated by SAM, and threonine deaminase which is activated by valine and feedback inhibited by isoleucine (Madison *et al.,* 1976; Gallagher *et al.,* 1998; Ereno-Orbea *et al.,* 2014).

The strucural similarity between CBS and *O*-acetylserine sulfhyrase (OASS), both members of fold-type II, enabled the structure of the truncated form of human CBS (hCBS), lacking the regulatory domain, to be solved in 2001, *via* molecular replacement (Meier *et al.,* 2001). As the presence of the hCBS regulatory domain results in aggregation that precludes crystal formation, the first structure of a full-length CBS was that of *Drosophila melanogaster* (dCBS), reported in 2010 (Figure 1.2A) (Koutmos *et al.,* (2010). The crystal structure of a modified full-length hCBS, lacking loop 516-525 (hCBSΔ516-525) was subsequently solved by Ereno-Orbea and colleagues in 2013 and shows an alternate conformation of the regulatory domain with respect to the active site, compared to dCBS (Ereno-Orbea *et al.,* 2013). Deletion of the 516-525 loop results in a dimeric form of hCBS with a reduced tendency to aggregation and Ereno-Orbea *et al.,* suggested that the tetrameric structure of the wild-type enzyme is stabilized by the interaction of loop region 513-529 and residues in the interdomain linker (Figure 1.2B) (Oyenarte *et al.,* 2012; Ereno-Orbea *et al.,* 2013). Recently, the crystal structure of the

hCBSΔ516-525/E201S variant, in which the glutamate residue at position 201 is replaced by serine, was solved with SAM bound to the regulatory domain (Ereno-Orbea *et al.,* 2014). Residue E201 plays a key role in anchoring the regulatory domain to the active-site entrance and removal of this residue results in a highly active hCBS-E201S enzyme. The crystal structure revealed that the relative orientation of the catalytic and regulatory domains in the activated state of the hCBS-SAM complex is similar to that observed in dCBS, in the absence of SAM (Figure 1.2C) (Ereno-Orbea *et al.,* 2014). Ereno-Orbea and coworkers proposed that in the absence of SAM, the "basal state", the C-terminal regulatory domain of hCBS occludes the entrance to the active site of the complementary catalytic domain of the dimer. The binding of SAM to hCBS causes a conformational change in which the regulatory domains of the two subunits rotate and associate, thereby leaving the active-site entrance unobstructed in the "activated state" (Figure 1.2) (Ereno-Orbea *et al.,* 2014). The conformation of the constitutively activated dCBS enzyme is similar to the activated state of hCBS (Koutmos *et al.,* 2010; Ereno-Orbea *et al.,* 2014).

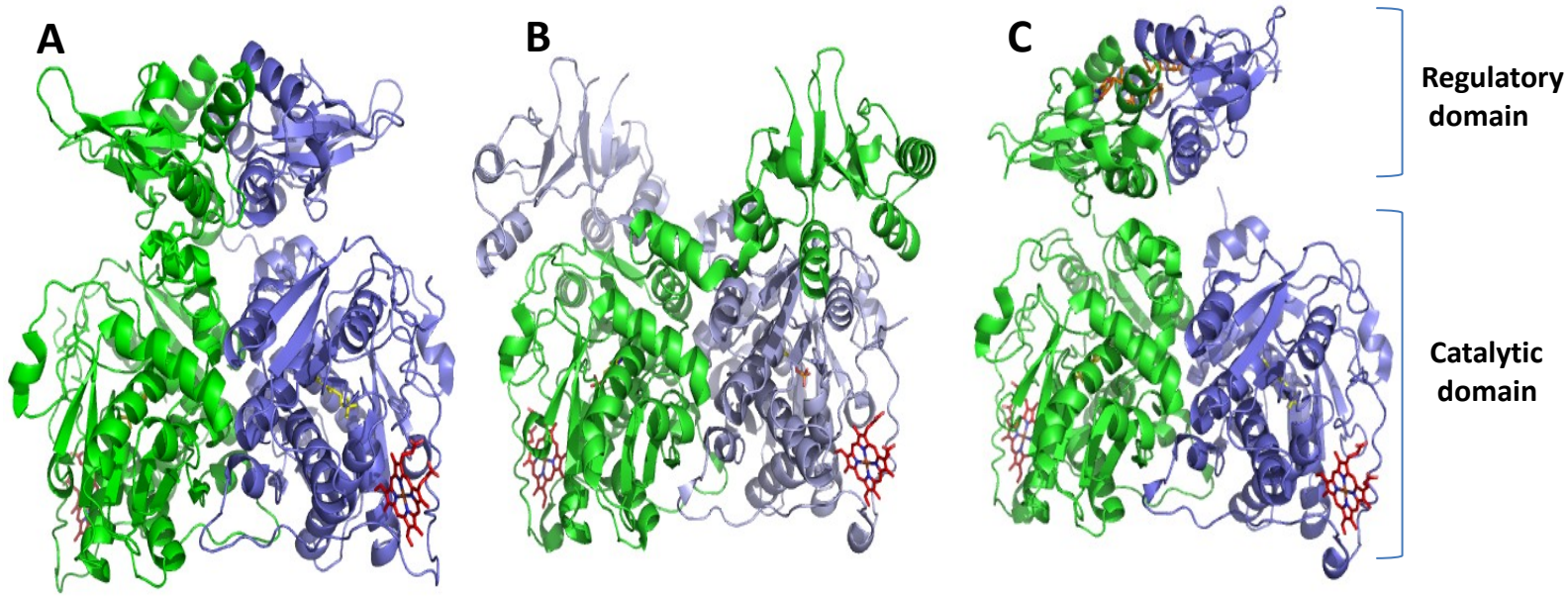

Figure 1.2: Comparison of the relative positions of the catalytic and regulatory domains in the structures of dimers dCBS, hCBSΔ516-525 and the SAM complex of hCBS Δ516-525/E201S. The relative orientation of the regulatory domain in the consititutively active (A) dCBS and (C) SAM-bound hCBSΔ516-525/E201S is strinkingly different from B) free hCBSΔ516-525, and allows unrestricted substrate access to the catalytic site (Koutmos *et al.,* 2010; Ereno-Orbea *et al.,* 2013; Ereno-Orbea *et al.,* 2014). This figure was generated using Pymol (The PyMOL Molecular Graphics System, Version 1.2r3pre, Schrödinger, LLC). Pdb code: 3PC2, 4L3V and 4PCU.

1.3.1.1. The heme-binding domain

The cofactor heme is versatile and plays a number of roles within proteins, including catalysis (e.g. catalase and peroxidases), oxygen binding and transport (e.g. hemoglobin and myoglobin) and allosteric activation (e.g. guanylate cyclase and bacterial transcription factor, CooA). Heme sensor proteins respond selectively, quickly and reversibly to molecular signals. For example, the soluble, ferrous form of guanylate cyclase (sGC) is activated up to 100-fold by NO-binding but does not interact with molecular oxygen (O_2) (Denninger *et al.,* 1999). The bacterial transcriptional factor CooA is activated by CO binding to the ferrous form of the heme iron (Shelver *et al.,* 1997), and returns to its original state once the signal molecule is released. Similarly, reversible conformational changes are observed for the heme-containing protein kinase FixL (Gilles *et al.,* 1994). Unlike CBS from lower eukaryotes, such as yeast, which lack the ~70-residue, N-terminal, heme-binding domain, the human and drosophila enzymes possess a heme cofactor (Jhee *et al.,* 2000a; Koutmos *et al.,* 2010; Ereno-Orbea *et al.,* 2013). The physiological role of the heme cofactor of hCBS remains contentious and catalytic, regulatory and structural roles have been suggested (Cherney *et al.,* 2007; Weeks *et al.,* 2009). The lack of heme cofactor in yeast CBS (yCBS), which catalyzes the same reaction as the human enzyme, in combination with the 25-Å distance between the hCBS active site and the heme cofactor, provide evidence that the heme cofactor is not involved directly in catalysis (Jhee *et al.,* 2000a; Meier *et al.,* 2001). The binding of CO or NO to the ferrous form of the heme iron (Fe^{II}) of hCBS results in inactivation of the enzyme, suggesting the possibility of a regulatory role (Toaka *et al.,* 2001; Weeks *et al.,* 2009). However, the formation of the inactive hCBS(Fe^{II}) was only observed under non-

physiological conditions of temperature (40˚C) and pH (pH of 9) (Pazicni *et al.,* 2005). The loss of enzyme activity associated with the ferrous state of hCBS is slow and irreversible, resembling protein denaturation behavior (Cherney *et al.,* 2007). As the slow loss of CBS activity seen upon heme reduction is irreversible and does not resemble other heme sensor proteins, Cherney and colleagues suggested that a simple redox-regulatory role is unlikely for the hCBS heme (Cherney *et al.,* 2007).

1.3.1.2. The catalytic domain

The catalytic domain binds the PLP cofactor and resembles other fold-type II PLP-dependent enzymes. The catalytic cofactor is deeply buried in a cleft that runs the length of the CBS dimer, and is only accessible via a narrow channel (Figure 1.3). The PLP cofactor is linked to the ε-amino group of an active-site lysine residue (K119 in hCBS) *via* a Schiff base linkage, and a glycine-rich loop of residues (256-260 of hCBS) binds the phosphate moiety (Meier *et al.,* 2001; Ereno-Orbea *et al.,* 2013). The nitrogen atom of the pyridine ring forms a hydrogen bond with the side chain hydroxyl group of a serine residue (hCBS-S349), as observed for the related enzymes OASS, TD and TrpS (Gallaher *et al.,* 1998; Quazi *et al.,* 2009). Upon binding of the serine substrate, the active site of CBS undergoes a conformational change and the mobile loop (hCBS residues 146-150) shifts S147 within hydrogen-bonding distance of the hydroxyl moiety of the substrate (Aitken *et al.,* 2004; Koutmos *et al.,* 2010). The homocysteine binding-site is not clearly defined and may involve water-mediated and/or backbone interactions, including G305 and G307 (Lodha *et al.,* 2009). The G307S homocystinuria-associated mutation was proposed to disrupt homocysteine binding (Meier *et al.,* 2003).

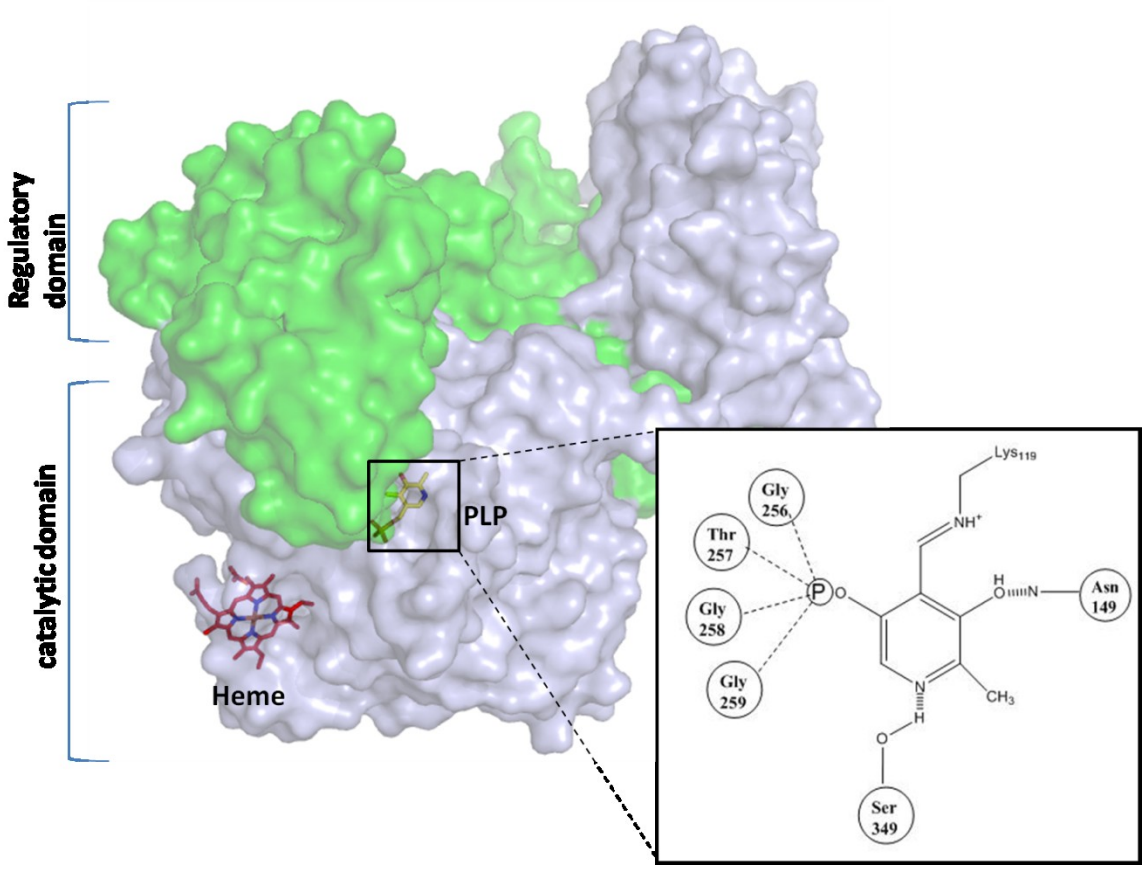

Figure 1.3: The overall structure of hCBSΔ516-525 dimer and the interactions of the PLP cofactor with residues in the active site. The PLP cofactor of hCBS is deeply buried in a cleft of the catalytic domain (blue) and, in the absence of SAM, obscured by the C-terminal regulatory domain (green) such that it is accessible only *via* a narrow channel. Several active-site residues, shown in the inset, interact with the cofactor to position it in a catalytically productive orientation. The heme and PLP cofactors are highlighted in red and yellow, respectively (Meier *et al.,* 2001; Ereno-Orbea *et al.,* 2013). This figure was generated using Pymol (The PyMOL Molecular Graphics System, Version 1.2r3pre, Schrödinger, LLC). Pdb code: 4L3V.

1.3.1.3. Regulatory domain

The C-terminal domain of hCBS contains the binding site for the allosteric regulator SAM (Ereno-Orbea *et al.,* 2014). Residues 415-468 and 486-543 of the regulatory domain adopt the characteristic α-β-α-β-β-α fold of CBS motifs and are referred to as CBS1 and CBS2, respectively (Figure 1.4). These motifs, first observed in CBS, and so named CBS domains, are found in a wide range of proteins, including inosine monophosphate dehydrogenase (IMPDH), chloride channels and AMP-activated protein kinase, and are observed in proteins from bacterial, archaebacterial and eukaryotic species (Kemp, 2004). The CBS2 motif of CBS enzymes from various sources, including yeast and human, is less conserved than CBS1 (Miles *et al.,* 2004). The crystal structures of several proteins containing 1-4 CBS domains have been solved and show that CBS domains generally assemble to form symmetrical pairs or tetrads in which the β-sheets of the two CBS domains interact in an antiparallel arrangement (Ignoul *et al.,* 2005). Deletion of the C-terminal regulatory domain of hCBS results in a dimeric enzyme that is ~2-3 fold more active than the tetrameric, full-length enzyme, demonstrating that, in the context of CBS, the regulatory domain is involved in both regulation of activity and the oligomeric status of the protein (Kery *et al.,* 1998).

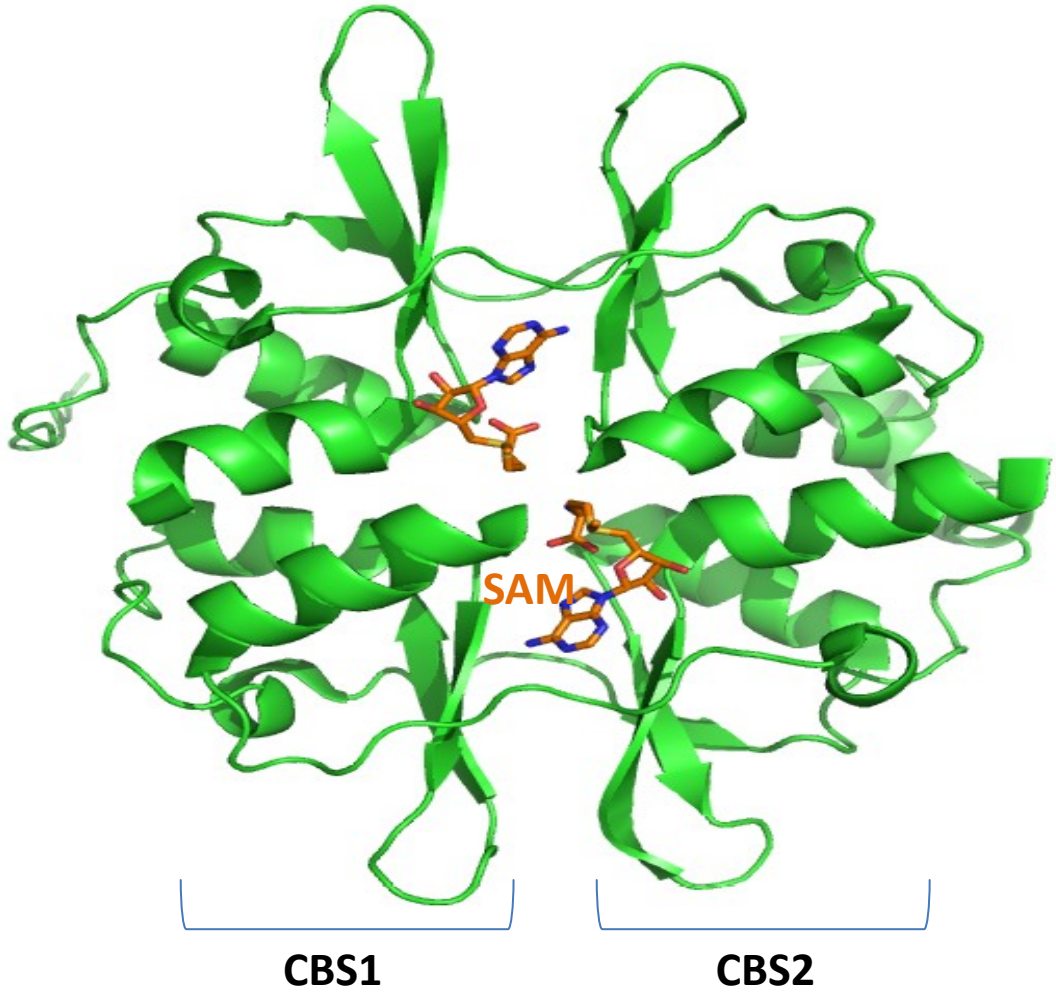

Figure 1.4: The regulatory domain of the hCBSΔ516-525 complex with SAM. A single CBS motif (β1-α1-β2-β3-α2) consists of a three-stranded β-sheet that packs against a pair of α-helices. Pairs of CBS motifs associate in a compact structure referred to as ‘‘Bateman module’’, that presents two binding cavities, referred to as site-1 (S1) and site-2 (S2), where SAM (orange) binds in the case of hCBS (McCorvie *et al.,* 2014). This figure was generated using Pymol (The PyMOL Molecular Graphics System, Version 1.2r3pre, Schrödinger, LLC). Pdb code: 4UUU.

1.3.2 Reaction mechanism

The ε-amino group of an active-site lysine residue (hCBS-K119), the catalytic base, is covalently bound to the PLP cofactor, *via* Schiff base linkage, in the internal aldimine, resting state of the cofactor (Meier *et al.,* 2001). The amino group of the substrate displaces the active-site lysine residue to form the external aldimine, *via* a transaldimination reaction, a step that is common to all PLP-dependent enzymes catalyzing the transformation of amino acids (Figure 1.5). The catalytic versatility of PLP has been well documented and cofactor chemistry is regulated by the protein component of the enzyme (Dunathan, 1966; Elliot and Kirsch 2004). The CBS reaction follows a ping-pong kinetic mechanism where the hydroxyl group of serine is exchanged for the thiol group of homocysteine to form cystathionine and a molecule of water (Jhee *et al.,* 2000b). As the first product is water, this reaction can also be considered to follow an ordered bi-uni mechanism (Aitken and Kirsch, 2003). Elimination of the hydroxyl moiety of the serine substrate results in formation of the aminoacrylate intermediate (E-AA), which reacts with homocysteine to form the external aldimine of cystathionine (E-L-Cth) before releasing the cystathionine product (Figure 1.5). Product inhibition results when cystathionine accumulates since serine and cystathionine compete for the unliganded form of the enzyme. The CBL/LDH continuous assay for the condensation of serine and homocysteine eliminates product inhibition by hydrolyzing the cystathionine product to recycle homocysteine and release ammonia and pyruvate, which is converted to lactate with the concomitant oxidation of NADH (ε_{340} = 6,200 $M^{-1}cm^{-1}$) (Aitken *et al.,* 2003). Two forms of substrate inhibition by homocysteine are observed for CBS as the homocysteine substrate can reduce activity by binding to the serine-binding site or to the

homocysteine site, but in advance of aminoacrylate formation (Jhee *et al.,* 2000). The full-length human enzyme is prone to aggregation and the strong Soret peak of the hCBS heme cofactor masks the absorbance of the PLP, complicating pre-steady state studies of reaction intermediates. Therefore yCBS, which lacks the N-terminal, heme-binding domain of the human enzyme, provides a useful model enzyme for mechanistic studies (Figures 1.5; 1.6) (Jhee *et al.,* 2000; Aitken and Kirsch 2004; Lodha *et al.,* 2010, Singh *et al.,* 2011).

Cystathionine β-synthase can also catalyze the condensation of two molecules of cysteine or cysteine and homocysteine to produce lanthionine or cystathionine, respectively, and hydrogen sulfide (H_2S) (Figure 1.6) (Singh *et al.,* 2009). This reaction follows the same mechanism as the condensation of serine and homocysteine, with the exception that the thiol group of cysteine is released to generate H_2S (Singh *et al.,* 2011). Hydrogen sulfide is a gaseous signaling molecule that has been implicated in a range of physiological responses and is proposed to act on the cardiovascular, central nervous system and energy metabolism. For example, H_2S induces long term potentiation in hippocampal neurons *via* activation of the *N*-methyl-D-aspartic acid receptor (Abe *et al.,* 1996). It also acts as a vasorelaxant for the cardiovascular system and smooth muscle cells by increasing potassium-ATP channel currents (Zhao *et al.,* 2001). Hydrogen sulfide has also been reported to lower the metabolic rate and body temperature by reversible inhibition of cytochrome c oxidase (Blackstone *et al.,* 2005). Investigation of the complex regulation of CBS is expected to shed light on the role of this enzyme in processes involving H_2S production and homocysteine homeostasis.

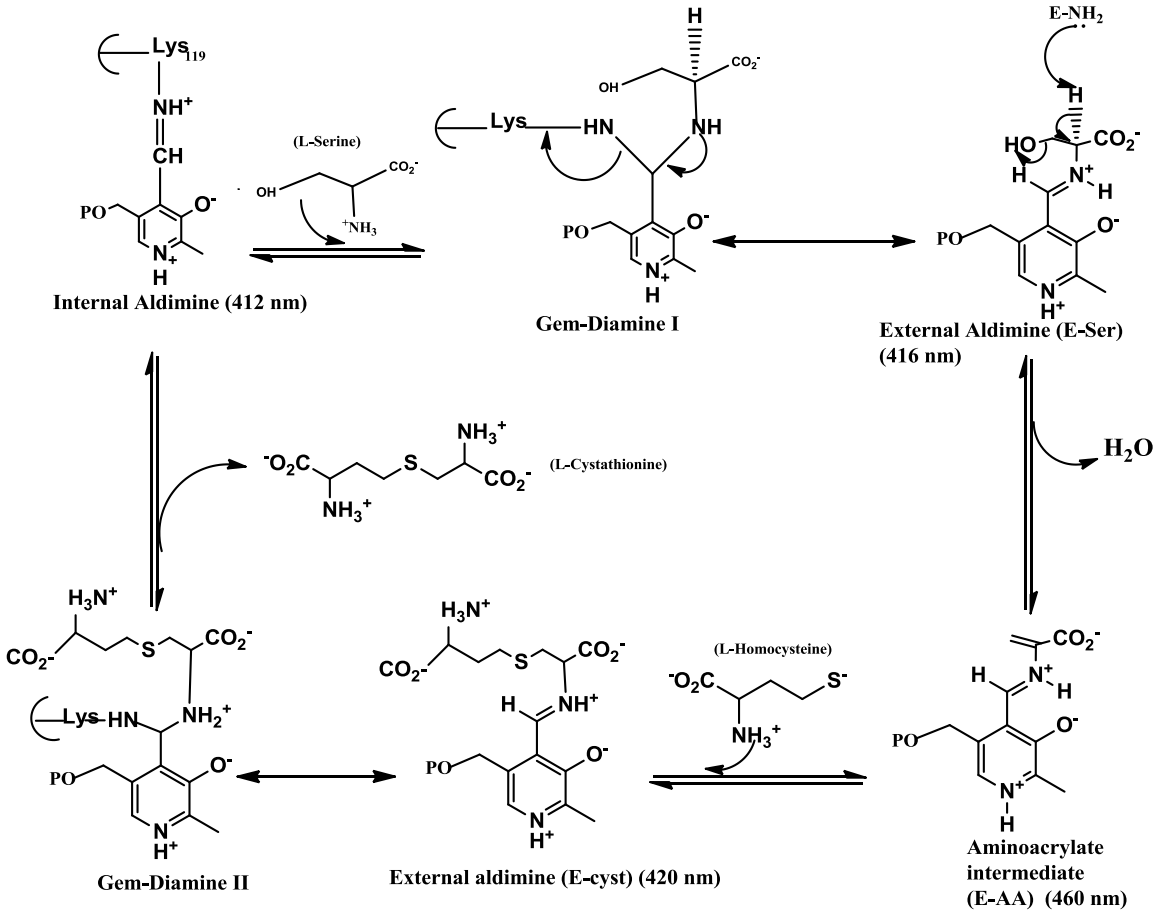

Figure 1.5: Reaction mechanism of the condensation of serine and homocysteine by yeast CBS. Abbreviations: GD: germinal diamine, E-Ser: external aldimine of serine, E-AA: aminoacrylate intermediate, E-Cyst: external aldimine of cystathionine (Jhee *et al.,* 2001).

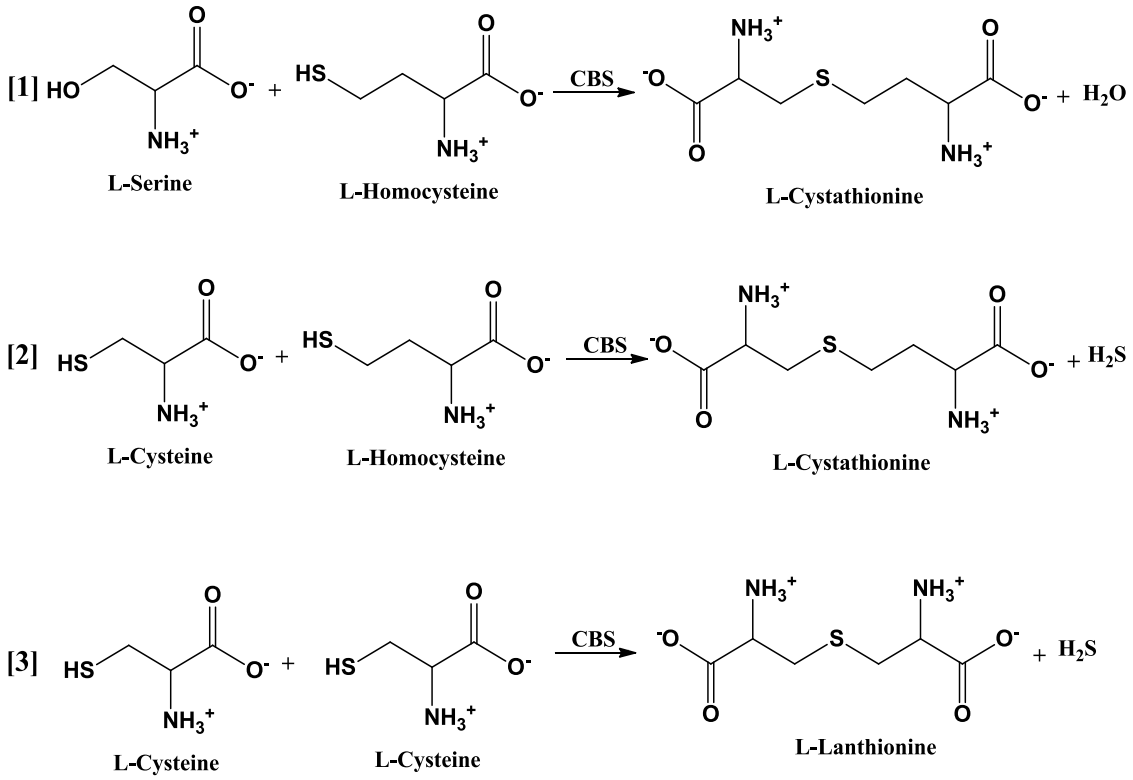

Figure 1.6: The reactions catalyzed by CBS. 1) CBS catalyzes the condensation of serine and homocysteine to produce cystathionine. 2) CBS can also produce cystathionine and H_2S by condensation of cysteine and homocysteine. 3) CBS is also capable of condensing two cysteine molecules to produce lanthionine and H_2S (Singh *et al.,* 2009).

1.4. Objectives of study

The homocysteine substrate of the highly regulated enzyme cystathionine β-synthase is situated at the branch-point between the activated methyl cycle, and the central metabolite SAM, and the transsulfuration pathway, which leads to glutathione biosynthesis. Despite the recent availability of structures for the full-length form of drosophila and human CBS, the mechanism(s) underlying the regulation of this enzyme and the effects of homocystinuria-associated, amino-acid substitutions remain to be explored. The research aims described in this PhD thesis are as follow:

1. Investigation of the effect and mechanism of homocystinuria-associated mutations situated in proximity to the active site of yeast CBS, with the ultimate goal of refining current therapeutic regimes for homocystinuria,
2. Exploration of the fluorescence properties of the four tryptophan residues of yeast CBS (an enzyme which lacks the fluorescence-quenching heme cofactor) in order to assess their potential as probes of conformational change and/or interactions between the catalytic and regulatory domains,
3. Investigation of the binding of SAM and other adenosyl derivatives to the regulatory domains of human and yeast CBS, as a step towards understanding the role of this domain in the context of the yeast enzyme.

2. METHODS

This section provides the general methods used in all the research chapters, including site-directed mutagenesis, protein purification and steady-state measurement of enzyme activity. The modifications to each technique as well as any unique methods are described in the appropriate thesis chapter.

2.1. Construction of site-directed variants

Mutations were constructed using overlap-extension polymerase chain reaction (PCR) to create single or multiple amino acid substitutions in the gene of interest (Higuichi, 1990). The 5'-flanking and the reverse mutagenic primers and the forward mutagenic and 3'-flanking primers, were used in separate polymerase chain reactions to produce overlapping 5' and 3' amplicons, respectively, of the target template sequence. The amplification products and expression vector were digested using appropriate restriction enzymes (New England BioLabs). The digested vector was subsequently treated with Antarctic phosphatase (New England BioLabs) to remove the 5'-phosphate group, thereby reducing background by preventing self-ligation. Following gel purification the digested amplicons and vector were ligated using T4 DNA ligase and transformed into the *E. coli* strain DH10B (Gibco BRL) *via* the heat shock method. Site-directed mutants were subsequently sequenced to verify the presence of the desired substitution(s) and to ensure no unanticipated mutations are present.

2.2. Expression and Purification of the CBS variants

Plasmid constructs of wild-type and site-directed variants of yCBS were expressed and purified using the same procedure (Aitken and Kirsch, 2004). A 300-mL culture of *E. coli* strain DH10B, containing the appropriate construct, was grown overnight at 37ºC and 200 rpm. This culture was used to inoculate 3 L of CBS growth media (50 mM K_2HPO_4, 50 mM KH_2PO_4, 50X V.B Salt, 7.2g Tryptone, 14.4g Yeast extract, Glycerol) in baffled, 2.8-L Fernbach flasks (1 L per flask), at a 1:10 ratio. Cells were grown at 30°C and 200 rpm and IPTG was added to a concentration of 0.2 mM when the OD_{600} reached 0.5. The cells were incubated at 30 °C and 200 rpm for an additional 16 hours, and harvested by centrifugation at 4000 rpm for 10 min at 4°C. The cell pellets were washed by resuspension in 100 mL of 0.85% NaCl, followed by centrifugation at 5000 rpm for 10 min and storage at -80ºC. Cell pellets were resuspended in 100 mL of buffer A (50 mM potassium phosphate, pH 7.8, 20 μM PLP, 10 mM imidazole) containing one "EDTA-free" protease inhibitor tablet (Roche). Lysozyme (1 mg/mL) was added to cell solution and the mixture was incubated on ice for 20 minutes prior to sonication (8 cycles of 30 sec at 50% duty cycle; Vibra Cell sonicator, Sonic and Material, Inc.). The cell lysate was centrifuged at 15000 rpm for 45 min at 4°C and the supernatant was applied into a 1.5 x 10 cm column of Ni-NTA resin (Qiagen), equilibrated with buffer A. The column was washed with at least 20 column volumes of buffer A and eluted with a 200-mL linear gradient of 10-200 mM imidazole in buffer A. Fractions were assessed by SDS-PAGE and those containing pure enzyme were pooled, concentrated and dialyzed against storage buffer (50 mM potassium phosphate, pH 7.8, 20 μM PLP, 1 mM EDTA and 1 mM dithiotrietol). Glycerol was added to 20% (v/v) and

the aliquoted enzyme was stored at -80ºC. The protein monomer concentration was determined *via* UV spectroscopy, by calculating the molar extinction coefficient of the protein, as described by Gill *et al.,* (1989).

The hCBS constructs, wild-type hCBS and hCBSΔ516-525, were expressed using the procedure outlined in Belew *et al.,* 2009. Briefly, 100-mL, overnight culture of *E. coli* strain DH10B, containing the hCBS expression construct, was grown in LB media containing 100 μg/mL ampicillin. Three liters of LB media, containing 75 mg/L δ-aminolevulinic acid (δ-ALA), were inoculated with the overnight culture media (at a 1:50 inoculant-to-media ratio) in baffled, 2.8-L Fernbach flasks (1 L per flask). Cells were grown at 30˚C and IPTG was added to a final concentration of 0.2 mM when the OD_{600} reached 0.5. The cells were grown at 30˚C for a further 16 h and harvested by centrifugation at 4000 rpm for 10 min at 4˚C. Protein purification and storage of the hCBS enzyme(s), followed the same procedure described for the yCBS enzyme (Aitken and Kirsch, 2004).

2.3. Enzyme assays

Enzyme activity was measured in a total volume of 100 μL at 25°C with a Molecular Devices Spectramax 390 spectrophotometer. The assay buffer was comprised of 50 mM Tris, pH 8.6, and 20 μM PLP. A background rate, for all components except the test enzyme, was recorded for each sample before initiating the reaction by the addition of CBS. Data was fit by nonlinear regression with SAS program (SAS Institute, Cary, NC).

2.3.1. Hydrolysis of L-cystathionine

The reverse-physiological, CBS-catalyzed hydrolysis of L-Cth to L-Ser and L-Hcys was detected *via* the reaction of 5,5'-dithiobis-(2-nitrobenzoic acid) (DTNB) with the free thiol of the L-Hcys product (Figure 2.1) (Aitken and Kirsch, 2003). Reactions were carried out in assay buffer containing 2 mM DTNB, 0.004 - 6.2 mM L-Cth. Reactions were initiated by the addition of either wild-type enzyme or site-directed variants. Absorbance changes were monitored at 412 nm ($\Delta\varepsilon_{412}$ = 13,600 $M^{-1}cm^{-1}$) and the data were fit to the Michaelis-Menten equation (1) to determine k_{cat} and K_m, while k_{cat}/K_m was obtained independently from equation (2).

$$\frac{v}{[E]} = \frac{k_{cat} \times [S]}{K_m + [S]} \quad (1) \qquad \frac{v}{[E]} = \frac{k_{cat}/K_m \times [S]}{1 + [S]/K_m} \quad (2)$$

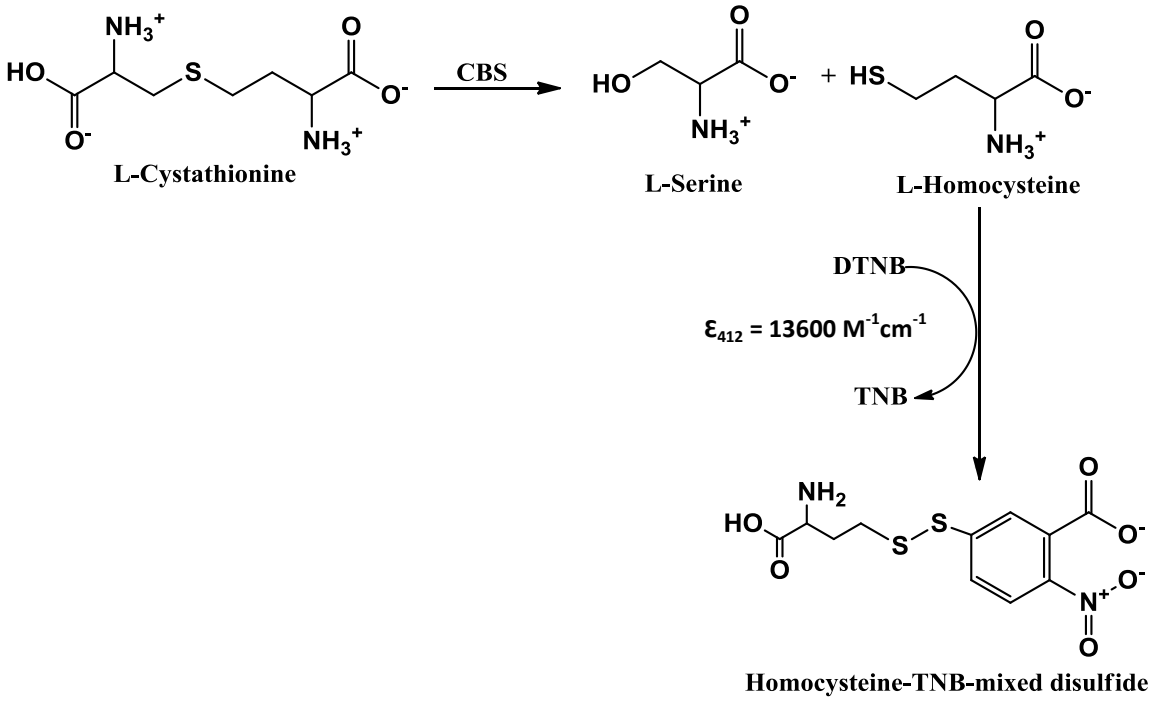

Figure 2.1: The assay for detection of the reverse-physiological hydrolysis of L-Cystathionine by CBS. L-Cystathionine hydrolysis is detected *via* the reaction of 5,5'-dithiobis-(2-nitrobenzoic acid) (DTNB) with the free thiol of the L-Hcys product. The increase in absorbance can be monitored at 412 nm ($\Delta\varepsilon_{412}$ = 13,600 $M^{-1}cm^{-1}$) (Aikten and Kirsch, 2003).

2.3.2. Condensation of L-Ser and L-Hcys

The CBS-catalyzed condensation of L-Ser and L-Hcys to produce L-Cth was assayed *via* the continuous CBL-LDH assay (Figure 2.2) (Aitken and Kirsch, 2003). Reactions were carried out in assay buffer containing 1.5 mM NADH, 0.5 μM CBL, 1.4 μM LDH, 0.1-11.3 mM L-Hcys and 0.2-36 mM L-Ser and were initiated by the addition of wild-type enzyme or site-directed variants. In this continuous assay, CBL converts L-Cth to L-Hcys, NH_3^+ and pyruvate, which is subsequently reduced to lactate by LDH, with the concomitant oxidation of NADH to NAD^+, monitored at 340nm ($\Delta\varepsilon_{340}$ = 6,200 $M^{-1}cm^{-1}$). The concentration of LDH and CBL were optimized by varying their concentrations independently and 1.4 μM LDH and 0.5 μM CBL were selected as sufficient to ensure that neither coupling enzyme would be rate-limiting for the range of CBS concentrations assayed. The values of the kinetic parameters were determined from the fit of the data to the models described by Jhee *et al.,* (2000a) for ytCBS.

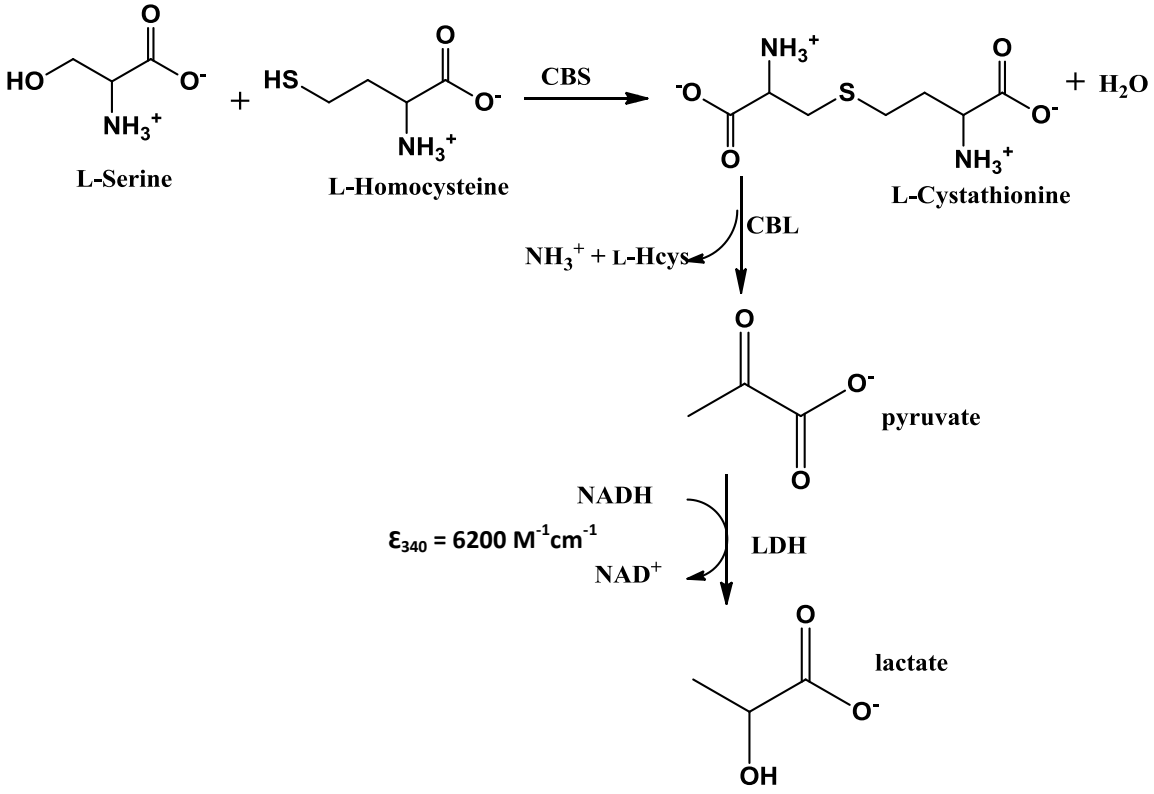

Figure 2.2: The assay for detection of the CBS-catalyzed condensation of L-Ser and L-Hcys. The CBL coupling enzyme converts cystathionine to homocysteine, NH_3^+ and pyruvate, which is subsequently reduced to lactate by LDH, with the concomitant oxidation of NADH to NAD^+, monitored at 340 nm ($\Delta\varepsilon_{340}$ = 6,200 $M^{-1}cm^{-1}$) (Aitken and Kirsch, 2003).

Chapter 3:

Exploration of the Mechanism of Homocystinuria-Associated Mutations in the Active Site of Cystathionine β-Synthase

3.1. Abstract

Cystathionine β-synthase (CBS; E.C. 4.2.1.22) is a pyridoxal 5'-phosphate dependent enzyme that catalyzes the condensation of serine with homocysteine, a toxic metabolic intermediate of methionine metabolism, to produce cystathionine. The gene encoding CBS is located on the 21st chromosome in humans and is linked to the hereditary disorder homocystinuria. Residues E111, K112, E244, T326 and K327 form the core of a hydrogen bonding network that participates in holding together the 81-85, 236-256 and 317-331 loops (yeast CBS numbering, corresponding to 146-150, 296- 316 and 374-388 of the human enzyme), which comprise much of the surface of the active-site entrance of CBS. Adjacent to E244 are residues Y241, G245, I246 and G247 that line the entrance of the CBS active-site, while T197 binds the phosphate loop of the PLP cofactor. In this study, the role of a series of 20 site-directed variants of these 10 residues was characterized to investigate the effect of six previously identified homocystinuria-associated active-site hCBS amino acid replacements, E176K, K384E/N, T257M, G305R and G307S (corresponding to E111K, K327E/N, T197M, G245R and G247S of yCBS). The impact of these substitutions on the kinetic parameters of yeast CBS is illustrated by the 30 to74-fold reductions in the k_{catF} of the E244 and G247 variants and the 16 to 25-fold increases in the K_m values for serine and homocysteine of the K327E, G245A and I246G variants. The effect of selected substitutions on stability is exemplified by the 1.6-M decrease in the midpoint for urea denaturation of the E111K (hCBS-E176K) variant. Our results support a role of the K112 hydrogen bonding network as a determinant of active-site architecture and dynamics. Residues G245-I246-G247, situated adjacent to the

cofactor, are likely required to maintain a catalytically productive orientation of the PLP cofactor.

3.2. Introduction

Homocysteine is formed upon cleavage of *S*-adenosylhomocysteine (SAH), the product of methyl-group donation by *S*-adenosylmethionine (SAM), the ubiquitous methyl donor of cellular metabolism. The transmethylation and transsulfuration pathways compete for homocysteine, converting it to methionine and cysteine, respectively. Cystathionine β-synthase (CBS) catalyzes the pyridoxal 5'-phosphate (PLP)-dependent condensation of serine and homocysteine to produce cystathionine in the first step of the transsulfuration pathway (Aitken and Kirsch, 2005). Deficiency of CBS activity is the most common cause of the disease homocystinuria. The clinical manifestations of this metabolic disorder include thromoembolism and connective tissue defects (Mudd *et al.,* 2001). More than 150 homocystinuria-associated mutations have been identified in the human gene encoding CBS (Kraus *et al.,* 2010; http://cbs.lf1.cuni.cz/mutations.php). Although the majority of disease-associated mutations are restricted to a small number of patients, some are prevalent in specific populations. For example, G307S accounts for >70% of homocystinuria alleles in Ireland (Kraus *et al.,* 1999). Elucidation of the structure-function relationships underlying the various disease-associated mutations of this enzyme will facilitate the efficient optimization of personalized treatment regimes, thereby reducing the impact of elevated homocysteine concentration, particularly during development.

The human CBS (hCBS) enzyme comprises: 1) an N-terminal domain of ~70 residues, unique to CBS from animal species, including humans and fruit flies, 2) a highly conserved catalytic core of ~340 residues, 3) a C-terminal, regulatory domain of ~140 residues (Koutmos *et al.,* 2010; Ereno-Orbea *et al.,* 2013). Structures are available

for the truncated form of hCBS (htCBS; residues 1-413, lacking the C-terminal, regulatory domain), the full-length form of *Drosophila melanogaster* CBS (dCBS) and a modified form of full-length hCBS lacking loop 516-525 (hCBSΔ516-525) (Meier *et al.,* 2001; Koutmos *et al.,* 2010; Orbea *et al.,* 2013). The heme cofactor is not involved in catalysis (Jhee *et al.,* 2000a; Meier *et al.,* 2001) and the Soret peak masks the absorbance of PLP intermediates, complicating presteady state studies. Therefore, the yeast enzyme, which lacks the N-terminal, heme-binding domain has provided an effective model system for mechanistic studies. The roles of several active-site residues have been characterized in yeast CBS (Jhee *et al.,* 2000a; Jhee *et al.,* 2001; Aitken and Kirsch, 2004; Quazi and Aitken, 2009; Lodha *et al.,* 2009; Lodha *et al.,* 2010).

The reported homocystinuria-associated point mutations are broadly distributed throughout the coding sequence of hCBS, including eight within the active-site cleft (G148E/R, E176K, T257M, G259D/M, G305R, G307S, S349N and K384E/N) (Kraus *et al.,* 1999; Meier *et al.,* 2003). Residues G305 and G307 form part of the surface of the entrance of the active site and Meier *et al.,* (2003) suggested that substitution of G307 with serine alters the conformation of an adjacent loop containing residue Y301. Similarly, based on *in silico* modeling, Lodha *et al.,* (2009) proposed the formation of a hydrogen bond, not present in the wild-type enzyme, between the side chain hydroxyl moieties of S307 (of hCBS-G307S) and Y301. Formation of this hydrogen bond was predicted to disrupt the wild-type interactions of Y301, resulting in the loss of a pair of hydrogen bonds between residues G256/T257 and the phosphate moiety of PLP and allowing the cofactor to shift ~1 Å toward the mouth of the active site. The residue adjacent to hCBS-G305 is a conserved glutamate residue (E304) that bridges a pair of

lysine residues (K177 and K384 of hCBS, corresponding to K112 and K327 of yCBS) as part of a hydrogen-bonding network (E176, K177, E304, K384, T383) that links the two sides of the active-site cleft. Residues E176 and K384 of this network are the site of homocystinuria-associated mutations (Kraus *et al.,* 1999). A series of 20 site-directed variants of 10 active-site residues was characterized to investigate the mechanism of the homocystinuria-associated active-site hCBS mutations E176K, K384E/N, T257M, G305R and G307S (corresponding to E111K, K327E/N, T197M, G245R and G247S of yCBS).

3.3. Material and Methods

3.3.1. Reagents

L-Cth, β-NADH (β-nicotinamide adenine dinucleotide, reduced form), L-Ser, L-Hcys thiolactone and L-lactate dehydrogenase (LDH) were purchased from Sigma. Dithiothreitol (DTT), ampicillin, 5,5′-dithio-bis-(2-nitrobenzoic acid) (DTNB) and imidazole were obtained from Fisher Scientific. Restriction endonucleases and T4 DNA ligase were from New England Biolabs. Nickel-nitrilotriacetic acid (Ni-NTA) resin was from Qiagen. Cystathionine β-lyase (CBL) was expressed and purified as described previously (Aitken and Kirsch, 2003). Oligonucleotide primers were synthesized by Integrated DNA Technologies and site-directed mutants were sequenced by BioBasic prior to expression and purification to ensure only the desired mutation(s) were present.

3.3.2. Construction, expression and purification of the site-directed yCBS mutants

Overlap-extension polymerase chain reaction (PCR) with the pSECseq0 (GGC GTC AGG CAG CCA TCG GAA GCT G) and pSECseq7r (GCC CGC CAC CCT CCG GGC CGT TGC TTC GC) flanking primers and the respective mutagenic primers was employed for the construction of site-directed mutants. The amplification products were inserted between the internal *BamH*I site of ytCBS and the vector *Pst*I site of the pTSECb-His plasmid, which contains the gene encoding ytCBS with a C-terminal 6-His affinity tag. The site-directed mutants were expressed and the resulting enzymes were purified via Ni-NTA affinity chromatography (Qiagen) as described by Aitken and Kirsch (2004). Protein monomer concentration was determined *via* UV-Vis spectroscopy. The ε_{280} value for ytCBS is 44500 $M^{-1}cm^{-1}$ (Jhee *et al.,* 2000b).

3.3.3. Steady-state kinetics

Enzyme activity was measured in a total volume of 100 μL at 25°C with a Molecular Devices Spectramax 390 spectrophotometer. The assay buffer was comprised of 50 mM Tris, pH 8.6, and 20 μM PLP. A background rate, for all components except the yCBS enzyme, was recorded for each sample before initiation of the reaction by the addition of yCBS. Data was fit by nonlinear regression with SAS (SAS Institute, Cary, NC). The reverse-physiological, yCBS-catalyzed hydrolysis of L-Cth to L-Ser and L-Hcys was detected *via* the reaction of 5,5'-dithiobis-(2-nitrobenzoic acid) (DTNB) with the free thiol of the L-Hcys product (Aitken and Kirsch, 2003). Reactions were carried out in assay buffer containing 2 mM DTNB, 0.004-6.2 mM L-Cth and 1.6-12 μM ytCBS, depending on the activity of the particular site-directed mutant. Absorbance changes were monitored at 412 nm ($\Delta\varepsilon_{412}$ = 13,600 $M^{-1}cm^{-1}$) and the data were fit to the Michaelis-Menten equation (equation 1) to determine k_{cat} and K_m, while k_{cat}/K_m was obtained independently from equation 2.

$$\frac{v}{[E]} = \frac{k_{cat} \times [S]}{K_m + [S]} \tag{1}$$

$$\frac{v}{[E]} = \frac{k_{cat}/K_m \times [S]}{1 + [S]/K_m} \tag{2}$$

The CBS-catalyzed condensation of L-Ser and L-Hcys to produce L-Cth was monitored *via* the continuous CBL-LDH assay (Aitken and Kirsch, 2003). Reactions were carried out in assay buffer containing 1.5 mM NADH, 0.5 μM CBL, 1.4 μM LDH, 0.1-11.3 mM L-Hcys and 0.2-36 mM L-Ser and were initiated by the addition of 0.66 μM wild-type ytCBS or 1-31 μM site-directed variant, depending on the activity of the

specific enzyme. In this continuous assay the CBL coupling enzyme converts L-Cth, produced by CBS, to L-Hcys, NH_3^+ and pyruvate, which is subsequently reduced to lactate by LDH, with the concomitant oxidation of NADH (ε_{340} = 6,200 $M^{-1}cm^{-1}$) to NAD^+. The concentration of LDH and CBL were optimized by varying their concentrations independently and 1.4 μM LDH and 0.5 μM CBL were selected as sufficient to ensure that neither coupling enzyme would be rate-limiting for the range of ytCBS concentrations assayed. The ytCBS kinetic parameters were determined, *via* global analysis, from the fit of the data to equation 3, in which $K_{iF1}^{L\text{-}Hcys}$ and $K_{iF2}^{L\text{-}Hcys}$ are inhibition constants for substrate inhibition by L-Hcys (Jhee *et al.,* 2000).

$$\frac{v}{[E]} = \frac{k_{cat}[L-Ser][L-Hcys]}{K_m^{L-Hcys}[L-Ser] + K_m^{L-Ser}[L-Hcys]\left(1+\frac{[L-Hcys]}{K_{iF1}^{L-Hcys}}\right) + [L-Ser][L-Hcys]\left(1+\frac{[L-Hcys]}{K_{iF2}^{L-Hcys}}\right)} \quad (3)$$

A term for substrate inhibition by L-Ser was added to equation 3 to produce equation 4 and the $K_{iF2}^{L\text{-}Hcys}$ was removed from equations 3 and 4 to produce equations 5 and 6 in order to fit the β-replacement data for variants with substrate inhibition patterns distinct from the wild-type enzyme.

$$\frac{v}{[E]} = \frac{k_{cat}[L-Ser][L-Hcys]}{K_m^{L-Hcys}[L-Ser]\left(1+\frac{[L-Ser]}{K_{iF}^{L-Ser}}\right) + K_m^{L-Ser}[L-Hcys]\left(1+\frac{[L-Hcys]}{K_{iF1}^{L-Hcys}}\right) + [L-Ser][L-Hcys]\left(1+\frac{[L-Hcys]}{K_{iF2}^{L-Hcys}}\right)} \quad (4)$$

$$\frac{v}{[E]} = \frac{k_{cat}[L-Ser][L-Hcys]}{K_m^{L-Hcys}[L-Ser] + K_m^{L-Ser}[L-Hcys]\left(1+\frac{[L-Hcys]}{K_{iF1}^{L-Hcys}}\right) + [L-Ser][L-Hcys]} \quad (5)$$

$$\frac{v}{[E]} = \frac{k_{cat}[L-Ser][L-Hcys]}{K_m^{L-Hcys}[L-Ser]\left(1+\frac{[L-Ser]}{K_{iF}^{L-Ser}}\right) + K_m^{L-Ser}[L-Hcys]\left(1+\frac{[L-Hcys]}{K_{iF1}^{L-Hcys}}\right) + [L-Ser][L-Hcys]} \quad (6)$$

The kinetic parameters for the β-replacement reaction of the T197S and T197A variants were determined from the fit to equations (7) and (8), respectively (Aitken and Kirsch, 2004). The terms k_{catE} and $K_{mE}^{L\text{-}SER}$ reflect the β-elimination of L-Ser that was uniquely observed for the T197A/S variants.

$$\frac{v}{[E]} = \frac{k_{catE}K_m^{L-Hcys}[L-Ser] + k_{cat}[L-Ser][L-Hcys]}{K_{mE}^{L-Ser}K_m^{L-Hcys} + K_m^{L-Hcys}[L-Ser]\left(1+\frac{[L-Ser]}{K_{iF}^{L-Ser}}\right) + K_m^{L-Ser}[L-Hcys]\left(1+\frac{[L-Hcys]}{K_{iF1}^{L-Hcys}}\right) + [L-Ser][L-Hcys]\left(1+\frac{[L-Hcys]}{K_{iF2}^{L-Hcys}}\right)} \quad (7)$$

$$\frac{v}{[E]} = \frac{k_{catE}K_m^{L-Hcys}[L-Ser] + k_{cat}[L-Ser][L-Hcys]}{K_{mE}^{L-Ser}K_m^{L-Hcys} + K_m^{L-Hcys}[L-Ser]\left(1+\frac{[L-Ser]}{K_{iF}^{L-Ser}}\right) + K_m^{L-Ser}[L-Hcys]\left(1+\frac{[L-Hcys]}{K_{iF1}^{L-Hcys}}\right) + [L-Ser][L-Hcys]} \quad (8)$$

3.3.4. Single turnover measurements

The formation of the external aldimine of the aminoacrylate intermediate, upon reaction of wild-type and site-directed variants of ytCBS with the serine substrate was monitored using a UV-visible diode array spectrophotometer (Agilent model 8450). The reaction of 20 μM enzyme with 50 mM L-Serine, in pH 8.6 Tris buffer, was monitored at 320 and 460 nm for 40 min at 25°C. The reaction of 20 μM I246A and G245A with 5–200 mM L-Ser was monitored at 460 nm, under the same conditions, for the formation of the aminoacrylate intermediate at each concentration of L-Ser.

3.3.5. Fluorescence spectroscopy

Fluorescence spectra were acquired with a Cary Eclipse spectrofluorimeter (Varian) at 25°C in 50 mM Tris, pH 8.6. The apparent dissociation constant for the enzyme-aminoacrylate (E-AA) complex due to L-Ser association with the free enzyme ($Kd_{(app)}^{L-Ser}$) was determined, as described by Jhee and coworkers, by titrating a 1 μM

solution of ytCBS with L-Ser (Jhee *et al.,* 2000). The increase in fluorescence intensity at 540 (λ_{ex} = 460 nm), due to the formation of the aminoacrylate intermediate was recorded and the change in fluorescence intensity ΔF was plotted versus [L-Ser] and fit to equation (9):

$$\Delta F = \frac{\Delta F_{max}\,[L-Ser]}{Kd_{app}^{L-Ser} + \,[L-Ser]} \quad (9)$$

3.3.6. Urea denaturation stability studies

The chaotropic agent urea, was employed to denature ytCBS in order to compare the relative effect of the 20 site-directed substitutions compared to the wild-type enzyme. The ytCBS protein was diluted to a final concentration of 1 μM in 20 mM phosphate buffer, pH 7.5, containing 0-7.6 M urea. Samples were incubated for 16 hours at room temperature and emission spectra were recorded at 25˚C using the Cary Eclipse (Varian) spectrofluorometer. Emission spectra (λ_{ex}=295 nm) were recorded between 300 - 380 nm (excitation, emission slit = 5 nm). The fluorescence intensity at the single wavelength (λ_{em}=356 nm) providing the greatest difference in fluorescence between the folded and unfolded states was plotted versus urea concentration (Pace *et al.,* 1997; Walters *et al.,* 2009). Data were fitted to the equation of a two-state model for equilibrium unfolding using KaleidaGraph (10):

$$y = \frac{\{(Yf+mf[D]+(Yu+mu[D])*e^{\left[m*\frac{[D]-Cm}{RT}\right]}\}}{1+\,e^{\left[m*\frac{[D]-Cm}{RT}\right]}} \quad (10)$$

Y_f and Y_u represent the intercept and m_f and m_u are the slope of the pre- and post-transition zones, respectively, while C_m is the midpoint of the transition zone between the folded and unfolded states.

3.4. Results

3.4.1. Steady-state kinetic characterization of site-directed variants

The kinetic parameters of all ytCBS variants, for the condensation of L-Ser and L-Hcys and L-Cth hydrolysis, were compared to the wild-type ytCBS. The F and R subscripts (e.g. k_{catF} and k_{catR}) represent the kinetic parameters of the physiological condensation of L-Ser and L-Hcys and the reverse-physiological hydrolysis of L-Cth, respectively (Tables 3.1, 3.2, 3.3A and 3.3B).

Residues E111, K112, E244, T326 and K327 comprise a hydrogen-bonding network that links the opposing sides of the active-site cleft. The $K_{mF}^{L\text{-}Ser}$ values of E111K and E111V are increased by 5 and 12-fold, respectively, while $K_{mF}^{L\text{-}Hcys}$ is unchanged and the k_{catF} of the β-replacement reaction is decreased by only 5-fold. The k_{catR} of the reverse-physiological, L-Cth hydrolysis reaction of E111K and E111V is decreased by 3 and 8-fold, respectively, while $K_m^{L\text{-}Cth}$ is increased by 48 and 81-fold (Table 3.1).

The $K_{mF}^{L\text{-}Hcys}$ is unchanged for the three E244 variants and $K_{mF}^{L\text{-}Ser}$ is increased by only 3, 4 and 5-fold for E244D, E244Q and E244V respectively, compared to wild-type ytCBS, indicating that this residue does not play a direct role in substrate binding. In contrast, the k_{catF} of the physiological, β-replacement reaction is decreased by 49, 30 and 74-fold for E244D, E244Q and E244V, respectively (Table 3.1). A similar trend is observed for the reverse-physiological, L-Cth hydrolysis reaction, as the k_{catR} of the three E244 variants is decreased by two orders of magnitude, while $K_m^{L\text{-}Cth}$ is only increased by 3-fold.

Substitution of residue T326 with alanine (T326A) has a negligible effect on the kinetic parameters of ytCBS, as the k_{cat} of the β-replacement and L-Cth-hydrolysis reactions are decreased by only 1.5 and 3-fold, respectively, compared to the wild type enzyme. The k_{cat} values of the K327E charge-reversal variant for the β-replacement and L-Cth hydrolysis reactions are decreased by 18 and 22-fold, respectively, and, while $K_{mF}^{L\text{-}Hcys}$ is unchanged, the $K_{mF}^{L\text{-}Ser}$ and $K_{mF}^{L\text{-}Cth}$ are increased by 10 and 51-fold, respectively. Therefore, the catalytic efficiency for the L-Cth hydrolysis reaction is reduced by three orders of magnitude (Table 3.3A). Correspondingly, the apparent dissociation constant of L-Ser ($K_{d(app)}^{L\text{-}Ser}$) is increased by 14-fold, compared to the wild-type enzyme. The 51-fold increase in the $K_m^{L\text{-}Cth}$ of the K327E variant is of similar magnitude to that observed for the replacement E111 with valine and lysine. The $K_{mF}^{L\text{-}Ser}$ of ytCBS-K327N is increased by 12-fold, while $K_{mF}^{L\text{-}Hcys}$ unchanged and k_{catF} and k_{catR} are decreased by only 4 and 5-fold, respectively. Althought residues E111, E244 and K327 are located at the periphery of the active site, distant from the PLP cofactor, the altered activity observed for these variants suggest that this hydrogen-bonding network influences active-site architecture and/or dynamics.

In order to investigate the mechanism of the prevalent, homocystinturia-associated G307S substitution (ytCBS-G247S), several active-site residues were targeted for site-directed mutagenesis. The substituted hCBS-S307 is proposed to interact with Y301 (ytCBS-Y241), leading to a conformational change and the resulting loss of hydrogen bonds between the phosphate moiety of PLP and T257 (ytCBS-T197) (Lodha *et al.,* 2009). Substitution hCBS-G305R (ytCBS-G245R) is another homocystinuria-associated mutation expected to affect the PLP cofactor binding (Meier *et al.,* 2003). The

$K_{mF}^{L\text{-}Ser}$ values of ytCBS-T197A and T197S are increased by only 3-fold and $K_{mF}^{L\text{-}Hcys}$ is unchanged and while the k_{catF} of the β-replacement reaction is unchanged by the T197S substitution, it is decreased by 32-fold for T197A, suggesting a role for the side-chain hydroxyl in the catalytically productive positioning of the cofactor. A similar trend is observed for the reverse-physiological L-Cth hydrolysis reaction as the k_{catR} of T197A is decreased by 7-fold and $K_{mR}^{L\text{-}Cth}$ is increased by 10-fold (Table 3.3B). A β-elimination activity was detected for the T197 variants, which is not present in the wt-ytCBS enzyme (Figure 3.1). The k_{catE} for the β-elimination of L-Ser by the alanine and serine substitution variants of ytCBS-T197 is 2-3 orders of magnitude lower (0.0107 ± 0.0007 and 0.0067 ± 0.0002 s^{-1}, respectively) than for the physiological reaction and the $k_{cat}/K_{mE}^{L\text{-}Ser}$ is only 5.9 ± 1.6 and 91.9 ± 16.7 $M^{-1}s^{-1}$, respectively.

The turnover of the physiological (k_{catF}) and L-Cth hydrolysis (k_{catR}) reactions are unchanged by the I246A substitution and $K_{mF}^{L\text{-}Ser}$ and $K_{mR}^{L\text{-}Cth}$ are increased by only 7 and 4-fold, respectively. In contrast, substitution of this residue with glycine (I246G) reduces k_{catF} and k_{catR} by 11 and 43-fold respectively and increases $K_{mF}^{L\text{-}Ser}$ and $K_{mR}^{L\text{-}Cth}$ by 25 and 2-fold, respectively, compared to the wild-type enzyme (Table 3.2). The ytCBS-G245R variant did not purify, due to aggregation, precluding steady-state kinetic characterization. The $K_{mF}^{L\text{-}Ser}$ of the G245L and G245A variants is increased by 7 and 16-fold, respectively, similar to the effect of replacement of the adjacent I246 by glycine. Similarly, the $K_{d(app)}^{L\text{-}Ser}$ of G245A is increased by 11-fold, and k_{catF} is decreased by 15 and 33-fold, respectively. The 16 and 25-fold increase in the $K_{mF}^{L\text{-}Ser}$ of G245A and I246G variants respectively, are suggestive of roles for the backbone amide or carbonyl

groups in the binding of L-Ser substrate. The $K_{mF}^{L\text{-}Hcys}$ of the G245A variant is also increased by 15-fold, compared to the wild-type enzyme (Table 3.2).

The Y241F substitution variant displays no change in k_{catF} and only a 3-fold reduction in k_{catR}, although the $K_m^{L\text{-}Ser}$ and $K_m^{L\text{-}Hcys}$ are increased by 13 and 6-fold, respectively (Table 3.2). Substitution of ytCBS-G247 with alanine or serine results in 57 and 32-fold reductions in k_{catF}, of the physiological, β-replacement reaction of ytCBS. The similarity in kinetic parameters of the Y241F/G247S double substitution variant and the G247S variant suggests that S247 does not form a hydrogen bond with Y241 (Table 3.2).

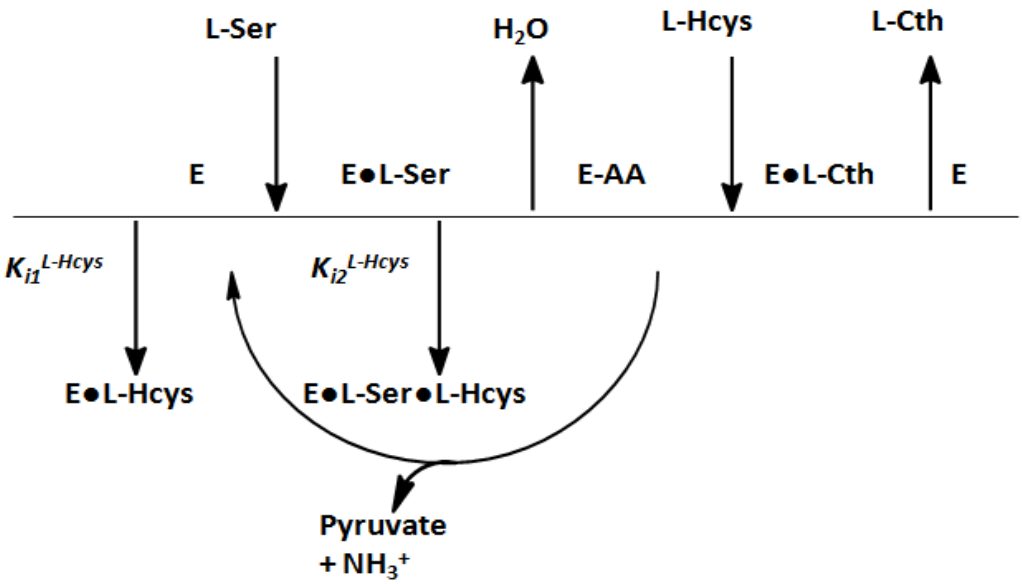

Figure 3.1: Cleland diagram illustrating the kinetic mechanism of the β-replacement reaction catalyzed by CBS including the β-elimination reaction observed for the T197 substitution variants. The ytCBS enzyme catalyzes the condensation of serine and homocysteine to produce cystathionine. Substrate inhibition by L-Hcys can occur by competing with L-Ser for the free enzyme form or by binding to the E-L-Ser complex prior to formation of the aminoacrylate intermediate, $K_{i1}^{L\text{-}Hcys}$ and $K_{i1}^{L\text{-}Hcys}$, respectively. The external aldimine E-AA is stable in wt-ytCBS, but this complex decomposes to pyruvate and ammonia and return to the internal aldimine form in the T197A and T197S variants (Aitken *et al.,* 2004).

Table 3.1: Kinetic parameters for the condensation of L-Ser and L-Hcys by wild-type ytCBS and the site-directed variants of the K112 network.[a]

Enzyme	k_{cat} (s^{-1})	$K_m^{L\text{-}Ser}$ (mM)	$K_m^{L\text{-}Hcys}$ (mM)	$K_{i1}^{L\text{-}Hcys}$ (mM)	$K_{i2}^{L\text{-}Hcys}$ (mM)	$K_i^{L\text{-}Ser}$ (mM)	$K_{D(app)}^{L\text{-}Ser}$ (µM)
ytCBS[b]	6.0 ± 0.3	0.8 ± 0.2	0.39 ± 0.04	0.9 ± 0.3	4.8 ± 0.6		
ytCBS	6.0 ± 0.3	0.8 ± 0.2	0.38 ± 0.06	0.8 ± 0.3	9 ± 2		12 ± 1
E111K	1.56 ± 0.08	4.1 ± 0.7	0.49 ± 0.05	1.2 ± 0.3	23 ± 10		59 ± 3
E111V	1.11 ± 0.06	9 ± 2	0.54 ± 0.05	2.4 ± 0.6	14 ± 3		160 ± 10
K112L	1.1 ± 0.1	43 ± 7	0.8 ± 0.3	6.2 ± 0.6		5 ± 2	
K112R	1.2 ± 0.2	70 ± 10	1.5 ± 0.3	7.2 ± 0.7		17 ± 5	
E244D	0.123 ± 0.003	2.1 ± 0.2	0.2 ± 0.1	1.3 ± 0.2	31 ± 8		30 ± 1
E244Q	0.20 ± 0.01	3.4 ± 0.3	0.14 ± 0.01	2.4 ± 0.3	22 ± 4		11 ± 3
E244V	0.082 ± 0.004	3.9 ± 0.6	0.27 ± 0.02	1.0 ± 0.2	30 ± 20		47 ± 3
T326A	5.2 ± 0.1	2.7 ± 0.2	0.31 ± 0.02	2.0 ± 0.2	18 ± 2		72 ± 2
K327E	0.33 ± 0.02	6 ± 2	0.7 ± 0.1	1.9 ± 0.8	4 ± 2		170 ± 20
K327L	0.96 ± 0.05	0.8 ± 0.2	0.44 ± 0.05	0.8 ± 0.3	-		28 ± 3
K327N	1.11 ± 0.06	9 ± 2	0.54 ± 0.05	2.4 ± 0.6	15 ± 3		30 ± 1

[a]Kinetic parameters reported are for the condensation of L-Hcys and L-Ser. Reaction conditions: 0.2-36 mM L-Ser, 0.1-11.3 mM L-Cys, 1.5 mM NADH, 0.5 µM eCBL, 1.4 µM LDH and 0.66-31 µM wild-type or variant yCBS, depending on the activity of the enzyme, in assay buffer at 25 ºC. The data were fit to the equations 3-6.

[b]Lodha *et al.,* 2009

Table 3.2: Kinetic parameters for the condensation of L-Ser and L-Hcys by wild-type ytCBS and the site-directed variants of the G247 network.[a]

Enzyme	k_{cat} (s^{-1})	$K_m^{L\text{-}Ser}$ (mM)	$K_m^{L\text{-}Hcys}$ (mM)	$K_{i1}^{L\text{-}Hcys}$ (mM)	$K_{i2}^{L\text{-}Hcys}$ (mM)	$K_i^{L\text{-}Ser}$ (mM)	$K_{D(app)}^{L\text{-}Ser}$ (mM)
ytCBS	6.0 ± 0.3	0.8 ± 0.2	0.38 ± 0.06	0.8 ± 0.3	9 ± 2	-	12 ± 1
T197A[b]	0.19 ± 0.01	2.7 ± 0.4	0.11 ± 0.03	1.6 ± 0.3	6 ± 1	-	n.d.[c]
T197S[b]	5.5 ± 0.6	2.7 ± 0.7	1.3 ± 0.2	1.0 ± 0.3	-	13 ± 3	11 ± 1
Y241F	4.8 ± 0.3	11 ± 1	2.1 ± 0.4	10 ± 5	-	12 ± 2	7 ± 2
G245A	0.54 ± 0.05	13 ± 2	5.8 ± 0.9	159 ± 9	-	-	140 ± 20
G245L	0.18 ± 0.01	5.1 ± 0.8	0.50 ± 0.07	5 ± 1	7 ± 1	-	n.d.
I246G	0.56 ± 0.08	20 ± 5	0.36 ± 0.08	5 ± 2	4 ± 1	-	n.d.
I246A	7 ± 1	6 ± 2	1.2 ± 0.3	1.6 ± 0.5	6 ± 2	23 ± 6	28 ± 3
G247A	0.11 ± 0.01	2.2 ± 0.4	0.11 ± 0.03	0.7 ± 0.2	6 ± 1	-	n.d.
G247S	0.185 ± 0.003	2.2 ± 0.5	0.11 ± 0.04	1.0 ± 0.2	14 ± 3	-	n.d.
Y241F-G247S	0.129 ± 0.003	1.23 ± 0.16	0.17 ± 0.07	1.1 ± 0.6	10 ± 3	-	n.d.

[a]Kinetic parameters reported are for the condensation of L-Hcys and L-Ser. Reaction conditions: 0.2-36 mM L-Ser, 0.1-11.3 mM L-cys, 1.5 mM NADH, 0.5 μM eCBL, 1.4 μM LDH and 0.66-31 μM wild-type or mutant yCBS, depending on the activity of the enzyme, in assay buffer at 25 ºC. The data were fit to the equations 3-6.

[b]Data were fitted to equations 7 and 8

[c]n.d. indicates not detectable. The shift in fluorescence peak at 540 nm was not observed for these variants upon reaction with L-Ser.

Table 3.3A: Kinetic parameters of the L-Cth hydrolysis activity of wild-type ytCBS and the site-directed variants of the K112 network.[a]

Enzyme	Mutation	k_{cat} (s^{-1})	$K_m^{L\text{-}Cth}$ (mM)	$k_{cat}/K_{mE}^{L\text{-}Cth}$ ($M^{-1}s^{-1}$)
ytCBS[b]	-	0.329 ± 0.02	0.069 ± 0.004	$(4.7 \pm 0.2)\times10^{3}$
ytCBS	-	0.370 ± 0.004	0.069 ± 0.004	$(3.4 \pm 0.5)\times10^{3}$
ytCBS-K112 (hCBS-K176) network	**E111K**	0.108 ± 0.001	3.3 ± 0.6	33 ± 4
	E111V	0.07 ± 0.01	6 ± 2	13 ± 2
	K112L[c]			1.41 ± 0.04
	K112Q[c]			$(3.9 \pm 0.6)\times10^{-2}$
	K112R[c]			$(8.1 \pm 0.9)\times10^{-2}$
	E244D	$(0.60 \pm 0.05)\times10^{-2}$	0.12 ± 0.05	80 ± 28
	E244Q	$(0.19 \pm 0.01)\times10^{-2}$	0.20 ± 0.05	52 ± 12
	E244V	$(0.25 \pm 0.03)\times10^{-2}$	0.17 ± 0.09	13 ± 7
	T326A	0.210 ± 0.002	0.41 ± 0.18	$(0.41 \pm 0.02)\times10^{3}$
	K327E	0.017 ± 0.003	3.5 ± 1.6	4.8 ± 1.2
	K327L	0.081 ± 0.001	0.45 ± 0.03	$(0.18 \pm 0.01)\times10^{3}$
	K327N	0.087 ± 0.001	0.31 ± 0.02	$(0.29 \pm 0.01)\times10^{3}$

[a]Kinetic parameters reported are for hydrolysis of L-Cth. Reaction conditions: 0.004-6.2 mM L-Cth and 1-26.25 μM wild-type or mutant yCBS, depending on the activity of the enzyme, in assay buffer at 25 ºC. The data were fit to the Michaelis-Menten equation to obtain k_{cat} and $K_m^{L\text{-}CTH}$ and equation 6 to obtain $k_{cat}/K_m^{L\text{-}CTH}$.

[b]Values for wild-type ytCBS are from Lodha *et al.,* (2009).

[c]Saturation was not achieved within the solubility limits of L-Cth substrate. Data were fitted to equation 2.

Table 3.3B: Kinetic parameters of the L-Cth hydrolysis activity of wild-type ytCBS and the site-directed variants of the G247 network.[a]

Enzyme	Mutation	k_{cat} (s^{-1})	$K_m^{L\text{-}Cth}$ (mM)	$k_{cat}/K_{mE}^{L\text{-}Cth}$ ($M^{-1}s^{-1}$)
ytCBS[b]	-	0.329 ± 0.02	0.069 ± 0.004	$(4.7 \pm 0.2)x10^3$
ytCBS	-	0.370 ± 0.004	0.069 ± 0.004	$(3.4 \pm 0.5)x10^3$
ytCBS-G247 (hCBS-G307) network	**T197A**	0.0107 ± 0.0007	1.81 ± 0.56	6 ± 2
	T197S	0.0067 ± 0.0002	0.08 ± 0.01	92 ± 17
	Y241F	0.127 ± 0.005	0.32 ± 0.05	$(4 \pm 0.5)x10^2$
	G245A	n.d.[d]	n.d.	n.d.
	G245L	n.d.	n.d.	n.d.
	I246G	0.0087 ± 0.0004	0.15 ± 0.03	60 ± 12
	I246A	0.177 ± 0.004	0.30 ± 0.03	$(7.5 \pm 0.4)x10^2$
	G247A	n.d.	n.d.	n.d.
	G247S	n.d.	n.d.	n.d.
	Y241F/ G247S	n.d.	n.d.	n.d.

[a]Kinetic parameters reported are for hydrolysis of L-Cth. Reaction conditions: 0.004-6.2 mM L-Cth and 1-26.25 μM wild-type or mutant yCBS, depending on the activity of the enzyme, in assay buffer at 25 ºC. The data were fit to the Michaelis-Menten equation to obtain k_{cat} and $K_m^{L\text{-}CTH}$ and equation 6 to obtain $k_{cat}/K_m^{L\text{-}CTH}$.
[b]Values for wild-type ytCBS are from Lodha *et al.,* (2009).
[d]n.d. indicates activity was not detected.

3.4.2. Fluoresence spectroscopy

Addition of L-Serine to yeast CBS results in the appearance of a fluorescence emission maximum centered at 540 nm upon excitation at 460 nm, attributed to the aminoacrylate intermediate. The increase in fluorescence at 540 nm allows determination of the apparent dissociation constant when L-Ser binds to the free enzyme, which yielded a $K_{D(app)}^{L\text{-}Ser}$ value of 12 μM for ytCBS (Figure 3.2). The 14-fold increase in $K_{D(app)}^{L\text{-}Ser}$ of the K327E is in accordance with the increase in $K_{mF}^{L\text{-}Ser}$ observed for this variant, suggesting that the charge reversal substitution plays an indirect role in L-Ser binding (Figure 3.2; Table 3.1). The fluorescence peak at 540 nm, for the formation of the aminoacrylate intermediate, was not observed for several variants G245A, T197A, I246G and G247A/S. This indicates that these residues might play a role in the cofactor orientation between the open and closed conformation of the active site.

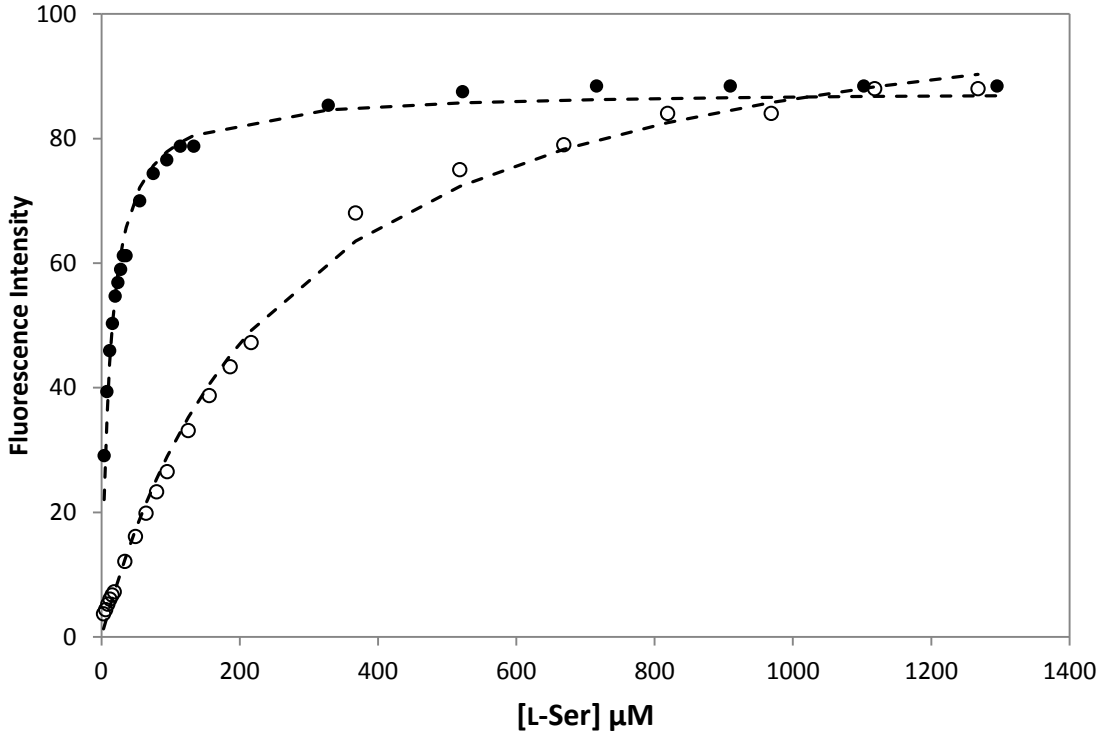

Figure 3.2: Aminoacrylate formation of wild-type (●) and K327E (○) site-directed variant of truncated yCBS enzyme. Titration with L-Ser increases the fluorescence intensity at 540 nm which is then plotted to determine $K_{D(app)}^{L\text{-}Ser}$. Data were fitted to equation (9) (Jhee *et al.,* 2000).

3.4.3. Effect of single residue replacements on CBS enzyme stability

The four tryptophan residues in the catalytic domain of ytCBS provide a sensitive fluorescence probe of conformational changes and comparison of the relative stabilities of the ytCBS variants compared to the wild-type enzyme. The enzyme appears to follow a two-state unfolding model with defined pre-transition (0-2 M urea), transition (2-3 M urea) and post-transition regions (4-8 M urea) (Pace *et al.,* 1997). Therefore, in order to compare the relative stability of each variant with the wild-type enzyme, equation 10 was employed to determine the midpoint (C_m) of the unfolding transition. The dependence of the fluorescence emission intensity on urea concentration for the wild-type ytCBS and a representative selection of site-directed variants are shown in figure 3.3. The C_m of the wt-ytCBS is 3 M urea. The refolding of ytCBS is not reversible and chemical equilibrium was not achieved, which precludes the determination of thermodynamic parameters of the unfolding reaction. Therefore, the unfolding transitions of ytCBS variants were qualitatively compared to the wild-type ytCBS for assessment of the relative effect of the site-directed substitutions on protein stability.

The E244D/Q/V, G245A/L, I246G and G247A/S replacements, lining the entrance of the active site, eliminate the pre-transition region (0-2 M urea) and correspondingly reduce the midpoint of the transition, compared to the wild-type enzyme. The near wild-type curve of the I246A variant is the sole exception of this group of 9 substitutions targeting residues 244-247 (Figure 3.3; Figure A1-3). This correlates well with the k_{catF} observed for the I246A variant, which is similar to the wild-type enzyme (Table 3.2). Interestingly, the K327E/N (K384E/N-hCBS) homocystinuria-assiocated mutation exhibits a similar unfolding behavior as wt-ytCBS, demonstrating only a ~0.5

M urea decrease in C_m. In contrast, the C_m of the ytCBS-E111K homocystinuria-associated variant (hCBS-E176K) is reduced by ~1.6 M. These results suggest that substitution of active-site residues can lead to changes in CBS stability. The resulting decrease in folded and active enzyme would be expected to reduce the *in vivo* flux through the transsulfuration pathway, thereby leading to the observed accumulation of homocysteine in plasma.

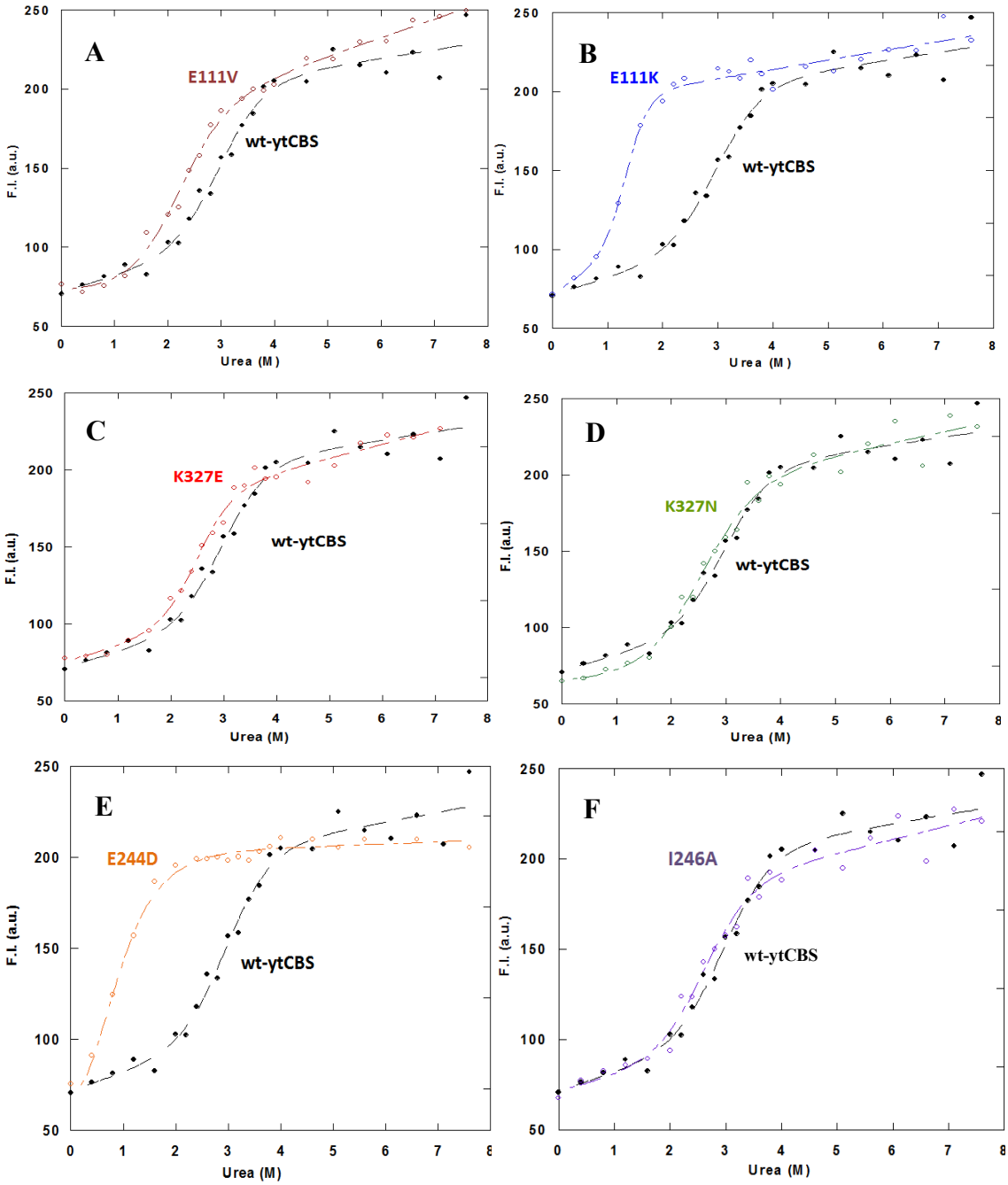

Figure 3.3: Fluorescence-monitored urea denaturation of wild-type and site-directed variants of truncated yCBS enzyme. Dependence of fluorescence emission on urea concentration for 1 µM wt-ytCBS (●) and A) E111K, B) E111V, C) K327E, D) K327N, E) E244D and F) I246A variants (○). Spectra were recorded between 300 and 380 nm (λ_{ex} = 295 nm and λ_{em} = 356 nm). Data were fitted to equation (10).

Table 3.4: Midpoint values (C_m) of urea-induced unfolding for the wild-type enzyme and site-directed variants of ytCBS[a].

Protein	C_m (M)
ytCBS	3.0 ± 0.2
E111K	1.4 ± 0.1
E111V	2.1 ± 0.2
K112L	1.1 ± 0.2
K112R	n.d.
E244D	n.d
E244Q	n.d
E244V	n.d
T326A	1.8 ± 0.1
K327E	2.5 ± 0.1
K327L	3.77 ± 0.05
K327N	2.5 ± 0.3

Protein	C_m (M)
ytCBS	3.0 ± 0.2
T197A	n.d.
T197S	2 ± 1
Y241F	1.4 ± 0.7
G245A	n.d
G245L	n.d.
I246G	n.d.
I246A	2.6 ± 0.3
G247A	n.d.
G247S	n.d.

[a]ytCBS and site-directed variants were diluted to a final monomer concentration of 1 μM in 20 mM phosphate buffer, pH 7.5, containing 0 -7.6 M urea. Samples were incubated for 16 hours at room temperature and emission spectra were recorded at 25˚C using the Cary Eclipse (Varian) spectrofluorometer. Emission spectra (λ_{ex}=295 nm) were recorded between 300 - 380 nm (excitation, emission slit = 5 nm) and emission wavelength (λ_{em}=356 nm) was selected. Data were fitted to a two-state model for protein unfolding, equation (10) (Pace *et al.,* 1997). n.d. indicates that the denaturation curves, for the corresponding site-directed variants, could not fit to a two-state model equation.

3.4.4. Spectroscopic studies and formation of the aminoacrylate intermediate

The spectroscopic properties of PLP provide a sensitive probe for detecting reaction intermediates in yCBS. As a result, these studies were conducted with the model yeast enzyme as it lacks the heme cofactor that masks the absorbance of PLP reaction intermediates in hCBS. Upon reaction with the L-Ser substrate the absorbance maximum of ytCBS shifts from the 412 nm peak, attributed to the internal aldimine (E), to 460-nm characteristic of the aminoacrylate intermediate (E-AA) (Jhee *et al.,* 2000). The difference in the spectra of the PLP cofactor for the hydrogen-bonding network variants E111K/V, E244D/V/Q and K327E/N was negligible compared to the wt-ytCBS enzyme. In contrast, the formation of the aminoacrylate intermediate at 460 nm is reduced by 50% and 75% for I246G and T197A, respectively, and is not detectable for G245Land G247S.The spectra of I246A and G245A are similar to that of the wt-ytCBS enzyme (Figure 3.4). This follows the trend observed for the catalytic activity of these two variants, to a lesser extent for G245A, which display kinetic parameters similar to the wild-type enzyme. Substitution of residues G245 with a larger side chain, such as leucine or arginine, likely affects PLP positioning in the active-site of ytCBS. In contrast with T197A, accumulation of the aminoacrylate intermediate is observed for the T197S variant, although the E-AA peak intensity is reduced by 50%, compared to wt-ytCBS.

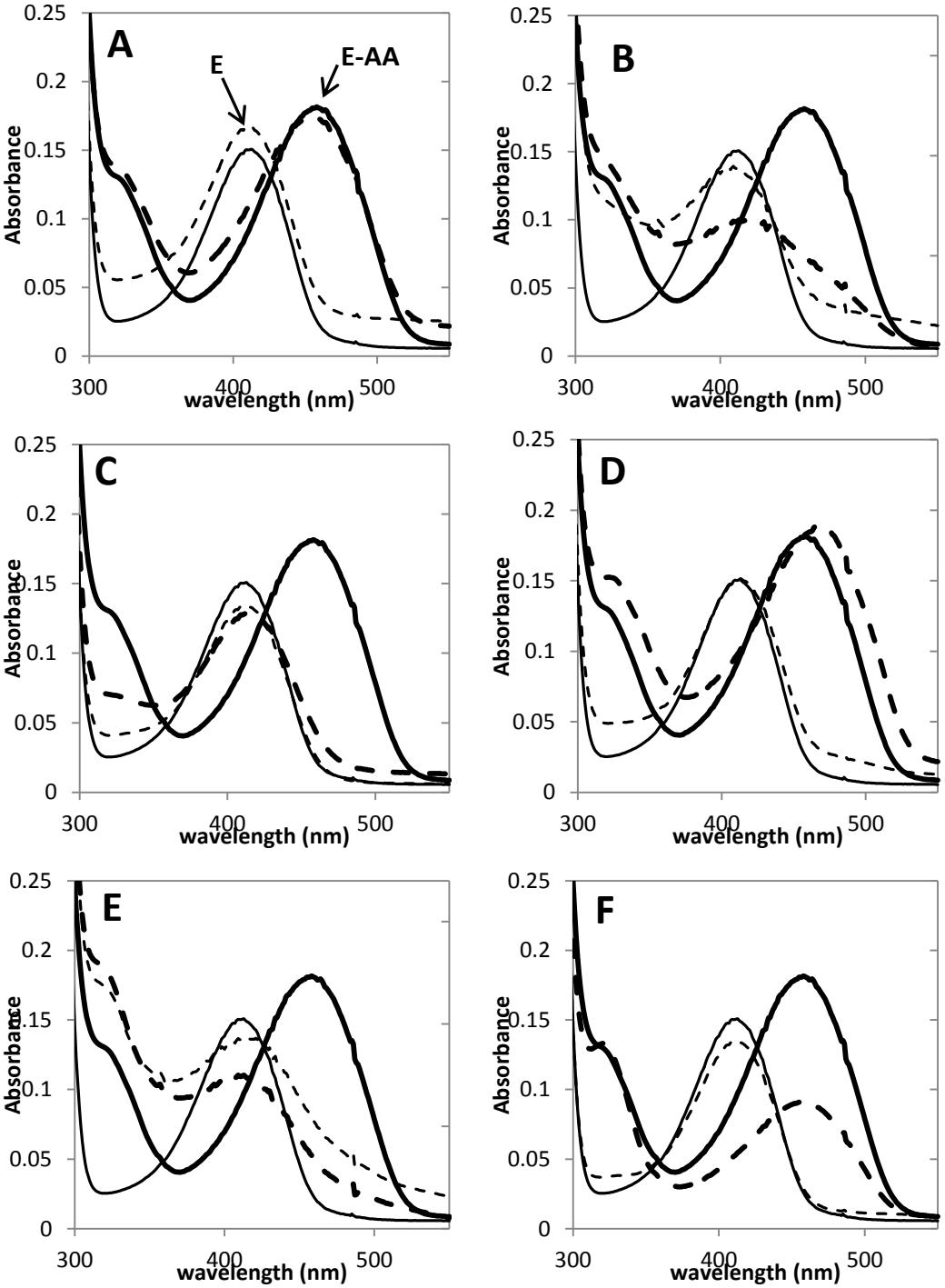

Figure 3.4: Formation of the aminoacrylate intermediate for the wild-type and site-directed variants of truncated yCBS. Spectra of PLP cofactor of wild-type ytCBS (solid lines) and the ytCBS variants (dashed lines), A) I246A, B) I246G, C) G245L, D) G245A, E) T197A and F) T197S alone and following the addition of 50 mM L-Ser (thick lines). The internal aldimine or free enzyme is denoted as (E) at 412 nm and (E-AA) is the aminoacrylate intermediate in the presence of L-Ser substrate at 460 nm (Jhee *et al.,* 2000).

3.5. Discussion

The crystal structure of *Drosophila melanogaster* CBS, dCBS, was solved in the absence and presence of the serine substrate, representing the open conformation of the vacant active site and the substrate-bound, closed conformation (Figure 3.5), respectively (Koutmos *et al.,* 2010). These structures facilitate interpretation of biochemical studies characterizing active-site residues. In order to investigate the effect of homocystinuria-associated mutations situated in proximity to the active site, a series of 20 site-directed variants of 10 residues were constructed and characterized and the results are interpreted in the context of the available CBS structures.

Docking of L-Cystathionine to the active site of a modeled ytCBS structure was employed by Lodha and colleagues to determine key residues involved in substrate binding. Accordingly, residue K112 was selected for site-directed mutagenesis based on its proposed interaction with the distal carboxylate group of L-Cth in the closed conformation of ytCBS (Lodha *et al.,* 2009). Residue K112 belongs to a hydrogen-bonding network (K112-E111-T326-K327-E244) that bridges the three loops (81-85, 236-256 and 317-331 of yCBS; 146-150, 296- 316 and 374-388 of the human enzyme) that comprise a large segment of the surface of the active site (Koutmos *et al.,* 2010). Residues E111 and K327 are of particular interest, as they are the site of homocystinuria-associated mutations in the human CBS enzyme (Kraus *et al.,* 1999). Residue E244 links the K112 hydrogen-bonding network to the active-site entrance as it is situated adjacent to residues G245 and G247, which are located at the entrance of the active site, and are also the sites of homocystinuria-associated mutations, in the human enzyme (Figure 3.5).

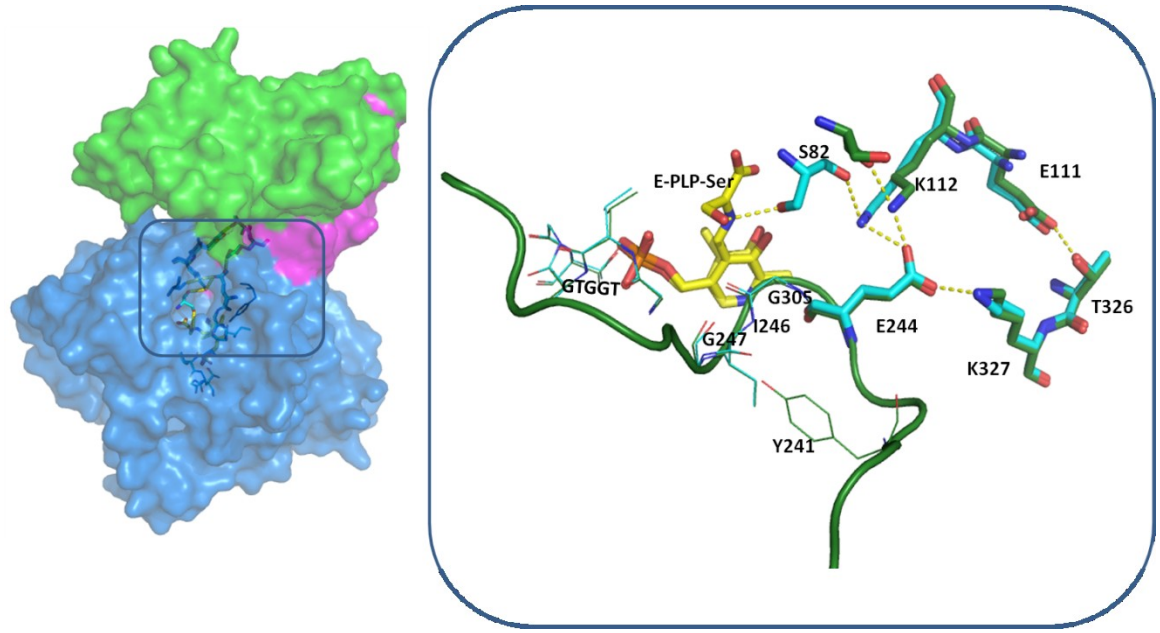

Figure 3.5: View of the Drosophila CBS (dCBS) monomer showing the catalytic (blue), linker (pink) and regulatory domain (green). The residues corresponding to the yCBS-K112 (hCBS-K177) hydrogen-bonding network are conserved in drosophila, human and yeast CBS (K112-E244-K327-E111-T326). This network bridges the two sides of the active site cleft and, *via* K112, links to the mobile loop of residues 80-85 of yCBS, which interacts with the α-carboxylate group of the L-Ser substrate. The inset compares the open (green) and closed L-Ser-bound (cyan) conformations of the dCBS active site. Residues corresponding to yCBS-S82 and K112 shift 5.3 and 3.4 Å, respectively, toward the PLP upon closure of the active site and residues E111 and K327 undergo a corresponding, but smaller conformational change (Koutmos *et al.,* 2010). This figure was generated using Pymol (The PyMOL Molecular Graphics System, Version 1.2r3pre, Schrödinger, LLC). Pdb code: 3PC2 and 3PC4.

3.5.1. The K112 hydrogen bonding network

3.5.1.1. E111K and E111V

Individuals with the hCBS-E176K substitution (yCBS-E111K) suffer from a severe form of homocystinuria (Kozich *et al.,* 1997). The ytCBS-E111K variant was constructed to investigate the effect the disease-associated hCBS-E176K charge-reversal mutation, in the context of ytCBS, and E111V was constructed to further probe the role of this residue by eliminating its hydrogen bonding capacity and thereby preventing its interaction with residue T326. The 5 and 12-fold increase in the $K_{mF}^{L\text{-}Ser}$ and the 48 and 81-fold increase in the $K_m^{L\text{-}Cth}$ for the E111K and E111V, respectively, demonstrate that E111 may be involved in binding L-Cth and L-Ser. However, given its position at the dimer interface between the catalytic subunits, it is more likely that residue E111 plays an indirect role by maintaining the active-site in a conformation that enables productive binding, upon closure of the active site. Lodha *et al.,* (2009) determined that replacement of residue K112, immediately adjacent to residue E111, to leucine or arginine results in an increase of ~50-90-fold in $K_{mF}^{L\text{-}Ser}$. Residue K112 forms a hydrogen bond with S82, of the mobile loop (residues 81-85 of yCBS), which binds the L-Ser substrate (Burkhard *et al.,* 1999; Aitken *et al.,* 2004; Koutmos *et al.,* 2010). Therefore, the observed increases in the $K_m^{L\text{-}Ser}$ and $K_m^{L\text{-}Cth}$ of the E111K and E111V variants may be caused by disturbance of the S82-K112 interaction. The crystal structure of dCBS, in complex with the L-Ser substrate, shows that the hydroxyl group of dCBS-S116 (yCBS-S82) moves ~5.3 Å toward the active site to interact with the side-chain hydroxyl of the L-Ser substrate while residue K112 (dCBS-K146) shift ~3.4 Å and E111 undergoes a similar but smaller conformational change (Figure 3.5) (Koutmos *et al.,* 2010). The ytCBS-E111K variant

(hCBS-E176K) also shows a decrease in stability, compared to the wild-type ytCBS (Figure 3.3). The corresponding E176K variant of hCBS was reported to aggregate in *E.coli* crude extract, suggesting a similar destabilizing effect in the context of the human enzyme (Janosik *et al.,* 2001). These results are also in accordance with a recent study, using circular dichroism, which demonstrated that hCBS-E176K exhibits partial destabilization of helical elements of secondary structure and decreased stability, compared to the wild-type enzyme (Hnizda *et al.,* 2012a). The observed *in vitro* decrease in enzyme stability may indicate changes of protein conformation, in addition to shifting the equilibrium between the folded and unfolded states, leading to more rapid degradation *in vivo*. Enzyme misfolding due to missense mutations has been suggested to be a common mechanism of CBS deficiency resulting from homocystinuria-associated mutations (Janosik *et al.,* 2001). The resulting reduction in active enzyme would cause a decrease in flux through the transulfuration pathway, leading to the observed accumulation of homocysteine in patients with the E176K allele. Missense mutations affect protein structure by preventing correct enzyme folding. This results in protein misfolding as observed for the E176K variant (ytCBS-E111K). Proteasome inhibitors prevent the degradation of misfolded mutant protein and could stimulate proper folding by inducing expression of liver chaperone proteins Hsp70, Hsp40 and Hsp27 which increase levels of active CBS (Singh *et al.,* 2010; Gupta *et al.,* 2013). This could provide an alternative treatment for vitamin supplementation, in the case of substitutions resulting in protein misfolding, such as in individuals carrying the E176K mutation.

3.5.1.2. T326A

Residue T326 (hCBS-T383) forms a hydrogen bond with E111 (hCBS-K176) and is immediately adjacent to residue K327 (hCBS-K384), which are both the sites of homocystinuria associated mutations of hCBS (E176K, K384E/N) (Figure 3.5). The corresponding T383 of the human enzyme is situated at the interface of the hCBS dimer and is not expected to contact the substrate in the active site. The ytCBS-T326A variant was investigated to provide further insight on the role of E111 (hCBS-E176) by removing the E111-T326 hydrogen bond without altering the glutamate side chain of E111. The k_{catF} and k_{catR} are decreased by only 1.5 and 3-fold, respectively, for the T326A variant, indicating that this residue is not a determinant of active-site conformation or dynamics. These results suggest that the changes in activity and stability observed for the E111K (E176K-hCBS) variant are a direct effect of the side chain modification of this residue, rather than the loss of the E111-T326 interaction.

3.5.1.3. E244D, E244Q and E244V

Residue ytCBS-E244 (hCBS-E304) interacts with a pair of lysine residues to bridge the active-site cleft (Figure 3.5) (Koutmos *et al.,* 2010). A series of three site-directed mutants was constructed to investigate the role of E244, by modifying (E244D, E244Q) or eliminating (E244V) the capacity of this residue to form hydrogen bonds with lysines K112 and K327. The ~50-100-fold reductions in k_{catF} and k_{catR}, for the E244 variants (Table 3.1, 3.3A), suggest that residue E244 plays a role in defining a catalytically competent active-site conformation. The reduced stability of the three E244 substitution variants (Figure 3.3), including the conservative, glutamate to aspartate substitution, is an indication of the central role this residue plays in bridging the opposing sides of the active-site cleft. Residue E244 is situated in the centre of the 235-255 loop,

one of three loop segments that form the majority of the active-site surface. The K112-E244-K327 hydrogen bonds bridge loops 76-158, 235-255 and 316-339 of ytCBS, thereby likely acting as a determinant of active-site conformation and dynamics. In addition to the role that E244 (hCBS-E304) plays as an anchor of the K112 network, it also aids in maintaining a stable closed conformation of the hCBS active-site. Upon substrate binding, and closure of the active site, the corresponding E304 of hCBS forms a hydrogen bond with S174 and stabilizes loop 171-174, corresponding to residues 106-109 in yCBS (Figure 3.6) (Koutmos *et al.,* 2010; Ereno-Orbea *et al.,* 2013). Therefore, substitution of E244 may result in a shift in the equilibrium between the open and closed conformations of the active site. However, as no β-elimination activity was observed for any of the E244 variants, the conformational equilibrium of the active site is not sufficiently disturbed to suggest that residue E244 is a determinant of reaction specificity.

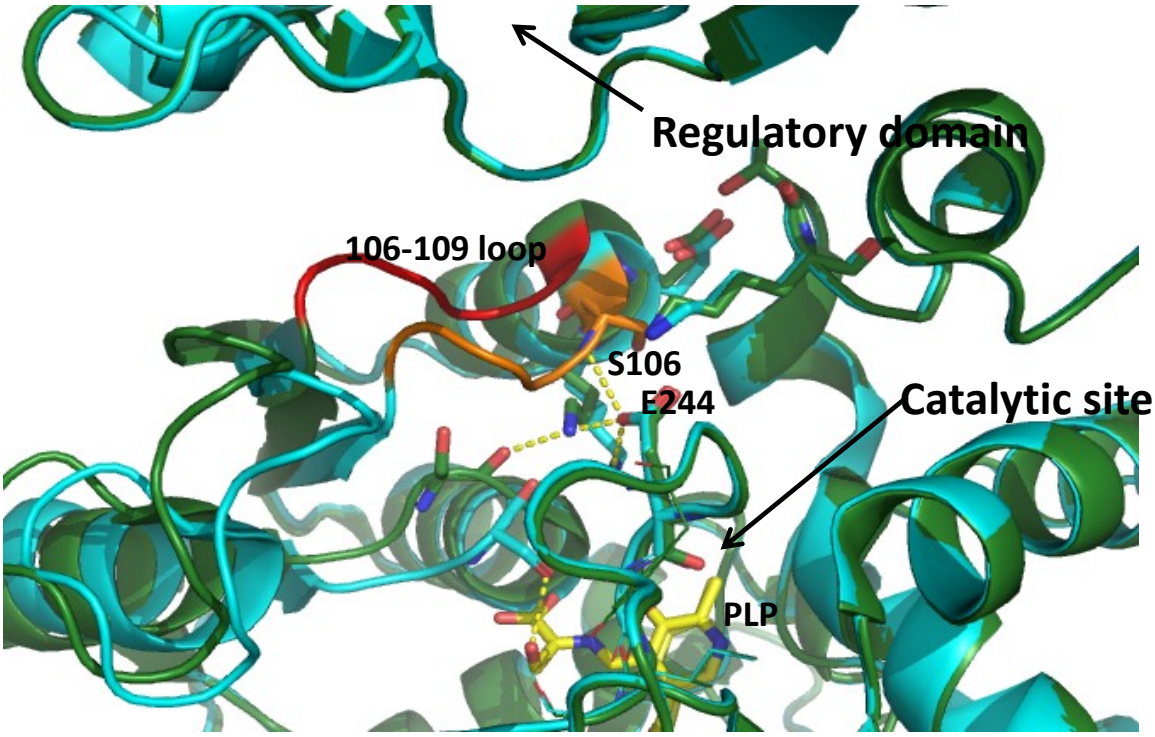

Figure 3.6: Residue E244 of yCBS (hCBS-E304) stabilizes the closed conformation of CBS. In the open conformation (green), the 106-109 loop of yCBS (171-174; hCBS numbering) (red) cannot interact with residue E244. Upon L-Ser binding (cyan), the 106-109 loop (orange) undergoes a conformational change toward the active site, bringing S106 within 3Å of E244 and enables hydrogen-bonding between the two residues (Koutmos *et al.,* 2010). This figure was generated using Pymol (The PyMOL Molecular Graphics System, Version 1.2r3pre, Schrödinger, LLC). Pdb code: 3PC2 and 3PC4.

3.5.1.4. K327E, K327N and K327L

Residue K327 of ytCBS was targeted for investigation because the corresponding K384 of hCBS is the site of two homocystinuria-associated mutations (K384E/N) (Kraus *et al.,* 1999; Meier *et al.,* 2001). This residue also contributes to the K112 hydrogen bonding network and is situated adjacent in sequence to T326, which interacts with E111 (Figure 3.5). Three site-directed variants were constructed in the model ytCBS enzyme. The K327E and K327N variants correspond to the homocystinuria-associated substitutions of residue K384 of hCBS, while ytCBS-K327L was designed to remove the hydrogen-bonding capacity of the lysine side chain, while maintaining the hydrophobic packing interactions of this residue. The catalytic efficieny for the L-Cth hydrolysis of the K327E variant is reduced by three order of magnitude (Table 3.3A), and $K_{D(app)}^{L\text{-}Ser}$ is increased by 10-fold (Table 3.1). Replacing the basic side chain of K327 with an acidic glutamate residue would disrupt the E244-K327 hydrogen bond and likely alter the architecture of the entrance of the ytCBS active site, due to repulsion between these two negatively charged residues, thereby indirectly perturbing the binding of L-Ser and L-Cth. The K384E allele is pyridoxine responsive, suggesting that the modified active-site architecture impedes productive cofactor binding (Kraus *et al.,* 1999). Comparison of the open and closed conformations of the active site, represented by the dCBS and the dCBS-L-Ser complex, respectively, demonstrates that upon binding of the L-Ser substrate, residue K327 (dCBS-K353) undergoes a slight conformation change to reposition the side chain while maintaining the position of the ε-amino group (Figure 3.7). Residue K327 (hCBS-K384) is located at the interface between the catalytic and the regulatory domains interacting with residues D330 (hCBS-S361) and W333 (hCBS-W364) in the

regulatory domain and could play a role in stabilizing the contact between those domains (Hnizda *et al.,* 2010).

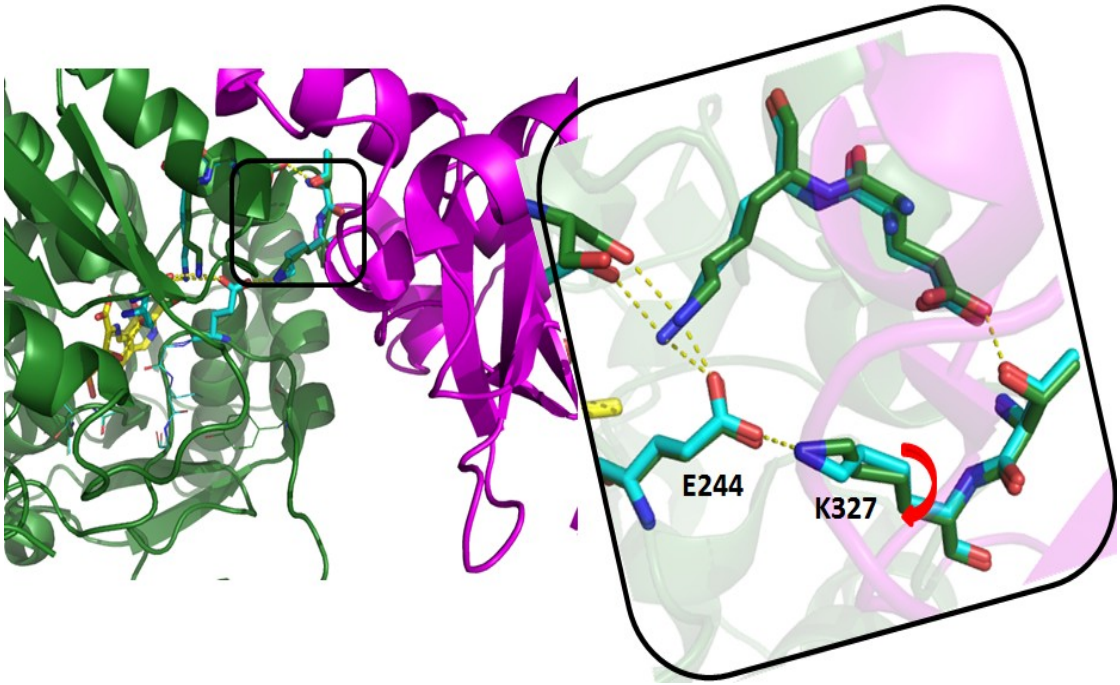

Figure 3.7: Position of residue yCBS-K327 (K353 of dCBS monomer) at the interface between the catalytic (green) and regulatory domain (pink). This lysine residue rotates between the open (green) and closed (cyan) conformation of the dCBS active site (Koutmos *et al.,* 2010). This figure was generated using Pymol (The PyMOL Molecular Graphics System, Version 1.2r3pre, Schrödinger, LLC). Pdb code: 3PC2 and 3PC4.

The asparagine side chain of the K327N substitution variant contains an amide group, which could form a hydrogen bond with residue E244, but the shorter N327 side chain may weaken or eliminate this interaction, as suggested by the 11-fold increase in $K_m^{L\text{-}Ser}$. However, k_{catF} and $K_m^{L\text{-}Hcys}$, k_{catR} and $K_m^{L\text{-}Cth}$ are all within 3-fold of the wild-type enzyme and both K327E/N variants had negligible effect on enzyme stability, compared to the wild-type truncated yeast enzyme (Figure 3.3; Table 3.4). The approximately 5-fold reduction in k_{catF} and k_{catR} observed for the K327L substitution is similar to that found with an asparagine replacement at this position. The observed changes in kinetic parameters resulting from the homocystinuria-associated substitutions of this residue result in perturbance of the *in vivo* flux through the reverse transsulfuration pathway. These changes are sufficient to result in the observed severe clinical manifestations of homocystinuria for the corresponding K384E mutation (Aral *et al.,* 1997). The negligible effect on stability (Figure 3.3) and k_{catF} (Table 3.1) observed for the K327E/N variants compared to the wild-type enzyme suggest that supplementation with vitamin B_6, B_{12} and folic acid would be sufficient to reduce homocysteine levels and restore enzyme activity in patients carrying the K384E/N mutations (Aral *et al.,* 1997).

3.5.2. Investigating the mechanism of the G307S homocystinuria-associated mutation

3.5.2.1. Residues G245-I246-G247

Residues G245-I246-G247 (G305-I306-G307 of hCBS), also conserved in OASS (G228-I229-G230), are located at the active site entrance of the CBS enzyme and with 6.5 Å of the PLP cofactor (Burkhard *et al.,* 1998; Meier *et al.,* 2001). Meier and colleagues have also suggested that the substrate homocysteine could bind in this region,

such that the prevalent homocystinuria-associated substitution hCBS-G307S would inhibit the binding of this substrate (Meier *et al.,* 2003). The orientation of G307 does not allow accommodation of a serine, because the side chain of Y301 is tightly packed against this residue. Residues G305 (yCBS-G245) is located in the active site of CBS and forms a hydrophobic interaction with the PLP cofactor *via* Van der Waals contacts with the pyridine ring (Meier *et al.,* 2003). The G305R homocystinuria-associated mutation is expected to affect PLP binding and active-site architecture as the large and charged side chain of arginine cannot be accommodated in place of glycine. Residue I246 in yeast CBS (hCBS-I306) is also located at the active site entrance in proximity to the PLP cofactor. The location of this residue, between two homocystinuria-associated mutations, G305R and G307S, might suggest a role for I246 in stabilizing the architecture of the active-site entrance.

3.5.2.1.1. I246A and I246G

Upon binding of the L-Ser substrate in dCBS, the PLP cofactor tilts toward the side chain of dCBS-I275 (ytCBS-I246) which forms a hydrophobic contact with the PLP ring, thereby providing a packing interaction that aids in positioning the cofactor within the active site, such that it is in a catalytically productive orientation (Figure 3.8). Elimination of this stabilizing interaction by the I246G substitution results in 11 and 43-fold reductions in k_{catF} and k_{catR}, respectively, a 25-fold increase in $K_{mF}^{L\text{-}Ser}$ and a shift in the C_m for unfolding of the enzyme (Table 3.2, 3.3B). The aminoacrylate intermediate, observed for the wild-type enzyme, is not formed upon incubation of ytCBS-I246G with 50 mM L-Ser under equilibrium conditions (Figure 3.4). In contrast, the kinetic parameters and urea denaturation profile of the I246A substitution variant are similar to

the wild-type ytCBS enzyme (Figure 3.3; Table 3.2; Figure A1-3C). These results suggest that the effects observed for replacement of the hydrocarbon side chain of I246 with glycine are due primarily to the unique conformational flexibility of this residue and that the resulting GGG sequence, in place of the wild-type GIG, does not provide a tight binding pocket for the PLP cofactor.

3.5.2.1.2. G245A, G245L and G245R

Residue hCBS-G305 (yCBS-G245) contacts the *re* face of the pyridine ring of PLP and is the site of the G305R homocystinuria-associated mutation (Meier *et al.,* 2003). The ytCBS-G245R site-directed variant could not be purified, due to aggregation, indicating that substitution of this glycine residue with arginine reduces the ability of this enzyme to adopt a stable folded structure. This observation illustrates why pyridoxine supplementation would not be effective for patients with the hCBS-G305R allele, allowing treatments to focus on methionine restriction and supplementation with folate, vitamine B_{12} and betaine. Although the alanine and leucine substitution variants of G245 are soluble, their stability is also reduced, as demonstrated by elimination of the pre-transition zone in urea-denaturation plots (Figure A1-3A). No accumulation of the aminoacrylate intermediate was observed for G245L and an 11-fold increase in $K_{D(app)}^{L\text{-}Ser}$ was observed for the G245A variant (Figure 3.4; Table 3.2). The 16 and 15-fold increase in $K_{mF}^{L\text{-}Ser}$ and $K_{mF}^{L\text{-}Hcys}$ observed for the G245L variant suggest that substitution of Gly with a bulkier residue blocks the binding of both substrates. Comparison of the open and closed conformations of the dCBS active site demonstrates that upon binding of L-Ser, the cofactor tilts and shifts ~1Å toward G245, which in turn undergoes a slight conformational change that would favor the new position of PLP (Figure 3.8). These

results suggests that residue G245 (hCBS-G305) plays an important role in maintaining a catalytically productive conformation of the active site of ytCBS. Treatement with vitamin B_6, B_{12}, in combination with folic acid is the current treatment for the G305R CBS deficiency. However, the G305R substitution leads to a misfolded protein with an increased tendency for aggregation. Proteasome inhibitors could stimulate residual enzyme activity by preventing protein aggregation (Singh *et al.,* 2010). The 16-fold increase in the K_m of L-ser and L-hcys for the G245A variant suggests substitution of the glycine results in a conformational change that blocks substrate(s) access to the active site. Supplementation with L-Ser could be a useful alternative to lower homocysteine levels in G305R homocystinuric patients, by increasing the amount of available substrate in the active site. Recent study by Sim and colleagues demonstrated that supplementation with L-Ser lowered homocysteine concentrations in mice and rats, suggesting that L-Ser could be a candidate for treatment of homocysteine-related diseases such as homocystinuria (Sim *et al.,* 2015).

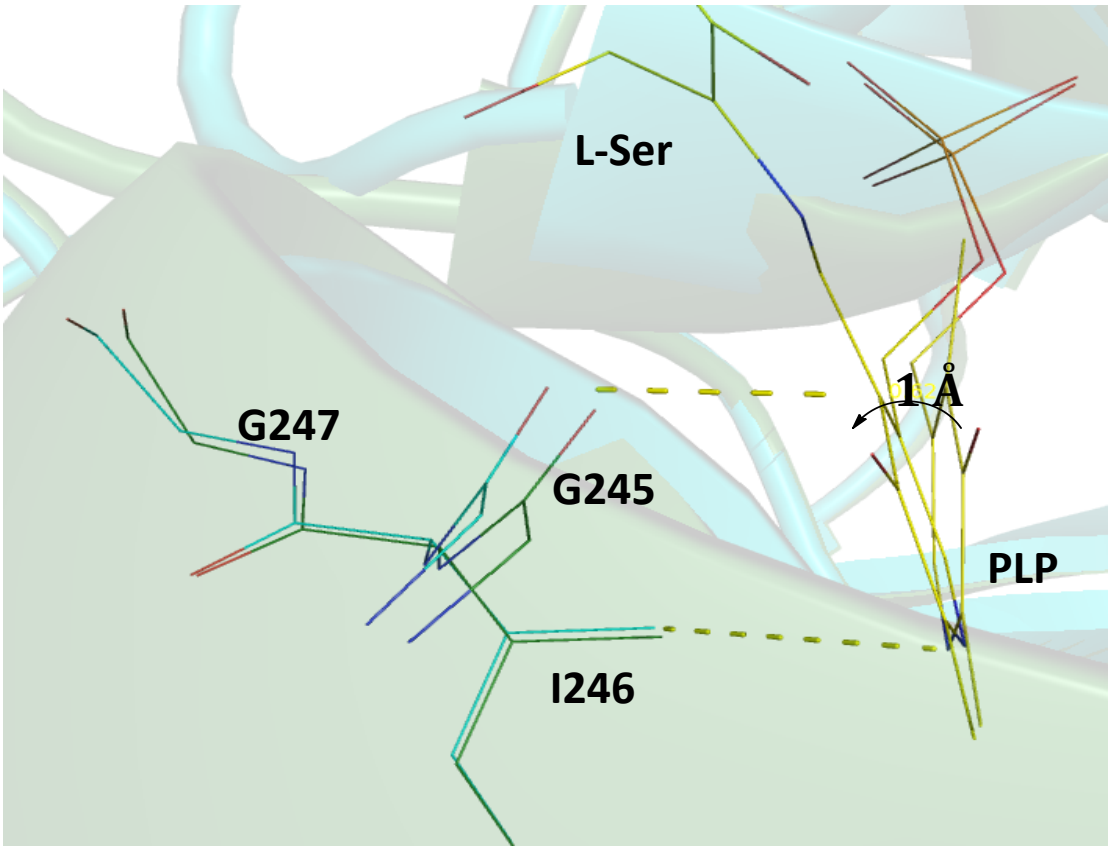

Figure 3.8: Overlay of the open (green) and closed conformation (cyan) of dCBS active-site. Upon L-Ser binding, the PLP cofactor (yellow) tilts ~1 Å toward the mouth of the active site (L-Ser). Residue G245 (G274-dCBS) undergoes a slight conformational change to allow the shift in the PLP position. The side chain of residue I246 (I275-dCBS) supports the PLP cofactor by forming hydrophobic interactions with the pyridine ring (Koutmos *et al.,* 2010). This figure was generated using Pymol (The PyMOL Molecular Graphics System, Version 1.2r3pre, Schrödinger, LLC). Pdb code: 3PC2 and 3PC4.

3.5.2.1.3. G247A, G247S, Y241F and Y241F-G247S double variant

Residue G307 of hCBS forms a hydrogen bond with V255, which is adjacent to residues G256 and T257, of the phosphate-binding loop (Meier *et al.,* 2003). Lodha *et al.,* (2009) employed *in silico* modeling to determine the structural effect of the hCBS-G307S substitution and suggested that an interaction between the side-chain hydroxyl groups of S307 and Y301 would lead to a shift in the position of both residues such that a pair of hydrogen bonds between residues G256/T257, of the GTGGT phosphate-binding loop (hCBS residues 256-260), and the phosphate moiety of the PLP cofactor are lost and the cofactor is shifted ~1 Å toward the mouth of the active site. Therefore, the G247A, Y241F and G247S/Y241F variants were constructed to investigate this hypothesis. If the premise is correct the G247A variants would be expected to have kinetic parameters closer to the wild-type enzyme than the G247S variant and addition of the Y241F substitution (G247S/Y241F) would at least partially rescue the loss in catalytic efficiency of G247S.

Residue Y241 (hCBS-Y301) is part of the 235-255 loop, which also includes E244, a residue that plays an important role in linking the opposite sides of the active site cleft to maintain a catalytically productive active-site architecture. The Y241F variant was constructed in order to investigate the proposed role of the hydroxyl moiety of this residue in hydrogen bonding to residue S247, in the context of the of G247S variant, which corresponds to the G307S homocystinuria-associated mutation of hCBS (Lodha *et al.,* 2009). Residue E242, immediately adjacent to yCBS-Y241, is also the site of a homocystinuria-associated mutation (E302K) in the human enzyme. The side chain of hCBS-E302 is solvent exposed and is located at the interface between the catalytic and the regulatory domain (Koutmos *et al.,* 2010). The increase in both $K_{mF}^{L\text{-}Ser}$ and $K_{mF}^{L\text{-}Hcys}$

suggest that the hydroxyl group of Y241 plays an indirect role in stabilizing active site in a catalytically productive conformation (Table 3.2). Interestingly, Y241 (hCBS-Y301) plays a similar active-site bridging role as residue E244 (hCBS-E304) by interacting with residue K172 to stabilize the closed conformation of the hCBS active-site (Ereno-Orbea *et al.,* 2013).

The similarity in the kinetic parameters of the G247A, G247S and the G247S/Y241F variants demonstrates that either the hydroxyl side chain of Y241 does not interact with the side chain of S247 in the context of the yCBS-G247S variant or that the this interaction is not the cause of the altered kinetic parameters of the latter. Residues Y301 and S285 are tightly packed against G307 (hCBS numbering) in the structure of the truncated form of hCBS. Meier *et al.,* (2003) predicted a role in G307 as a site for L-Hcys binding and suggested that the replacement of this residue with serine may affect the conformation of the active site entrance. Substitution of ytCBS-G247 with alanine or serine resulted in 57 and 32-fold reductions in k_{catF}, of the physiological, β-replacement reaction of ytCBS, demonstrating a role for this residue in maintaining the cofactor in a catalytically competent position. In contrast, the $K_m^{L\text{-}Hcys}$ was unchanged, suggesting that either this residue does not interact with the homocysteine substrate or that the G247A and G247S substitutions are not sufficient to result in disruption of this interaction. The G247S variant also reduced the relative stability of ytCBS (Figure A1-3B). Similarly, Hnizda and colleagues demonstrated that hCBS-G307S is rapidly degraded, even in the absence of urea (Hnizda *et al.,* 2012b).

3.5.2.2. T197A and T197S

Residue T197 of yCBS belongs to the G-T-G-G-T loop that binds the phosphate moiety of PLP, thereby anchoring this cofactor within the active site (Meier *et al.,* 2001). This residue corresponds to hCBS-T257, the site of the homocystinuria-associated T257M mutation in the context of hCBS. Site-directed variants were constructed to eliminate (T197A) or modify the hydrogen bonding capacity (T197S). Upon reaction with 50 mM L-Ser, a pronounced 320-nm peak is observed for ytCBS-T197A, while the 460-nm peak, indicative of the aminoacrylate intermediate was not observed. The formation of the E-AA is present, but reduced by approximately 2-fold in the T197S compared to the wild-type enzyme (Figure 3.4). β-elimination activity is observed for the alanine and serine substitution variants, which is an indicative of a change in the equilibrium between the open and closed conformations, allowing solvent to access the reactive aminoacrylate intermediate, as this activity is not detectable in the wild-type enzyme. Active-site ytCBS variants T81A, S82A, N84D/H, T85A, Q157A/E/H, Y158F and S289A also showed a β-elimination activity and aminoacrylate-mediated inactivation has been reported for three active-site variants (N84D, Q157H and Y158F) of ytCBS (Aitken *et al.,* 2004, Quazi *et al.,* 2009, Lodha *et al.,* 2010). These active-site variants possess a common mechanistic feature in that the characteristic peaks of the aminoacrylate intermediate, at 320 and 460 nm is not detected upon reaction with serine. The reduced native activity and the presence of β-elimination and inactivation activities is attributed to an improper orientation of the cofactor within the active-site of CBS and/or a change in the equilibrium between the open and closed conformations of the active site, as proposed for the Q157H and Y158F variants of ytCBS (Aitken *et al.,* 2004). The

hydrogen-bonding interaction between the hydroxyl group of T197 and the phosphate moiety of PLP, aids in maintaining a proper cofactor positioning during catalysis.

3.6. Conclusions

The results of this study show the importance of the K112 hydrogen-bonding network in maintaining active-site architecture and dynamics. The effect of homocystinuria-associated substitutions hCBS-E176K and K384E/N, corresponding to ytCBS residues E111 and K327, are conveyed to the cofactor and substrate-binding residues via residues K112 and E244, which bridge key structural elements to enforce a catalytically productive conformation on the active site. In contrast, disease-associated substitutions of residues G305, G307 and T257 of hCBS (corresponding to ytCBS-G245, G247 and T197) are the result of their direct contact with the cofactor. The similarity in the properties of the ytCBS-G247S and G247S/Y241F variants demonstrates that the effect of the corresponding hCBS-G307S substitution is likely not mediated by Y301. The detailed understanding of the effects of homocystinuria-associated substitutions on the activity and stability of CBS will support *in vivo* observations of pyridoxine responsiveness to minimize the early trial and error in the development of therapeutic regimes for patients with homocystinuria, thereby reducing the time required to balance homocysteine and methionine levels, particularly during development.

Chapter 4:

Characterization of the FourTryptophan Residues of Yeast Cystathionine β-Synthase with the Goal of Assessing their Potential as Probes of Conformational Change

4.1. Abstract

Cystathionine β-synthase (CBS; E.C. 4.2.1.22) is a pyridoxal 5'-phosphate (PLP) dependent enzyme that catalyzes the condensation of serine with homocysteine to produce cystathionine. The four tryptophan residues of yeast CBS (yCBS) are located in the catalytic domain (W132 and W263) and in the linker (W333 and W340) that connects the catalytic and regulatory domains. In this study, single and triple phenylalanine-substitution variants (W → F) of yCBS, were constructed to characterize the contribution of each tryptophan to the fluorescence spectrum and to fluorescence resonance energy transfer (FRET) to the PLP cofactor. A set of eight W → F variants was constructed in both the full-length and truncated (residues 1-353, lacking the regulatory domain) forms of the enzyme with the goal of assessing their potential as probes of conformational change and interactions between the catalytic and regulatory domains. The order of impact of these residues on catalytic efficiency and relative stability is W263 > W333 > W132 > W340. The accessibility of each tryptophan residue was determined *via* quenching with iodide in the truncated form (ytCBS), compared to the full-length yCBS enzyme (yfCBS), in the open and closed conformation. The fluorescence spectra and quenching results for the variants of the single and triple W→F substitutions indicate that W263 is buried, while W333 and W340 are solvent exposed. Residue W263 was determined to be the main contributor of FRET to the PLP cofactor and provides a useful probe of the active-site of yCBS. The increase in the quenching constant observed for the W333F and W340F-yfCBS variants and the limited quenching of these residues in the closed conformation suggest that these tryptophans are useful probe for catalytic-regulatory domain interactions, primarily those mediated by the linker region.

4.2. Introduction

Cystathionine β-synthase (CBS) catalyzes the pyridoxal 5'-phosphate (PLP)-dependent condensation of serine and homocysteine to produce cystathionine in the first step of the transsulfuration pathway (Aitken and Kirsch, 2005). Cystathionine β-synthase belongs to fold-type II of PLP-dependent enzymes, a structural class which includes enzymes catalyzing α,β-elimination and replacement reactions of amino acid substrates, as exemplified by CBS, *O*-acetylserine sulfhydrylase (OASS) and tryptophan synthase (TrpS). Typical of many fold-type II enzymes, such as threonine synthase (TS), CBS possesses a regulatory domain that is distinct from the PLP-binding, catalytic domain (Mehta *et al.,* 2000).

Deficiency of CBS activity is the most common cause of the disease homocystinuria, which is characterized by an elevated concentration of L-Hcys in plasma and urine. The clinical manifestations of this metabolic disorder include cardiovascular disease (thromoembolism), dislocation of the eye lens (ectopia lentis), mental retardation and skeletal deformities (Mudd *et al.,* 1995). More than 150 distinct, homocystinuria-associated mutations, primarily point mutations affecting a single codon, have been identified in the hCBS coding sequence (Kraus *et al.,* 1999; Kraus *et al., 2010*, http://cbs.lf1.cuni.cz/mutations.php). These mutations are distributed widely in the heme-binding, catalytic and regulatory domains of human CBS (hCBS) (Meier *et al.,* 2001; Meier *et al.,* 2003).

Until 2010, the only crystal structure available for CBS was the truncated form of hCBS, lacking the C-terminal regulatory domain (Meier *et al.,* 2001). Deletion of the C-terminal regulatory domain of both yeast and human CBS results in a ~2 fold increase in activity, compared to the full-length enzyme (Kery *et al.,* 1998; Jhee *et al.,* 2000). A

crystal structure of full-length drosophila CBS (dCBS), solved in 2010, shows that the regulatory domain is near the active-site of the catalytic domain, and that these two domains interact primarily through a linker region (Koutmos *et al.,* 2010). The crystal structure of a full-length hCBS variant, lacking the 516-525 loop (hCBSΔ516-525), was solved by Ereño-Orbea and colleagues (2013). The relative orientation of the regulatory domain to the catalytic domain is strikingly different between the drosophila and human enzymes, as in hCBS the regulatory domains of the two subunits do not interact and are shifted to the end of the catalytic cleft (Figure 4.1) (Ereño-Orbea *et al.,* 2013). The constitutively activated dCBS structure also shows that the linker region, situated between the catalytic and regulatory domains, is the primary site of contact between the two domains (Figure 4.1) (Koutmos *et al.,* 2010). The crystal structure of a variant of hCBS, with SAM bound to the regulatory domain, hCBSΔ516-525 E201S (hCBS E201S), was recently solved by Ereño-Orbea and colleagues (2014). Binding of SAM triggers a conformation change in the regulatory domain that favors the association of the Bateman module, similar to dCBS. This alleviates the inhibition imposed by the regulatory domain on the catalytic site. Ereño-Orbea proposed that the linker region facilitates the association of the regulatory domain (Ereño-Orbea *et al.,* 2014). However, the mechanism by which the regulatory and catalytic domains of CBS communicate has not yet been investigated.

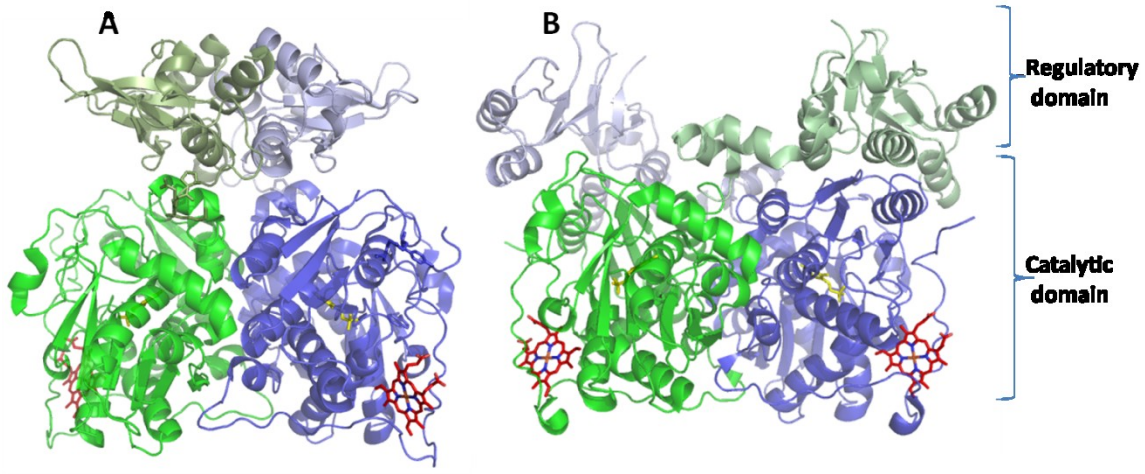

Figure 4.1: The structures of (A) dCBS and (B) hCBSΔ516-525 dimer showing the relative orientation of the regulatory domains (light green and light blue) with respect to the catalytic cores (dark green and dark blue). The heme and PLP cofactor are shown in red and yellow, respectively (Koutmos *et al.,* 2010; Ereno-Orbea *et al.,* 2013). This figure was generated using Pymol (The PyMOL Molecular Graphics System, Version 1.2r3pre, Schrödinger, LLC). Pdb code: 3PC2 and 4L3V.

The location of a pair of tryptophan residues at the interface between the catalytic and regulatory domains, in yCBS, provides the opportunity to employ fluorescence as probe to investigate the conformational changes that may underlie communication between the two domains. The human CBS enzyme, like that of other animals and *Drosophila melanogaster*, is not well-suited to the use of tryptophan fluorescence as a probe of conformational changes or domain interactions because its fluorescence spectrum is complicated by the presence of eight tryptophan residues (7 in dCBS) and the fluorescence-quenching ability of the heme cofactor. In contrast, the full-length yeast enzyme, which lacks the heme cofactor of hCBS (Jhee *et al.,* 2000a), possesses only four tryptophan residues, distributed between the catalytic domain (W132 and W263) and the linker (W333 and W340). The yeast enzyme, therefore, provides a useful model system to investigate the interface between the catalytic and regulatory domains of CBS. A series of eight single and triple Trp→Phe substitution variants were constructed in both the truncated (ytCBS, residues 1-354) and full-length (yfCBS) enzyme forms to enable the characterization of the fluorescence properties of each of the four tryptophan residues, and to assess their ability to act as probes of conformational change and inter-domain communication.

4.3. Material and Methods

4.3.1. Reagents

L-Cth was purchased from Sigma. Ni-nitrilotriacetic acid (Ni-NTA) resin and 5,5'-Dithiobis(2-nitrobenzoic acid) (DTNB) were obtained from Qiagen and Pierce, respectively. Oligonucleotide primers were synthesized by Integrated DNA Technologies and site-directed mutants were sequenced by BioBasic prior to expression and purification to ensure only the desired mutation(s) were present for each Trp → Phe variant.

4.3.2. Construction, expression and purification of yCBS mutants

Site-directed variants of yCBS, constructed *via* overlap-extension polymerase chain reaction, were inserted between the internal *BamH*I site of yCBS and the vector *Pst*I site of the pTSECb-His plasmid. This plasmid contains the gene encoding the truncated yCBS (ytCBS; residues 1–353, lacking the regulatory domain), with a C-terminal, 6-His affinity tag. The *Nde*I and *Pst*I restriction sites were used for the pTrc3 expression vector, which contains the gene encoding the full-length yCBS (yfCBS), containing a N-terminal 6-His affinity tag. Wild-type and site-directed variants of yCBS were expressed in *E. coli* strain DH10B. The yCBS enzymes were expressed and purified, *via* Ni-NTA affinity chromatography, as described by Aitken and Kirsch, (2004).

4.3.3. Determination of steady-state kinetic parameters

Enzyme activity was measured in a total volume of 100 μL at 25 °C on a Spectramax 340 microtiter plate spectrophotometer (Molecular Devices). The assay buffer was comprised of 50 mM Tris, pH 8.5, with 20 μM PLP. The hydrolysis of L-Cth was detected using 2 mM DTNB (ε_{412} = 13,600 $M^{-1}s^{-1}$), which reacts with the sulfhydryl group of the L-Hcys product (Aitken and Kirsch, 2003). A background reading was recorded before initiation of the reaction by addition of the yCBS enzyme. Values of $k_{cat}^{L\text{-}Cth}$ and $K_m^{L\text{-}Cth}$ were obtained by fitting of the data to the Michaelis-Menten equation and $k_{cat}^{L\text{-}Cth}/K_m^{L\text{-}Cth}$ was obtained independently from equation 1.

$$\frac{v}{[E]} = \frac{k_{cat}/K_m^{L-Cth} \times [L-Cth]}{1 + [L-Cth]/K_m^{L-Cth}} \quad (1)$$

4.3.4. Fluorescence Spectroscopy

Fluorescence spectra were acquired with a Cary Eclipse spectrofluorimeter (Varian) at 25°C in 20 mM phopshate buffer, pH 7.5. The fluorescence spectra for the variants carrying single and the triple W→F substitutions were recorded upon excitation at 295 nm between 300 - 380 nm with excitation and emission slit widths of 5 nm. To assess the possibility of energy transfer from one or more of the four tryptophan residues of yCBS to the PLP cofactor, the fluorescence spectrum (λ_{ex} = 295 nm) of 4 μM enzyme was recorded from 480–560 nm.

4.3.5. Urea denaturation of yCBS

Wild-type and tryptophan-substitution variants of yCBS were incubated at room temperature with 0 – 8 M urea for 16 hours. Equilibrium time for the unfolding transition to the midpoint was estimated by fitting a first-order kinetic progress curve to equation (2):

$$y(t) = y(\infty) + \Delta y * e^{-k_{app}t} \quad (2)$$

Y(∞) is the equilibrium signal at long times, Δy is the difference between the starting and the equilibrium signal, k_{app} is the apparent rate constant and (t) is the time (Street *el al.* 2008). Experiments were carried at 25˚C, in 20 mM phosphate buffer, pH 7.5. Fluorescence spectra of 1 μM wild-type yCBS and Trp → Phe variants were recorded. Emission spectra (λ_{ex} = 295 nm) were recorded between 300 - 380 nm (excitation, emission slit = 5 nm). The fluorescence intensity at the single wavelength providing the greatest difference in fluorescence (λ_{em} = 356 nm) between the folded and unfolded states was plotted versus urea concentration (Pace *et al.,* 1997; Walters *et al.,* 2009). Data were fitted to the equation of a two-state model for equilibrium unfolding using KaleidaGraph (3):

$$y = \frac{\{(Yf + mf[D] + (Yu + mu[D]) * e^{\left[m * \frac{[D]-Cm}{RT}\right]}\}}{1 + e^{\left[m * \frac{[D]-Cm}{RT}\right]}} \quad (3)$$

Y_f and Y_u represent the intercept and m_f and m_u are the slope of the pre- and post-transition regions, while C_m represent the midpoint of the transition.

4.3.6. Fluorescence Quenching Measurement

Determining K_q and f_a values for individual tryptophan can help provide information concerning the relative degree of exposure and/or the microenvironment surrounding the tryptophan residues (Eftnik *et al.,* 1981). Iodide is a negatively charged quencher and is limited to quenching solvent exposed tryptophan(s) or the neighboring charged residues. Fluorescence quenching experiments were performed by adding 5 μL of a 7.0 M iodide to 1 mL of 10 μM protein solution. The same procedure was followed for the quenching of ytCBS and yfCBS in the open and closed conformation and the latter was achieved by the addition of 10 mM L-Ser substrate to produce the aminoacrylate intermediate (Figure B1-3). Samples were excited at 295 nm and the emission intensity at 338 nm was recorded at 25˚C in 20 mM phosphate buffer, pH 7.5. The Stern-Volmer plot relates the decrease in fluorescence to the concentration of the collisional quencher, iodide (Figure B1-2A). The Stern-Volmer plots of ytCBS, yfCBS and the variants carrying the single W→F substitutions were found to be non-linear and showed a downward curvature (Figure B1-2B). This is characteristic of a protein with mutli-fluorophores with unequal iodine-accessibility to the quencher (Lehrer *et al.,* 1971; Eftnik *et al.,* 1981; Maruthamuthu *et al.,* 1995). These plots were linear for the triple substitutions variant and W263 was not quenched in the presence of iodide. A modified Stern-Volmer equation (4) was applied for enzymes with more than one tryptophan residue, where F_0 is the fluorescence intensity in the absence of the quencher, F the fluorescence intensity in presence of the quencher [Q], f_a is the fraction of accessible protein fluorescence and K_q is the effective Stern-Volmer quenching constant.

$$\frac{F0}{F0-F} = \frac{1}{fa} + \frac{1}{faKq[Q]} \quad (4)$$

4.4 Results

4.4.1. Effect of Trp → Phe substitution on yCBS activity

The kinetic parameters of the single and triple W→F substitution variants for the reverse-physiological, hydrolysis of L-Cth were compared to the truncated and full-length wild-type enzymes, as appropriate. The triple substitution variants (denoted as $_{TM}$), signifies that three tryptophan residues were replaced with phenylalanine and only one tryptophan residue remains. The kinetic parameters for the single W→F variants are within 2-fold of wild-type enzyme for both the truncated and full-length enzyme forms. However, substitution of W263 decreases k_{cat} by 20-fold for the triple substitution variants $W132_{TM}$ and $W333_{TM}$, while no activity was detected for $W340_{TM}$. However, $W263_{TM}$ decreases k_{cat} by only 2-fold in the context of both ytCBS and yfCBS enzymes (Table 4.1).

Table 4.1: Kinetic parameters of the L-Cth hydrolysis reaction catalyzed by wild-type and site-directed variants of yCBS[a]

Enzyme	k_{cat} (s^{-1})	K_m (mM)	k_{cat}/K_m ($M^{-1}s^{-1}$)
ytCBS	0.370 ± 0.004	0.085 ± 0.008	(3.9 ± 0.3) x 10^3
ytCBS-W132F	0.30 ± 0.01	0.15 ± 0.01	(2.0 ± 0.1) x 10^3
ytCBS-W263F	0.30 ± 0.01	0.39 ± 0.05	(0.8 ± 0.1) x 10^3
ytCBS-W333F	0.23 ± 0.01	0.14 ± 0.03	(1.6 ± 0.3) x 10^3
ytCBS-W340F	0.47 ± 0.03	0.40 ± 0.08	(1.1 ± 0.2) x 10^3
ytCBS-$W132_{TM}$	0.029 ± 0.001	0.13 ± 0.03	(0.2 ± 0.1) x 10^3
ytCBS-$W263_{TM}$	0.119 ± 0.002	0.16 ± 0.01	(0.7 ± 0.1) x 10^3
ytCBS-$W333_{TM}$	0.076 ± 0.002	0.15 ± 0.02	(0.5 ± 0.1) x 10^3
ytCBS-$W340_{TM}$	n.d.	n.d.	n.d.
yfCBS	0.261 ± 0.003	0.129 ± 0.008	(2.0 ± 0.1) x 10^3
yfCBS-W132F	0.259 ± 0.002	0.138 ± 0.006	(1.8 ± 0.1) x 10^3
yfCBS-W263F	0.119 ± 0.002	0.17 ± 0.01	(0.7 ± 0.1) x 10^3
yfCBS-W333F	0.233 ± 0.004	0.12 ± 0.01	(1.8 ± 0.1) x 10^3
yfCBS-W340F	0.234 ± 0.004	0.15 ± 0.01	(1.5 ± 0.1) x 10^3
yfCBS-$W132_{TM}$	0.013 ± 0.001	0.10 ± 0.03	(0.2 ± 0.1) x 10^3
yfCBS-$W263_{TM}$	0.147 ± 0.001	0.20 ± 0.03	(0.7 ± 0.1) x 10^3
yfCBS-$W333_{TM}$	0.018 ± 0.001	0.10 ± 0.03	(0.2 ± 0.1) x 10^3
yfCBS-$W340_{TM}$	n.d.	n.d.	n.d.

[a]Kinetic parameters reported are for hydrolysis of L-Cth. Reaction conditions: 2 mM DTNB, 0.01–6.4 mM L-Cth and 1.6-12 μM ytCBS, yfCBS wild-type or yCBS variants, depending on the activity of the enzyme, in assay buffer at 25°C. The data were fit to the Michaelis-Menten equation to obtain k_{cat} and $K_m^{L\text{-}Cth}$ and equation 1 to obtain k_{cat} and $K_m^{L\text{-}Cth}$.

n.d. indicates activity was not detected.

TM indicates that three tryptophan residues have been substituted with phenyalanine and only one tryptophan remains (i.e. $W340_{TM}$ indicates that only W340 is present in the enzyme).

4.4.2. Effect of W→F substitutions on enzyme stability

The urea denaturation of yCBS appears to follow a two-state unfolding pattern. However, unfolding appeared not fully reversible, thereby precluding the determination of thermodynamic parameters. Therefore, the single W→F substitution variants were qualitatively compared to that of wild-type yCBS and the relative changes in the midpoint of the denaturation were determined. The unfolding behavior for the W132F and W340F variants is similar to the wild-type enzyme for both the truncated and full-length enzymes (Table 4.2; Figure 4.3), while ytCBS-W333F exhibits a 1.8 M decrease in C_m and the pre-transition region is eliminated by the W263F subsitution (Figure 4.3). Although replacement of W263 with phenylalanine results in an enzyme that is only marginally stable, k_{cat}/K_m is only 4-fold lower than the wild-type enzyme, indicating that the conformation of the active site is not markedly perturbed.

Table 4.2: Transition midpoint values (C_m) for urea-induced unfolding of wild-type and tryptophan substitution variants of ytCBS and yfCBS[a].

Protein	C_m **(M)**
ytCBS	2.7 ± 0.1
W132F	2.8 ± 0.1
W263F[b]	n.d.
W333F	0.9 ± 0.2
W340F	2.3 ± 0.2
	C_m **(M)**
yfCBS	2.7 ± 0.1
W132F	2.6 ± 0.1
W263F	n.d.
W333F	n.d.
W340F	2.1 ± 0.5

[a]yCBS and site-directed variants were diluted to a final monomer concentration of 1 μM in 20 mM phosphate buffer, pH 7.5, containing 0-8 M urea. Samples were incubated for 16 hours at room temperature and emission spectra were recorded at 25˚C using the Cary Eclipse (Varian) spectrofluorometer. Emission spectra (λ_{ex} = 295 nm) were recorded between 300 - 380 nm (excitation, emission slit = 5 nm) and emission wavelength of (λ_{em} = 356 nm) was selected. Data were fitted to a two-state model for protein unfolding equilibrium (Pace *et al.,* 1997).
[b]n.d. indicates C_m was not determined because the enzyme variant does not follow a two-state model for urea-induced unfolding.

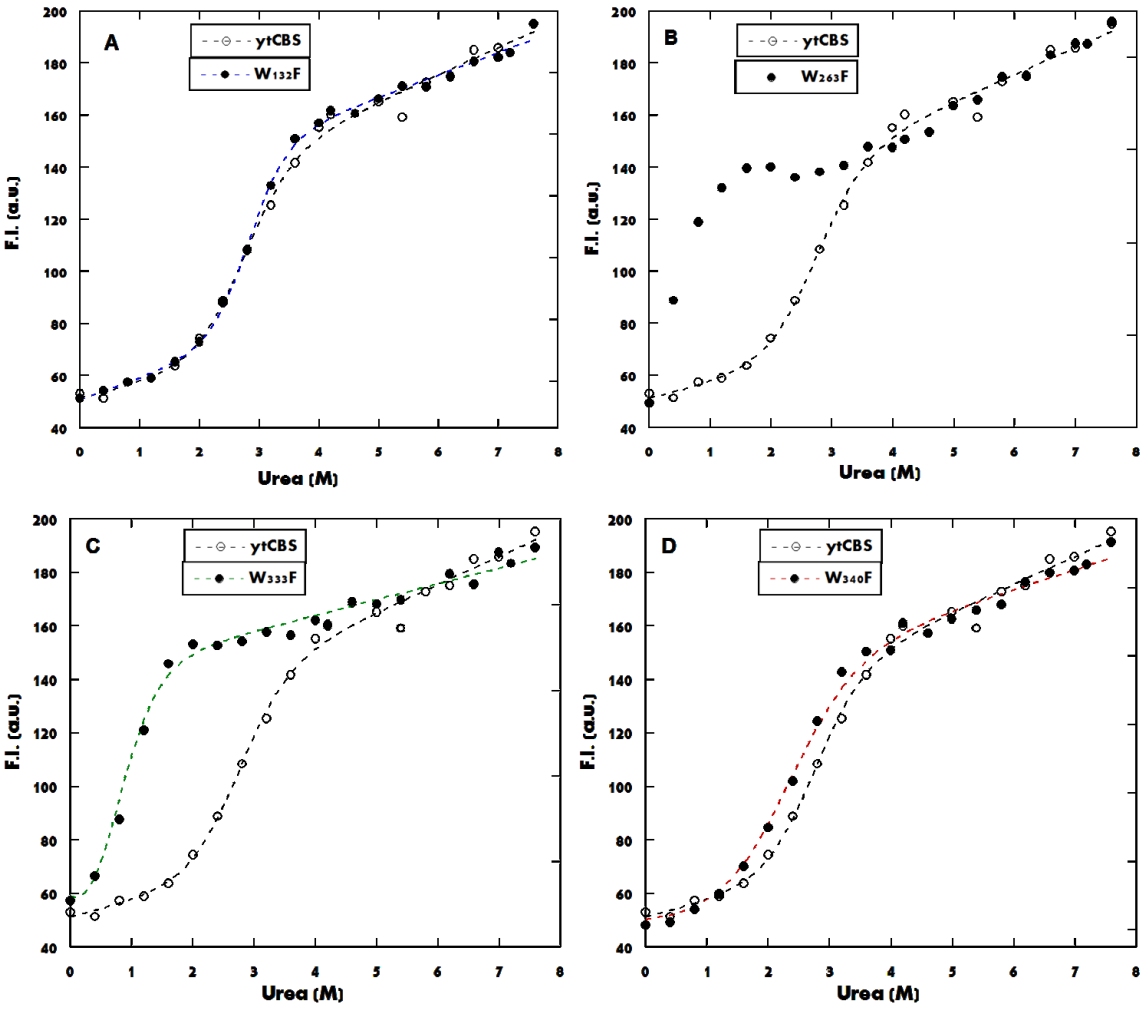

Figure 4.2: Fluorescence-monitored urea denaturation of wild-type and single W→F variants of truncated yCBS. Dependence on denaturant concentration of the fluorescence emission of wild-type ytCBS and the single tryptophan substitution variants A) W132F, B) W263F, C) W333F and D) W340F. Solutions containing 1.0 µM of ytCBS enzyme were incubated 16 hours at 25˚C in urea concentrations between 0 - 7.6 M. Samples were excited at 295 nm and the emission spectra were recorded between 320 - 380 nm (emission, excitation slit = 5 nm). The fluorescence intensity at 356 nm was plotted versus urea concentration. Data were fitted to equation 3.

4.4.3. Quenching studies and Förster energy transfer (FRET) for the single and triple W→F substitutions

The position of the maximal intensity in the fluorescence emission spectra and the quenching parameters provide information about the degree of exposure of tryptophan residues, as well as the microenvironment surrounding these fluorophores. Iodide is a negatively charged ion that is limited to quenching residues that are at least partially solvent exposed, as exemplified by W132, W333 and W340 in yCBS. Residues W333 and W340 are the most accessible for quenching, in both the truncated and full-length yCBS enzyme (Table 4.3). The 8 and 10-fold increase in the quenching constant of W333F and W340F-yfCBS is indicative of a change in the microenvironment of the remaining fluorophores, suggesting that substitution of either of the linker-situated tryptophan residues (W333 and W340) results in a local conformational change that increases the solvent exposure of the other one. W333 and W340 are the main residues being quenched by iodide (Table 4.3). These effects were less pronounced for the same variants in the truncated ytCBS enzyme as in the absence of the regulatory domain these residues are fully solvent exposed. The quenching of ytCBS and yfCBS in the open and closed conformation (upon addition of $_{L}$-Ser) was markedly different. The quenching of ytCBS in the closed conformation was unperturbed ressembling the quenching of residues W333 and W340 in the open conformation. In contrast, quenching of these tryptophan residues in the closed conformation was limited in the full-length enzyme form (Figure B1-3). This is likely due to the interactions between the catalytic and the linker/regulatory domains upon active-site closure, which shields the linker-situated tryptophan residues (W333 and W340) from being quenched by iodide.

Table 4.3: Quenching parameters, f_a and K_q, for ytCBS, yfCBS and the single substitution W→F variants[a].

Enzyme	**ytCBS**		**yfCBS**	
	K_q (M^{-1})	f_a	K_q (M^{-1})	f_a
Wild type	2.5 ± 0.6	0.52	2.4 ± 0.6	0.39
W132F	1.6 ± 0.3	0.49	5.8 ± 0.6	0.34
W263F	3.3 ± 0.3	0.47	6.5 ± 3.8	0.36
W333F	5.4 ± 0.6	0.23	18.2 ± 3.6	0.22
W340F	2.4 ± 0.7	0.31	25.1 ± 9.3	0.20

[a]Fluorescence quenching experiments were performed by adding 5 µL of a 7.0 M Iodide to 10 µM monomer solution. Samples were excited at 295 nm and the emission wavelength at 338 nm was selected, experiments were done at 25˚C in 20 mM Phosphate buffer, pH 7.5. Data were fitted to a modified Stern-Volmer equation (4), where f_a and K_q are the fraction of accessible protein fluorescence and the effective Stern-Volmer quenching constant, respectively.

Emission spectra of the single and triple variants were recorded with excitation at 295 nm (Figure 4.4). The fluorescence emission of tryptophan residues depends on the local changes in the environment surrounding these residues. The spectrum of wild-type enzyme is characterized by a major peak around 338 nm, due to the combined emission of the four tryptophan residues present in yCBS. A minor peak is observed at ~500 nm attributed to the energy transfer from tryptophan residue(s) to the PLP cofactor. This energy transfer occurs predominantly between W263 and PLP, as substitution of this residue, but not the other three tryptophans, eliminates the 500-nm peak that results from FRET to the cofactor (Figure 4.4). Upon substrate binding, a shift in the fluorescence spectrum of the PLP cofactor is observed from 500 to 540 nm (Figure 4.4A). This is due to the formation of the aminoacrylate intermediate.

The red-shift of 7 nm (338 to 345 nm) in the emission spectrum of the W263F variant compared to the wild-type enzyme indicates that this substitution results in changes in the environment and/or increased solvent exposure for the remaining tryptophan residues. The blue-shift to ~330 nm for the $W263_{TM}$ triple variant (W132F/W333F/W340F context) confirms that W263 is less solvent exposed than the other tryptophan residues of yCBS (Figure 4.4B). In contrast, the fluorescence emission spectrum of the $W333_{TM}$ (W132F/W263F/W340F) and $W340_{TM}$ (W132F/W263F/W333F) is red-shifted to approximately ~350 nm, indicates that these tryptophan residues are more exposed to solvent. These results are in agreement with the relative position of these tryptophan residues in the active-site (W263) and the linker region (W333 and W340) of the yCBS enzyme.

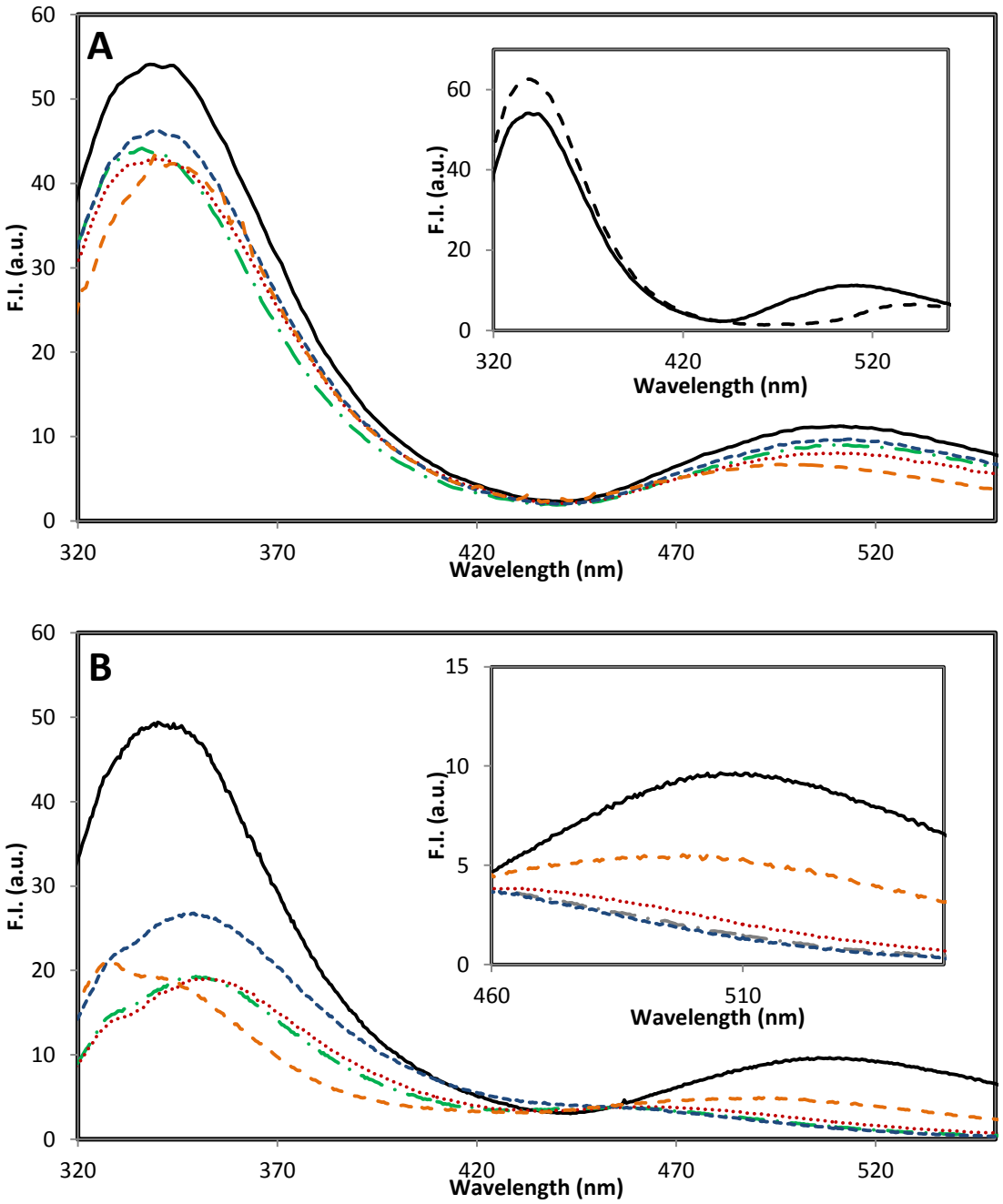

Figure 4.3: Emission spectra of wild-type, single and triple substitution varitants of yfCBS. A) Fluorescenc emission spectra of wt-yfCBS (solid lines), single substitution variants W132F (green), W263F (orange), W333F (red) and W340F (blue). Inset shows that upon L-Ser substrate binding (dashed lines) a shift in the fluorescence emission from 500 to 540 nm is observed. **B)** The triple substitution variants $W132_{TM}$ (green), $W263_{TM}$ (orange), $W333_{TM}$ (red) and $W340_{TM}$ (blue). Inset shows that $W263_{TM}$ (orange lines) is the main contributor of FRET to PLP. The enzymes (4 µM) were diluted in 20 mM phosphate buffer, pH 7.5 and measurements were recorded at 25˚C (λ_{ex} = 295 nm, λ_{em} = 310 - 550 nm and the excitation and emission slit widths were 5 nm).

4.5. Discussion

The recent crystal structures of the full-length drosophila and human CBS enzymes have revealed the relative positions of the catalytic and regulatory domains and suggest that SAM-mediated regulation of hCBS is accompanied by a large conformational change in the regulatory domain with respect to the active site of the catalytic domain (Koutmos *et al.,* 2010; Ereno-Orbea *et al.,* 2013; Ereno-Orbea *et al.,* 2014). However, the interactions between the catalytic and regulatory regions and the proposed role of the linker region in initiating the conformational change have not yet been elucidated. The development of tools to investigate the conformational changes, both between domains and within the catalytic domain, is required to further our understanding of the complex regulation of CBS. The presence of natural fluorophores (tryptophan residues and the PLP cofactor) in CBS provides the opportunity to use fluorescene spectroscopy as a probe of the conformational changes that underlie its catalytic function and the regulation. The location and environment of these fluorophores within the protein determines their effectiveness as probes of conformational change or domain interactions. For example, the eight tryptophan residues per monomer, as well as the quenching effect of the heme cofactor, of hCBS complicate its fluorescence spectrum, precluding interpretation of changes in the fluorescence spectrum in terms of localized conformational changes. In contrast, yCBS lacks the heme cofactor and possesses only four tryptophan residues per monomer (W132, W263, W333 and W340). Additionally, the placement of these tryptophan residues within the yeast enzyme suggests their potential as probes of conformational change as W263 is situated near the active-site cleft and the PLP cofactor, while W333 and W340 are located in the linker region that provides the main contact between the catalytic and regulatory

domains (Figure 4.4) (Koutmos *et al.,* 2010). Truncation of the CBS enzyme allows expression of the catalytic domain (residues 1-353 of yCBS) (Jhee *et al.,* 2000). The PLP cofactor is also a fluorophore and as its absorbance spectrum overlaps with the emission spectrum of tryptophan. Depending on the relative distances and orientations of these fluorophores, fluorescence resonance energy transfer (FRET) may be observed. This is exemplified by *O*-Acetylserine Sulfhydrylase (OASS), which also belongs to fold type-II PLP-dependent enzyme and contains a pair of tryptophan residues: W50 and W161. Campanini and colleagues reported that excitation of the tryptophans at 295 nm resulted in FRET to the PLP cofactor. As this can potentially provide a useful probe of both active-site dynamics and protein conformational changes, these authors constructed variants carrying tyrosine replacement at these positions and determined that W50 is primarily responsible for the energy transfer (Campanini *et al.,* 2003). In order to assess the suitability of yeast CBS's four tryptophan residues as probes of conformational change and to gain insight into the interactions between the catalytic and regulatory domains, variants were characterized housing single and triple W → F substitutions within the truncated (ytCBS) and full-length (yfCBS) forms of yCBS.

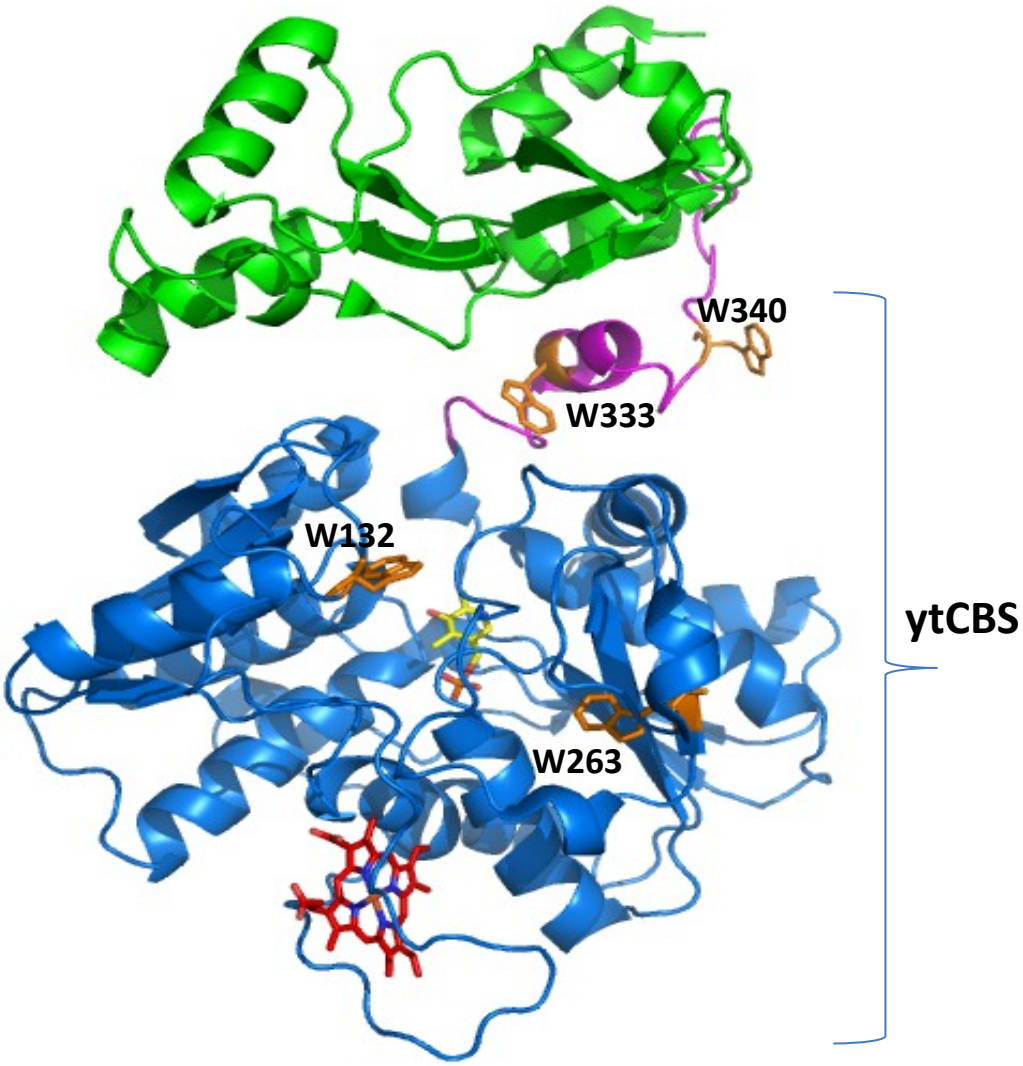

Figure 4.4: Cartoon representation of dCBS monomer showing the relative position of the four tryptophan residues of yCBS: W132, W263, W333 and W340. The catalytic domain is shown in blue, the linker in magenta and the regulatory domain in green. The truncated yeast CBS form (ytCBS) lacks the regulatory domain but contains residues W333 and W340. The heme and PLP cofactors are shown in red and yellow, respectively (Koutmos *et al.,* 2010). This figure was generated using Pymol (The PyMOL Molecular Graphics System, Version 1.2r3pre, Schrödinger, LLC). Pdb code: 3PC2.

4.5.1. Tryptophan residue(s) as probe(s) of active site conformation

4.5.1.1. Residue W132

Residue W132 is located in the catalytic domain of yCBS, approximately 10 Å from the PLP cofactor (Figure 4.4) (Koutmos *et al.,* 2010). The kinetic parameters of the W132F variant are within 2-fold of native truncated and full-length yCBS and the urea denaturation curves are coincident with the wild-type enzymes, demonstrating that replacement of W132 with phenylalanine does not alter the active site or stability of yCBS. These results indicate the feasibility of substituting W132 in order to simplify the fluorescence spectrum of yCBS for studies focusing on conformational change at the active site or domain interface. The emission spectrum of W132F displays similar FRET to the PLP cofactor as the wild-type enzyme and the $W132_{TM}$ triple-variant (W263F/W333F/W340F) shows no evidence of FRET, in both truncated and full-length yCBS, demonstrating that residue W132 is not responsible for the observed tryptophan-to-PLP energy transfer of the wild-type enzyme. Additionally, substitution of W132 with phenylalanine has no effect on the quenching constant in both ytCBS and yfCBS (Table 4.3). This is in accordance with the negligible effect of the W132F substitution on enzyme stability, a similar effect as observed for OASS-W161Y (Campanini *et al.,* 2003).

4.5.1.2. Residue W263

Residue W263 is situated in the catalytic domain of yCBS and within 9.6 Å of the PLP cofactor (Koutmos *et al.,* 2010). Although replacement of W263 with phenylalanine has negligible effect on the kinetic parameters of the yCBS catalyzed reaction, the

combination of this substitution with W132, W333 or W340 decreases k_{cat} by at least 20-fold. Therefore, substitution of W132 and W263 with phenylalanine, to focus on the spectrum of the two tryptophan residues situated at the domain interface (W333 and W340), is not recommended as the resulting double-substitution variant (W132F/W263F) would likely not be reflective of the wild-type enzyme.

In contrast to W132F, substitution of W263 with phenylalanine reduces the stability and/or perturbes the unfolding mechanism of yCBS, in both the truncated and full-length enzymes. Substitution of conserved tryptophan residues has been reported to destabilize protein structure as exemplified by the W214A variant of human serum albumin (Watanabe *et al.,* 2001). Residue W263 is the main contributor of the energy transfer to the PLP as demonstrated by the lack of a 500-nm absorbance for W263F and the similarity of this peak for the W263 triple variant (W132F/W333F/W340F) and the wild-type ytCBS and yfCBS enzymes. Similarly, of the two tryptophan residues within the homologous enzyme OASS, only W50 is positioned to enable FRET to the PLP cofactor (Bettati *et al.,* 2002; Campanini *et al.,* 2003). Future studies probing substrate/inhibitor binding and conformational changes in the active-site may find the observed W263→PLP FRET a useful probe of subtle changes at the active-site. For example, W263 could be employed to investigate the binding of inhibitors that affect H_2S production by CBS, identified by Thorson *et al.,* (2013).

The accessibility of tryptophan residues in W263F to iodide, f_a, is not changed compared to the wild-type enzyme and the W263 triple variant (W132F/W333F/W340F) is not quenched by iodide. This suggests that, W263 is also buried and shielded from the solvent in the yeast enzyme, and in agreement with the structure of hCBS and dCBS. The

3-fold increase in the degree of solvent exposure, K_q, for the W263F variant is likely due to a change in the local environment surrounding one or more of the remaining tryptophan fluorophores in response to the phenylalanine replacement. This is in agreement with the observed reduction in stability observed for this variant, compared to the wild-type enzyme.

4.5.2. Tryptophan residue(s) as probe(s) of catalytic-regulatory domain interaction

4.5.2.1. Residue W333

Residue W333 is located at the junction between the catalytic domain and the linker, and is expected to be solvent exposed in ytCBS, but shielded by the regulatory domain in yfCBS. The kinetic parameters of the W333F variant are within 2-fold of the wild-type truncated and full-length enzymes, demonstrating that this phenylalanine replacement does not significantly impact the active site of yCBS. The red-shift in the emission spectrum of the W333 triple variant (W132F/W263F/W340F), from 338 nm for the wild-type enzyme to 348 and 360 nm in the full-length and truncated enzyme, respectively, indicates that W333 is solvent exposed in yfCBS, but to a lesser degree than in ytCBS. Additionally, substitution of residue W333 reduces the stability of both the truncated and full-length enzyme forms (Table 4.2). This is surprising in the context of the truncated enzyme, as W333 is solvent exposed and situated close to the C-terminus of the protein and was expected to be in a relatively unstructured region, particularly in the context of the truncated enzyme.

The fraction of fluorophore accessible to the quencher, f_a, is decreased from 0.5 for the wild-type enzyme to 0.23 for the W333F variant, indicating that residue W333 is one of

the primary tryptophan residues quenched by iodide. The observed increase in K_q is likely result of the reduced stability of the W333F variant. Interestingly, the K_q of W333F is increased 8-fold in the full-length enzyme, compared to the 2-fold increase observed for ytCBS-W333F. This suggests that the W333F substitution results in a change of conformation which makes residue W340 more solvent exposed in yfCBS. This suggests that residue W340 is at least partially shielded by the regulatory domain in the full-length enzyme and that the W333F substitution destabilizes the structure and increases the solvent accessibility of the adjacent W340. Interestingly, residues hCBS-W390 (W333-yCBS) and the adjacent hCBS-M391, which form part of the α-helix in the linker region, are the sites of homocystinuria-associated mutations (Kraus *et al.,* 2010). The instability observed for the W333→F variant in yCBS implies that the α-helix region (α-15) of the linker is required to maintain the appropriate conformation of the linker region. Helix α-15 is also proposed to play a role in the hCBS tetramerization by interacting with loop region 513-529 of the regulatory domain (Ereno-Orbea *et al.,* 2013). Furthermore, quenching of yfCBS in the closed conformation demonstrates that active site closure is communicated to the regulatory domain through the linker region. Quenching of W333 and W340 in the closed conformation is limited suggesting that a change in conformation of the linker region shields these residues from being quenched by iodide (Figure B1-3). The flexibility of the linker region is proposed to facilitate the conformational changed associated with hCBS activation state upon SAM binding (Ereno-Orbea *et al.,* 2014). Therefore, W333 and W340 are useful probes to investigate conformational changes associated with the regulatory domain and of the oligomeric status of yCBS.

4.5.2.2. Residue W340

Residue W340 is located in the unstructured portion of the linker region following helix α-15. The kinetic parameters of the W340F variant are identical to the wild-type enzyme. In contrast, the activity of the W340 triple variant (W132F/W263F/W333F) was not detectable, indicating that while a single-site replacement at W340 is tolerated, combined substitutions at W132, W263 and W333 abolishes activity, precluding W340 from use as a solitary probe of conformational change in the linker region. In contrast to W333F, the stability of W340F is only slightly reduced. This suggests that the unstructured region of the linker is more tolerant of substitutions than helix α-15, which carries W333. Fluorescence resonance energy transfer is not observed from W340 to the PLP cofactor. These results are similar to those observed for solvent exposed tryptophans, W131 and W300 of the PLP-dependent enzyme *E.Coli* CBL (Jaworski *et al.,* 2013). The W340F substitution has no effect on the quenching constant in ytCBS, but the f_a value is decreased to 0.31, indicating that W333 is responsible for 31% of the overall quenching by iodide. In contrast, while the effect of W340F on stability is also negligible in the full-length enzyme, the quenching constant of yfCBS increased by 10-fold by substitution of W340. This may indicate that substitution of W340 with phenylalanine, in the full-length enzyme, results in a change in the local microenvironment of the linker that is sufficient to increase the exposure of the adjacent W333 to the iodide quencher.

4.6. Conclusions

Residue W263 is the major contributor of FRET to the PLP cofactor and provides a sensitive probe of conformational changes at the active site. Although residues W333 and W340 are both extensively solvent exposed in the absence (ytCBS) and presence (yfCBS) of the regulatory domain, subtle differences in their quenching by iodide, in the open and closed conformation, suggest that these residues may provide information about the relative positions of the catalytic and regulatory domains. This is in accordance with the crystal structure of dCBS which shows that residues W333 and W340 are located at the interface between the catalytic and regulatory domains and play a role in the proper interaction of the catalytic-regulatory domain in yfCBS (Koutmos *et al.,* 2010). The results of this study demonstrate that while substitutions of W132 and W340 with phenylalanine is tolerated, the triple W→F variants are not well suited to act as spectral probes for active-site conformation as the stability of the enzyme is affected by the combination of the three substitutions.

Chapter 5:

Investigation of the SAM-Binding Site of Yeast and Human Cystathionine β-Synthase *via* Mass Spectrometry

5.1. Abstract

The condensation of serine and homocysteine, catalyzed by the human cystathionine β-synthase (CBS; E.C. 4.2.1.22) enzyme, is increased 2-3-fold upon allosteric activation by *S*-Adenosyl-Methionine (SAM), which binds to the regulatory domain. In contrast, yeast CBS (yCBS) and Drosophila melanogaster CBS (dCBS) are not activated by SAM. Fluorescence spectroscopy and mass spectrometry were employed to investigate the interaction of SAM with full-length yeast and human CBS as well as with the isolated regulatory domains of both enzymes. Our results confirm that while the specific activity of hCBS is increased 2-fold in the presence of SAM, yCBS is not activated by SAM. The adenosine derivatives, methylthioadenosine (MTA), adenosine triphosphate (ATP) and adenosine monophosphate (AMP) have no effect on the activity of yCBS and hCBS. No changes in the fluorescence emission were observed upon titration of the soluble regulatory domain of yCBS with the four adenosyl compounds. The mass spectrometric analysis showed that the shift in mass peak *m/z 399*, characteristic of SAM presence, was not detected in the regulatory domain and full-length yCBS enzyme. These results show that, unlike hCBS, yCBS is not activated nor binds SAM. This indicates that yCBS is a highly active enzyme that is not regulated by SAM.

5.2. Introduction

The regulatory domain of cystathionine β-synthase contains a pair of conserved β_1-α_1-β_2-β_3-α_2 motifs, known as CBS domains. The CBS domain motif arose early as it is found in the proteins of archaebacteria, prokaryotes and eukaryotes (Bateman *et al.,* 1997). These domains commonly occur in pairs, as exemplified by chloride channels (ClC), inosine monophosphate dehydrogenase (IMPDH), adenosine monophoshate kinase (AMPK), the C-terminal domain of a *Methanococcus Janashii* protein of unknown function (MJ0100) and CBS. They are involved in regulation, *via* the binding of adenosine-containing ligands such as adenosine triphosphate (ATP), adenosine diphosphate (ADP), adenosine monophosphate (AMP), methylthioadenosine (MTA) and *S*-adenosylmethionine (SAM) (Figure 5.1) (Kery *et al.,* 1998; Maclean *et al.,* 2000; Kemp, 2004; Ignoul *et al.,* 2005; Lucas *et al.,* 2010; Koutmos *et al.,* 2010; Ereno-Orbea *et al.,* 2013). The role of these domains varies depending on the nature of the protein to which they are associated, and include oligomerization and regulation, *via* adenosine-derivative binding (Ignoul *et al.,* 2005, Ereno-Orbea *et al.,* 2013). Scott *et al.,* (2004) showed that IMPDH is activated by ATP binding to its pair of CBS sequences, thereby ensuring that guanine nucleotide synthesis only proceeds when sufficient ATP is available.

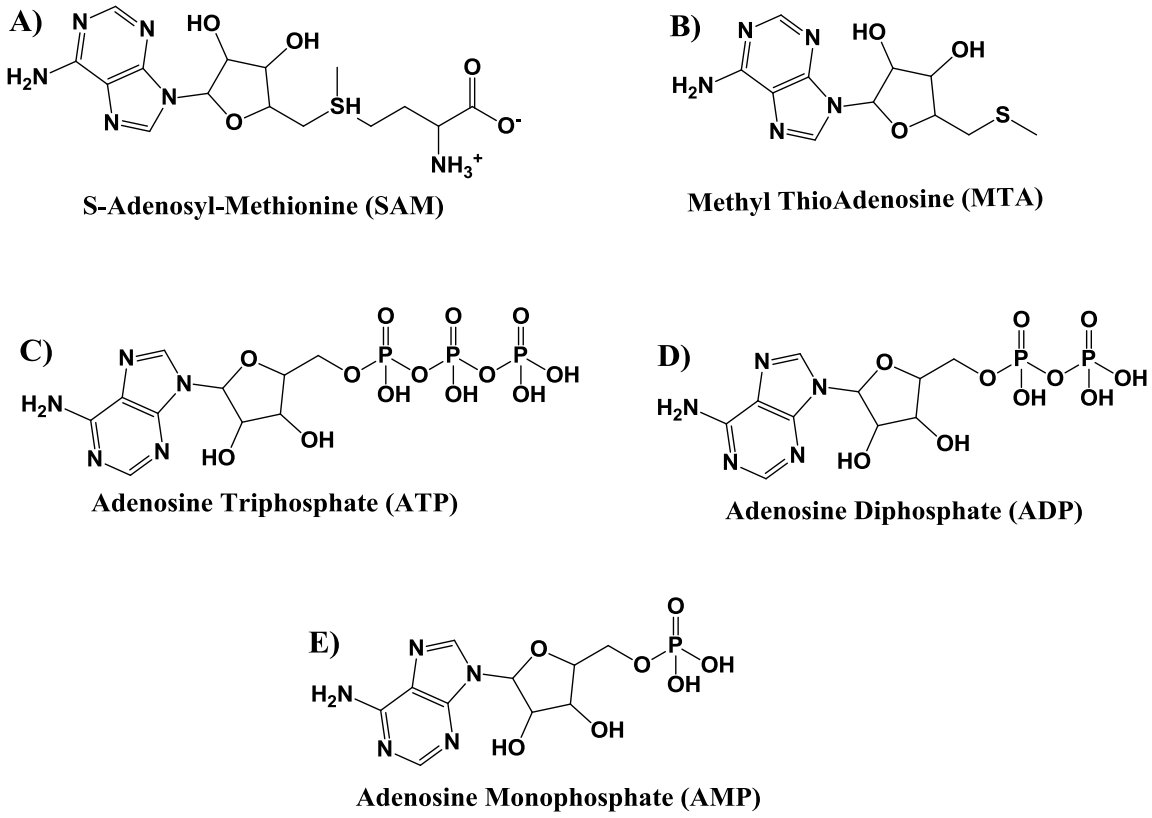

Figure 5.1: Chemical structures of A) *S*-adenosylmethionine (SAM), B) methylthioadenosine (MTA), C) adenosine triphosphate (ATP), D) adenosine diphosphate (ADP) and E) adenosine monophosphate (AMP). The CBS domains of a variety of prokaryotic and eukaryotic proteins bind these adenosine-containing ligands and play a role in protein regulation.

The structure of the modified full-length hCBSE201S enzyme (lacking loop 516-525 and containing the E201S substitution), in complex with SAM, confirms that the regulatory domain is the site of SAM binding, which results in allosteric activation (Ereno-Orbea *et al.,* 2014). Removal of the C-terminal domain generates an activated truncated form of CBS that is no longer activated by SAM, suggesting that the regulatory domain limits access to the active site in the absence of the allosteric regulator (Kery *et al.,* 1998). Although yeast CBS (yCBS) and drosophila CBS (dCBS) contain a C-terminal regulatory domain with a pair of conserved CBS domains, unlike hCBS, these enzymes are not activated by SAM (Maclean *et al.,* 2000; Su *et al.,* 2013). Removal of the regulatory domain of yCBS, results in a truncated enzyme form that is activated ~2-fold compared to the full-length enzyme.In contrast, full-length dCBS is fully activated and removal of its C-terminal domain has no effect on activity (Jhee *et al.,* 2000b; Su *et al.,* 2013). Su and colleagues also employed mass spectrometry to demonstrate that dCBS does not bind SAM (Su *et al.,* 2013). These observations bring into question the role of the regulatory domain in drosophila and yeast CBS, and whether an alternate adenosyl ligand may interact with these enzymes.

Comparison of the structures of the full-length human and drosophila enzymes, in the absence of SAM, shows that while their overall structures are similar, the relative orientation of the regulatory domain, with respect to the catalytic core, is strikingly different (Figure 4.1). The regulatory domains of the two dCBS subunits associate to form a disc structure (Bateman module), which interacts with the catalytic domain primarily through the linker, thereby allowing unrestricted flow of substrates to the active site (Koutmos *et al.,* 2010). In contrast to dCBS, the regulatory domains of hCBS do not

associate (Figure 4.1) (Ereno-Orbea *et al.,* 2013). In the absence of SAM, the regulatory domain blocks access to the entrance of the catalytic site of the adjacent monomer of hCBS (Ereño-Orbea *et al.,* 2013). Binding of SAM to the regulatory domain of hCBS induces a conformational change in the regulatory domain that favors the association of CBS domains, similar to dCBS, referred to as the activated form of the enzyme (Ereño-Orbea *et al.,* 2014).

The two CBS domains of each monomer are referred to as CBS1 and CBS2. The ligand-binding cleft of CBS1 cleft is less accessible to SAM than CBS2 due to steric hindrance (Ereño-Orbea *et al.,* 2013). The binding of SAM to the CBS2 site of the regulatory domain allows movement of the loops occluding the active site entrance and rearrangement of the regulatory domain to enable binding to the CBS1 site, thereby accommodating a second SAM molecule (Hnizda *et al.,* 2012; Ereño-Orbea *et al.,* 2013; Pey *et al.,* 2013). The mechanism of rearrangement/displacement of the regulatory domain was elucidated by the crystal structure of the SAM-bound hCBS, which revealed that the CBS domains rotate, relative to the catalytic core, to associate and form the disc structure observed for dCBS. Similar to dCBS, in the activated form of hCBS contact between the catalytic and regulatory domains is limited to the linker region (Ereño-Orbea *et al.,* 2014). Although the human, drosophila and yeast CBS enzymes all possess a C-terminal regulatory domain, only hCBS has been shown to bind and be activated by SAM (Ereno-Orbea *et al.,* 2014). The dCBS enzyme is not activated, nor does it bind to SAM (Su *et al.,* 2013). It was reported that yCBS is not activated by SAM, but the binding of SAM to the regulatory domain of yCBS has not been investigated (Jhee *et al.,* 2000). This brings into question the role of the CBS domain in drosophila and yeast CBS and the possibility that

these enzymes may be regulated by other adenosyl ligands, such as ATP, AMP or MTA. Therefore, we have investigated the interaction of adenosyl ligands with the regulatory domain of yeast CBS, employing the human enzyme as a control. TTruncated variants, lacking the regulatory domain, of both yeast and human CBS have been previously described (Kery *at al.* 1998; Jhee *et al.,* 2000). We report for the first time the expression of the yCBS regulatory domain, in the absence of the catalytic domain. Mass spectrometry and fluorescence spectroscopy were employed to probe the binding of SAM to the regulatory domains alone and in the full-length yeast and human CBS.

5.3. Materials and methods

5.3.1 Reagents

β-NADH (β-nicotinamide adenine dinucleotide, reduced form), L-Ser, L-Hcys thiolactone, L-lactate dehydrogenase (LDH), *S*-adenosylmethionine (SAM), adenosine triphosphate (ATP), adenosine monophosphate (AMP) and methylthioadenosine (MTA) were purchased from Sigma-Aldrich. Nickel-nitrilotriacetic acid (Ni-NTA) resin was from Qiagen.

5.3.2 Construction, expression and purification of hCBSΔ516-525 enzyme

A modified full-length hCBS lacking loop 516-525 (hCBSΔ516-525) from the CBS1 domain was constructed *via* overlap-extension PCR (Oyenarte *et al.,* 2012). This structure retains the regulatory domain and is activated by SAM. The identified 516-IQYHSTGKSS-525 loop was deleted by site-directed mutagenesis. The mutagenic primers were: forward (5'-GTGGTGCACGAGCAGCAGCGGCAGATGGTG-3') and reverse (5'- CACCATCTGCCGCTGCTGCTCGTGCACCAC-3'). The amplification products of the reassembly PCR amplification were digested (*Nde*I/*Sal*I) and inserted into the modified pTrc99a vector, which encodes an N-terminal, 6-His tag (Belew *et al.,* 2009). The mixture was transformed into *E. coli* ER1821 competent cells and the plasmid was sequenced in order to confirm the deletion. The hCBS construct was expressed and purified following the protocol described by Belew and coworkers (Belew *et al.,* 2009).

5.3.3. Mass Spectrometry.

In order to investigate SAM-binding, hCBS and yCBS regulatory domains and full-length enzymes were analyzed by mass spectrometry, in the absence and presence of SAM. Mass spectrometry is an analytical technique that can provide qualitative (structure) and quantitative (molecular weight) information on molecules/proteins after their conversion to ions (Ho *et al.,* 2003). Electrospray ionization mass spectrometry (ESI-MS) is a sensitive tool for studying large molecules and the addition of tandem mass spectrometry (ESI-MS/MS) allows rapid sample analysis and high sample throughput (Loo *et al.,* 2000). This soft ionization technique enables ionization of large molecules (such as proteins) without fragmenting them and hence can be useful for non-covalent binding complexes such as SAM-binding in CBS enzyme (Loo *et al.,* 2000; Ho *et al.,* 2003).

The purified hCBS and yCBS proteins (20 μM) were dialyzed overnight in 50 mM ammonium bicarbonate (pH 7.5) at 4˚C and then were concentrated using Amicon Ultra 3K 0.5 mL centrifugal filters. The SAM ligand was added to separate samples of yCBS and hCBS to a final concentration of 0.36 mM for an incubation time of 30 minutes. All samples were kept on ice. Mass spectra of 0.36 mM SAM, 20 μM hCBS and yCBS regulatory domains with and without 0.36 mM SAM were recorded. The same procedure was followed for full-length hCBS and yCBS in the absence and presence of SAM. Three microliters of the appropriate sample was loaded using a Proxeon nanoelectrospray emitter (Thermo Scientific, Odense, Denmark) followed by direct analysis of proteins using an AB Sciex QStar XL mass spectrometer equipped with a nanoESI source (AB Sciex, Framingham, MA, USA), which was externally calibrated prior to each experiment. Spectra were obtained using a nanoESI voltage of 1000 V, declustering and focusing

potentials of 30 and 120 V, respectively, and an MS/MS collision energy of 40 eV (Wasslen *et al.,* 2014). This work was performed in collaboration with Dr. Jeffrey Smith (Department of Chemistry, Carleton University).

5.3.4. Determination of Specific Activity.

Prior to mass spectrometry, the specific activity of full-length hCBS and yCBS enzymes were measured to determine the effect of SAM on CBS activity. The assay mixture contained 1.5 mM NADH, 0.5 μM CBL, 1.4 μM LDH, 7.5 mM L-Hcys and 25 mM L-Ser in 50 mM Tris buffer, 20 μM PLP, pH 8.6, and measurements were performed in the presence and absence of 0.36 mM of the adenosyl derivatives SAM, MTA, ATP and AMP. The yCBS and hCBS were incubated with the adenosyl derivatives for 5 minutes at 25˚C before measurements were recorded. The reactions were initiated by the addition of 0.017 mg/mL of wild-type yCBS or hCBS.

5.3.5. Fluorescence Spectroscopy.

To investigate the binding of SAM to the yeast CBS enzyme, the fluoresence emission spectrum of the PLP cofactor was recorded in the absence and presence of SAM, MTA, ATP and AMP, as described for threonine synthase from *Arabidopsis thaliana*, a fold-type II PLP-dependent enzyme that is also activated by SAM (Curien *et al.,* 1998). The change in the fluorescence properties of the PLP-bound cofactor in yfCBS, provides a tool to investigate the possibility of SAM-binding upon excitation at 410 nm (λ_{em} = 510 nm) (Curient *et al.,* 1998). Fluorescence spectra were acquired with a Cary Eclipse spectrofluorimeter (Varian) at 25°C. Fluorescence emission spectrum of 2

μM yfCBS in 20 mM phosphate buffer, pH 7.5, was measured upon excitation at 410 nm in the absence or the presence of 200 μM SAM. The emission spectrum was recorded from 420–560 nm with excitation and emission slit widths of 5 nm.

The regulatory domain of yCBS contains 9 phenyalanine and 4 tyrosine residues that might serve as useful probes for conformational change upon SAM binding. The regulatory domain of hCBS also contains aromatic residues and lacks the heme cofactor, when expressed in the absence of the catalytic domain. Therefore, the fluorescence spectrum of the aromatic residues was also employed to investigate SAM binding. Fluorescence emission spectra of yCBS and hCBS regulatory domains (λ_{ex} = 280nm) were recorded in the absence and presence of 200 μM SAM. The emission spectrum was recorded from 420–560 nm with excitation and emission slit widths of 5 nm.

5.4. Results

The hCBSΔ516-525 variant, as the full-length enzyme, is activated approximately 2 fold by SAM, while no change in specific activity was observed for yfCBS in the presence of SAM (Table 5.1). No increase in specific activity was observed for full-length yCBS or hCBS in the presence of MTA, ATP or AMP. Similarly, no change in the fluorescence emission at 510 nm (λ_{ex} = 410 nm) was observed for full-length yeast CBS upon addition of SAM or the other adenosyl-derivatives. In addition, no shift in the fluorescence emission spectrum of the yCBS regulatory domain was observed when excited at 280 nm in the presence of the adenosyl ligands. These results suggest that yCBS is not stimulated in the presence of SAM or other adenosyl derivatives. The regulatory domain of hCBS is red shifted, from 341 nm to 345 nm, upon addition of SAM suggesting that SAM binds to the regulatory domain of hCBS. In contrast, no change in the fluorescence spectrum of yCBS regulatory domain was detected suggesting that no conformational change is observed when yCBS is treated with SAM (Figure 5.2). Furthermore, no change in the PLP fluorescence properties was observed when yCBS was incubated with SAM or adenosyl derivatives.

Samples of the regulatory domains and full-length yeast and human CBS enzymes, in the presence and absence of SAM, were analyzed by mass spectrometry. The *m/z* 399 peak, characteristic of SAM, was not observed in spectra of yCBS regulatory domain, regardless of the presence of SAM, suggesting that the regulatory domain of yCBS does not bind SAM (Figure 5.4). Mass spectra of hCBS regulatory domain were recorded and the mass was determined to be 18398 Da, but no data could be registered when samples were treated with SAM, suggesting that the presence of SAM alters the conformation,

oligomeric status or stability of the free regulatory domains of the human enzyme (Figure 5.6). While the full-length yeast enzyme was visible in the absence (56954 Da) and presence (56976) of SAM, the 22 mass unit difference in the molecular weight confirms that yCBS does not bind SAM (Figure 5.5). However, low affinity binding might be a possibility. The hCBS enzyme could not be observed by mass spectrometry due to the tendency of the full-length enzyme to aggregate. Therefore, the hCBSΔ516-525 variant, which lacks residues 516-525 and displays reduced aggregation, was employed (Ereño-Orbea *et al.,* 2013). A full-length human CBS enzyme lacking amino acids residues 516-525, which belongs to an unordered loop in hCBS, was crystallized by Oyenarte *et al.,* (2012). This construct was reported to have an optimized expression and hence a better yield. The protein yield of the hCBSΔ516-525 variant is 5.2 mg/L, compared with 1.8 mg/L for the wild-type enzyme. The mass spectrum of the Δ516-525 variant enzyme shows the *m/z* 616, characteristic of heme, as well as the expected protein mass of 62596 Da (Figure 5.6). However, the spectra of hCBSΔ516-525 variant could not be observed in the presence of SAM. This result is consistent with that observed for the hCBS regulatory domain and likely reflects the observed conformational change reported for hCBS upon SAM binding (Ereno-Orbea *et al.,* 2014). The use of isothermal titration calorimetry (ITC) might provide a more sensitive measurement for SAM-binding in yCBS. The thermodynamics parameters for SAM-binding in hCBS were determined by Pey and colleagues and a binding affinity K_d of 5 ηM was reported (Pey *et al.,* 2013).

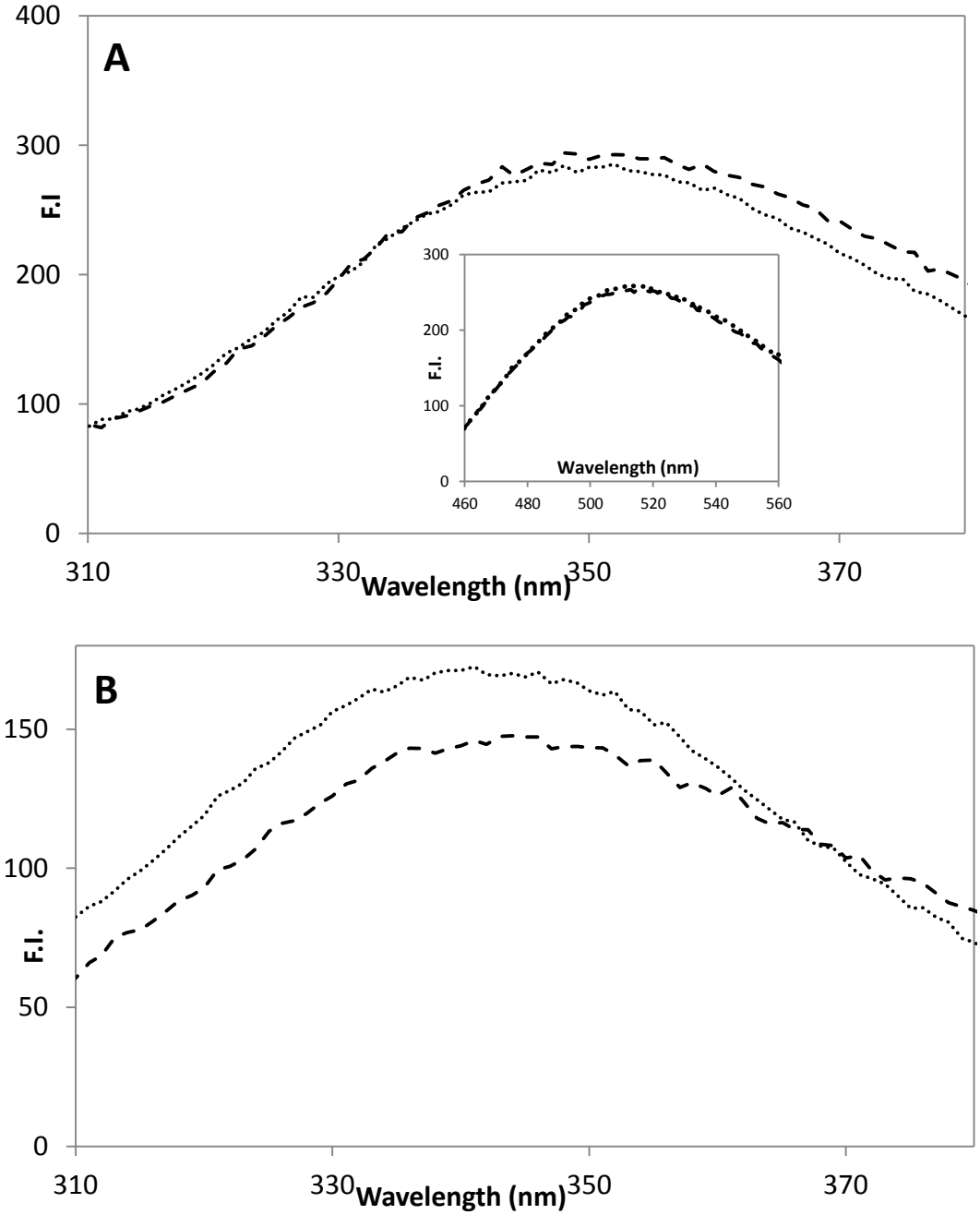

Figure 5.2: Fluorescence emission spectrum of the regulatory domains of A) yCBS and B) hCBS, in the absence (dotted lines) and presence (dashed lines) of SAM. The soluble regulatory domains (2 μM) were diluted in 20 mM phosphate buffer, pH 7.5 and measurements were recorded at 25˚C (λ_{ex} = 295 nm, λ_{em} = 310 - 550 nm and the excitation and emission slit widths were 5 nm, slow scan). 5 μL of 200 μM SAM was added to the solutions in a final volume of 200 μL.

Table 5.1: Specific activities of yCBS and hCBSΔ516-525 in the presence or absence of 0.36 mM SAM, MTA, ATP and AMP

Specific activity (units/mg) of protein[a]								
	SAM		**MTA**		**ATP**		**AMP**	
	--	+	**--**	+	**--**	+	**--**	+
dCBS[b]	1227 ± 94	1279 ± 33	-	-	-	-	-	-
hCBS	47 ± 4	116 ± 4	-	-	-	-	-	-
hCBSΔ516-525	125 ± 7	255 ± 9	110 ± 6	123 ± 2	108 ± 4	119 ± 16	124 ± 4	137 ± 9
yfCBS	489 ± 16	539 ± 6	678 ± 16	695 ± 8	629 ± 12	676 ± 3	706 ± 7	713 ± 22

[a]One unit of activity is defined as the formation of 1 μmol of product/minute. The assay mixture contained 1.5 mM NADH, 0.5 μM CBL, 1.4 μM LDH, 7.5 mM L-Hcys and 25 mM L-Ser in 50 mM Tris buffer, 20 μM PLP, pH 8.6 and -/+ 0.36 mM of SAM, MTA, ATP and AMP. The mixture of CBS and the corresponding adenosyl derivative were preincubated for 5 minutes at 25˚C. The reaction were initiated with 0.017 mg/mL CBS enzyme at 25˚C (n = 3).
[b]Specific activity of drosophila CBS for the formation of 1 μmol of product/hour, -/+ 0.36 mM SAM at 37˚C (Su *et al.,* 2013).

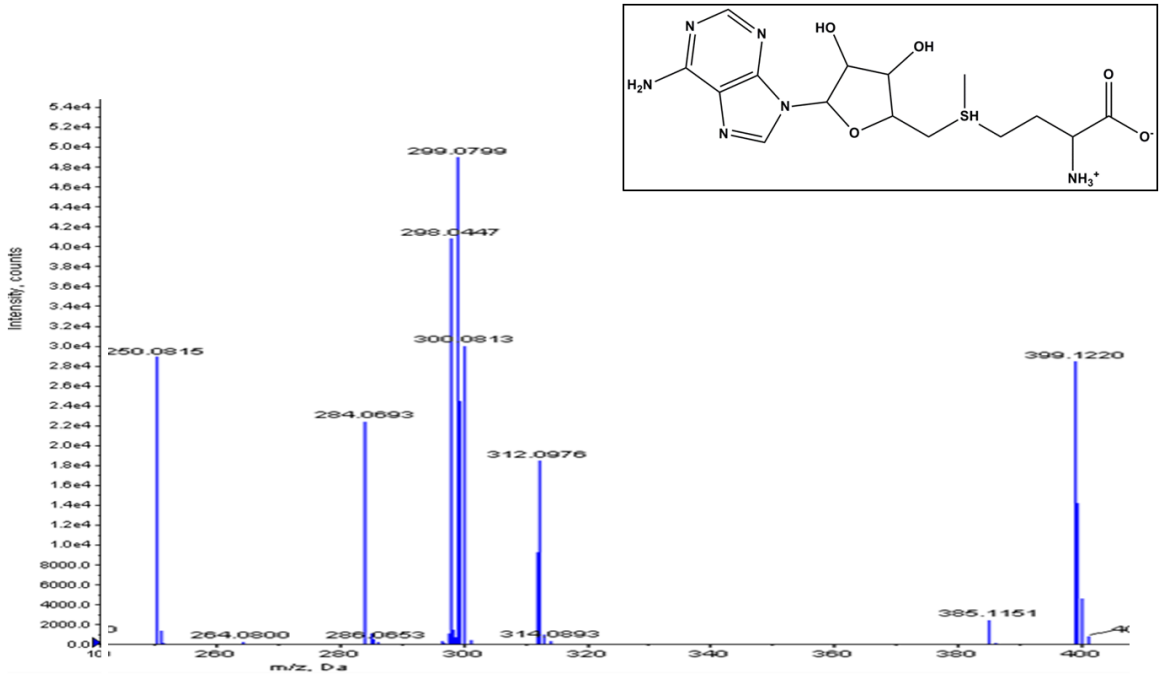

Figure 5.3: Mass Spectra of 1mM SAM. The peaks at *m/z* = 399.13 Da and *m/z* = 298.08 Da correspond to SAM and MTA, respectively. The peak at *m/z* = 250.07 Da is a fragmentation of SAM involving the loss of methionine group.

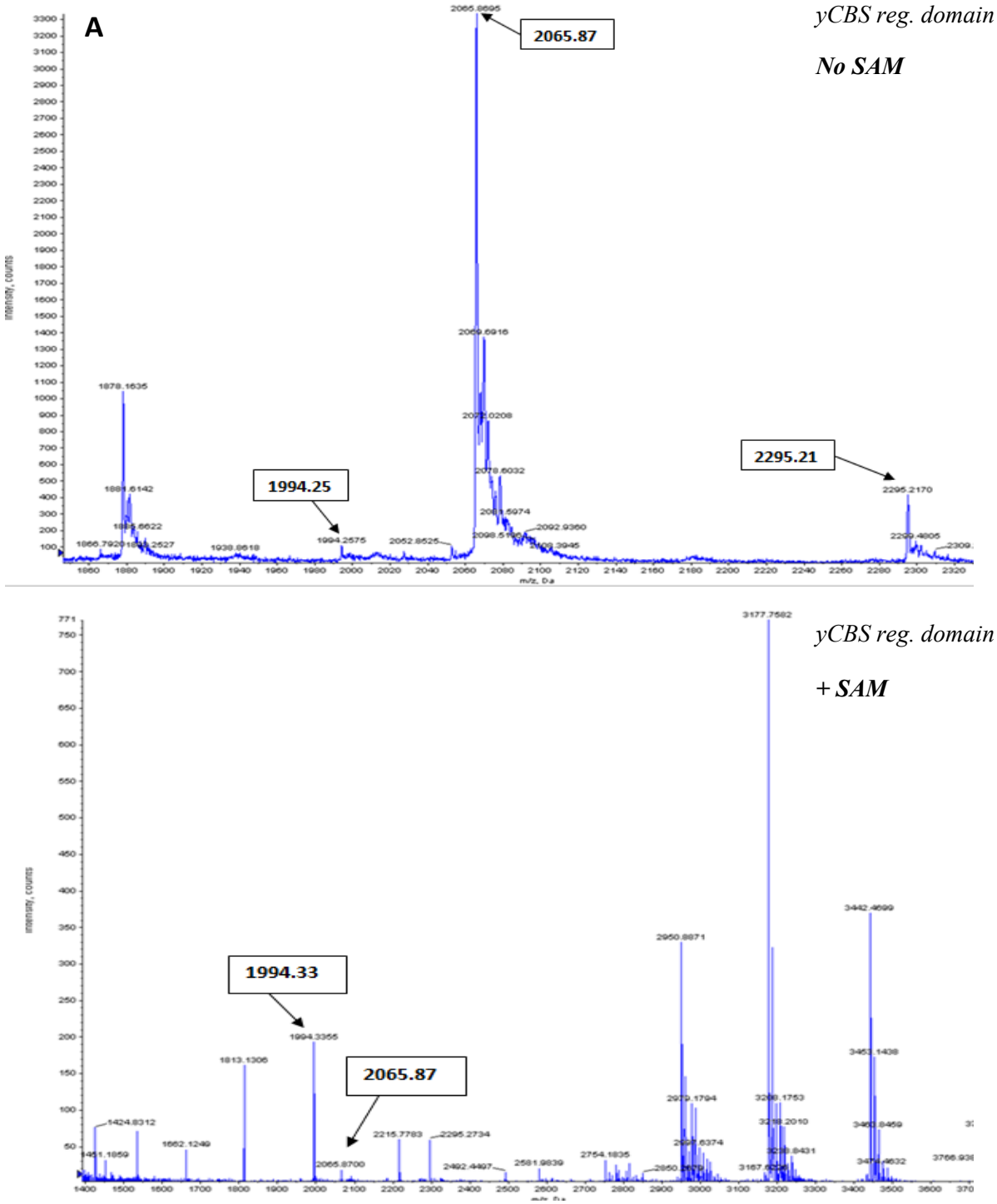

Figure 5.4: Mass spectra of the yCBS regulatory domain in the (A) absence and (B) presence of 0.36 mM SAM. Multiple charge states were used to determine the experimental mass of each protein sample: (A) 19933.68 Da and (B) 19933.49 Da.

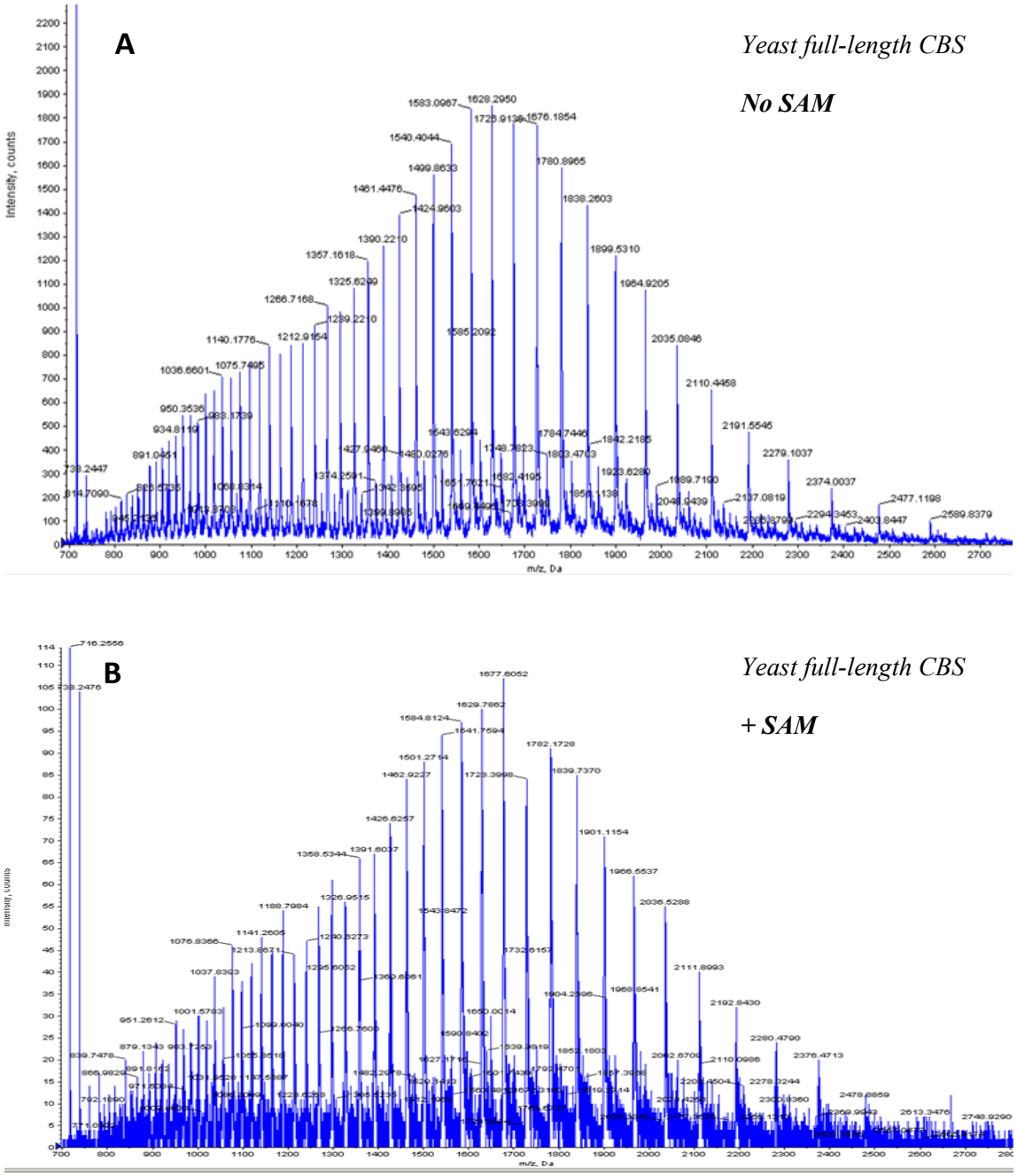

Figure 5.5: Mass spectra of full-length yeast CBS in the (A) absence and (B) presence of 0.36 mM SAM. Multiple charge states were used to determine the experimental mass of each protein sample: (A) 56954.19 Da, (B) 56976.21 Da.

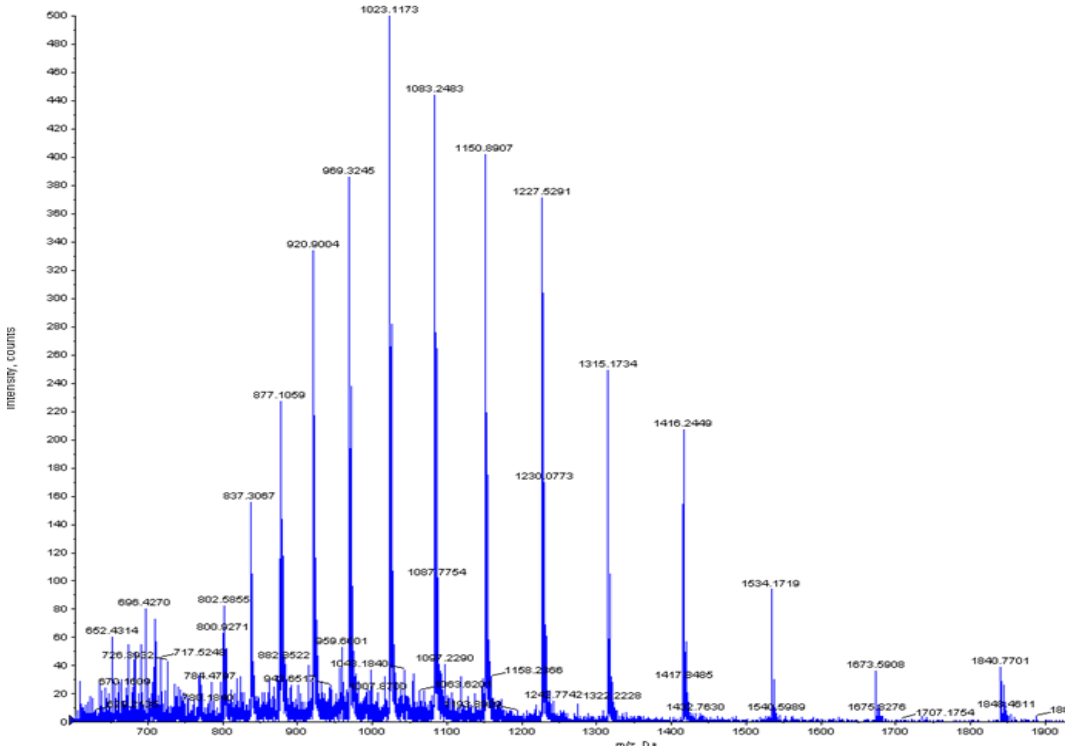

Figure 5.6: Mass spectrum of the hCBS regulatory domain. The calculated average mass of the hCBS-regulatory domain was determined to be 18398.03 Da and the expected mass was 18398.37 Da.

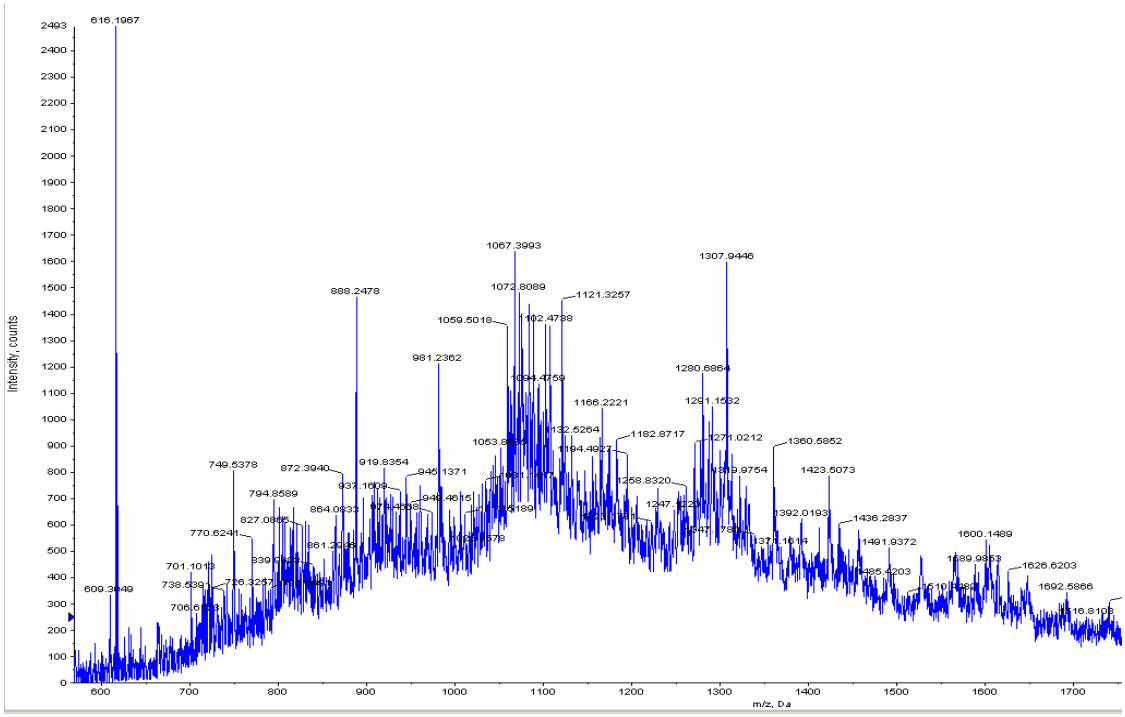

Figure 5.7: Mass spectrum of hCBSΔ516-525. The calculated average mass of the enzyme was determined to be 62596.21 Da and the expected mass was 61412.40 Da. The characteristic heme peak is shown at *m/z* = 616.2 Da.

Table 5.2: Observed and expected molecular weights of the CBS constructs, employed in the MS/MS study, calculated using manual spectral deconvolution[a].

	No SAM	**+ SAM**	**Expected M.W.**
Full-length hCBS	n.d.	n.d.	62501.57 Da
Full-length yCBS	56954.19 Da	56976.21 Da	56844.70 Da
yCBS regulatory domain	19933.68 Da	19933.49 Da	19933.42 Da
hCBS regulatory domain	18398.03 Da	n.d.	18398.37 Da
hCBSΔ516-525	62596.21 Da	n.d.	61412.40 Da

[a]The molecular mass (M) of neutral protein was calculated by determining charged state for several peaks using the equation $M = n \times (M_n - 1.008)$; M_n is the mass/charge, while n is the charge of the corresponding peak (Trauger *et al.,* 2002). Spectra were obtained using a nano ESI voltage of 1000 V, declustering and focusing potentials of 30 and 120 V, respectively, and a MS/MS collision energy of 40 eV (Wasslen *et al.,* 2014).
n.d. indicates that the spectra of these constructs was not detectable via mass spectrometry.

5.5. Discussion

Cystathionine β–Synthase (CBS) domains are conserved structural domains found in a variety of proteins from bacteria to human (Bateman *et al.,* 1997). The physiological importance of these domain have been emphasized by the observation that point mutations in CBS domains lead to perturbance of the protein function, such as homocystinuria disease in hCBS, retinal dystrophy in IMPDH and Wolff-Parkinson-White syndrome in AMPK (Shan *et al.,* 2001; Arad *et al.,* 2002; Kennan *et al.,* 2002). These CBS domains are usually involved in oligomerization and ligand binding (Ignoul *et al.,* 2005).

Although human, drosophila and yeast CBS all contain a C-terminal regulatory domain, the role of this domain in enzyme regulation likely differs between these species. The regulatory domain of hCBS contains the binding site for *S*-adenosyl-methionine, which is reported to increase enzyme activity 2-4-fold (Ereno-Orbea *et al.,* 2014). In contrast, yeast and drosophila CBS catalyze the same reaction as hCBS but are not activated by SAM (Jhee *et al.,* 2000; Koutmos *et al.,* 2010). This study explored the role of the regulatory domain of yCBS by investigating the binding of SAM, via mass spectrometry, and the binding of SAM, MTA, ATP and AMP via fluorescence spectroscopy. The human CBS enzyme, which binds and is activated by SAM (Ereno-Orbea *et al.,* 2014) was employed as a control.

A 2-fold activation of hCBS was observed in the presence of SAM, while no change in the specific activity was observed for yfCBS (Table 5.1). This is in accordance with previously reported results that yCBS is not activated by SAM, while hCBS exhibit 2 to 3-fold increase in activity (Ereno-Orbea *et al.,* 2014; Jhee *et al.,* 2000). Similar to yCBS,

dCBS is also reportedly not activated by SAM, at concentration as high as 5 mM (Su *et al.,* 2013). Su and coworkers employed mass spectrometry to demonstrate that dCBS also does not bind SAM (Su *et al.,* 2013).

The interaction of SAM to the regulatory domain of yCBS, expressed alone or with the catalytic domain, was assessed via mass spectrometry and fluorescence spectroscopy and binding was not observed using either technique. Interestingly, SAM-binding to dCBS was also tested using mass spectrometry by Su *et al.,* (2013) and no mass peaks corresponding to SAM (*m/z* 399), similarly suggesting that dCBS does not bind SAM. Full-length hCBS has a tendency to aggregate and could not be observed via mass spectrometry, but a mass spectrum of the modified hCBSΔ516-525 enzyme, was recorded and displayed the heme characteristic peak of *m/z* 616. This is the first mass spectrum reported for the human CBS enzyme. Incubation with SAM likely results in a conformational change that may predispose hCBS to aggregation because, as for the full-length enzyme in the absence of SAM, the hCBSΔ516-525 complex with SAM could not be recorded.

The results of this study suggest that, like dCBS, the yeast enzyme does not bind SAM (Su *et al.,* 2013). There are several reasons why CBS enzymes, other than hCBS, may not be activated by SAM. For example, dCBS appears to be locked in a constitutively active conformation (Koutmos *et al.,* 2010; Ereno-Orbea *et al.,* 2014). The C413S and S466L homocystinuria-associated variants are also not responsive to SAM and the latter is constitutively activated (Frank *et al.,* 2006; Janosik *et al.,* 2001). Docking studies of SAM to the regulatory domain of dCBS showed that there is not sufficient space to accommodate the SAM molecule (Koutmos *et al.,* 2010). However, in contrast with dCBS, the yeast enzyme is activated approximately 2-fold by removal of the regulatory domain. This

suggests the possibility that this domain is functional, as for hCBS, but may respond to an alternate ligand. A recent study by Majitan and colleagues demonstrated, using ITC, that SAM binds to the yCBS regulatory domain (Majitan *et al.,* 2014). However, the binding constant K_d of 5 μM is significantly lower (3 orders of magnitude) than SAM-binding in hCBS (K_d = 5 ηM). Furthermore, no effect on stability or activity was observed when yCBS was treated with SAM. Using differential scanning calorimetry (DSC), these authors observed that the thermal stability of yfCBS is unchanged by the presence of SAM and resembles the thermal denaturation of the truncated ytCBS enzyme (Majitan *et al.,* 2014). In contrast, SAM binding to the hCBS enzyme stabilizes the thermal transition in the presence of SAM.

The binding cavity of the CBS domains contains a conserved ribose-phosphate binding motifs (G-h-x-T/S-x-T/S-D) and substitution of the conserved aspartate/asparagine might impair nucleotide binding (Amodeo *et al.,* 2007). The residue preceding the last aspartate contributes significantly in determining the type of adenosine derivatives that could occupy the binding pocket. This is exemplified by the MJ0100 protein, which binds SAM and MTA (Lucas *et al.,* 2010). Both hCBS and MJ0100 bind SAM and contain an isoleucine and a glutamate preceding the conserved aspartate residue, in the ribose-binding motifs. In the case of yCBS, the conserved aspartate is replaced by a glutamate and the preceding residue is a serine. This sequence is similar to that of proteins able to bind adenosine mono-phosphate AMP, such as AMPK from *S.cervisiae* (Mayer *et al.,* 2011). This suggests that yCBS might be able to bind a different adenosyl ligand than SAM. However, the specific activity and the fluorescence spectrum of yfCBS were unaltered by the presence of the adenosine derivatives SAM, MTA, ATP and AMP. Future studies may

explore the ligand binding motifs of yCBS via site-directed mutagenesis to determine whether substitution with the corresponding residues of hCBS results in activation.

5.6. Conclusions

The results of this study show that, unlike hCBS, the regulatory domain of yCBS does not bind SAM. Mass spectrometry and fluorescence analysis of regulatory domain and yeast full-length enzyme showed that SAM-binding does not occur in yCBS, but low affinity binding might occur. In contrast, the emission maximum of the aromatic residues of the hCBS regulatory domain was red-shifted in the presence of SAM. These results are similar to the mass spectrometry analysis of dCBS, which demonstrated that SAM-binding does not occur in the regulatory domain of dCBS. Human CBS and the modified hCBSΔ516-525 are both activated 2-fold by SAM, while yCBS was not stimulated in the presence of SAM or other adenosines derivatives such as MTA, ATP and AMP. The role of the regulatory domain of the yeast enzyme is still under investigation.

6. CONCLUSIONS

Cysthationine β-Synthase (CBS) is a pyridoxal 5'-phosphate (PLP)-dependent enzyme that catalyzes the condensation of serine and homocysteine to form cysthathionine. Deficiency in CBS activity is the leading cause for homocystinuria, an inherited autosomal recessive disease in humans. More than 150 homocystinuria-associated mutations have been reported and these point mutations are distributed in the active site, dimer interface, heme-binding site and the regulatory domain of CBS.

A series of site-directed variants were characterized to investigate homocystinuria-associated mutations in the active site of the model yeast CBS (yCBS) enzyme that lacks the heme cofactor. Residue K112 is part of a hydrogen bonding network (K112-E111-K327-E244-T326) that bridges the opposing sides of the active site cleft and connects the loops that form much of its surface. Residues E111 and K327 are sites for homocystinuria-associated mutations (E176K and K384 of hCBS) and their effect is transferred to the cofactor and substrate-binding residues via K112 and E244. Residues E244 is also adjacent to residues G245-I246-G247 in the CBS active sitenear the PLP cofactor. Residues G245 and G247 are also sites for homocystinuria-associated mutations (G305R and G307S-hCBS). The decrease in the k_{catF} and the increase in $K_m^{L\text{-}Ser}$ for all the K112 network variants suggest a role for these residues as a determinant of active site architecture and dynamics. The decrease in stability observed for the E111K (E176K-hCBS) exemplifies the amino acid substitutions that impact folding and stability, which will result in increased protein degradation and reduced active and soluble enzyme *in vivo*. Residues G245, I246 and G247 are adjacent to the cofactor and play a role in maintaining the cofactor in a catalytically productive orientation. The work described in

chapter 3 sheds more light on the mechanism of several homocystinuria-associated mutations in the active site of CBS and might potentially aid to refine supplementation/diet treatments. The G305-hCBS (G245R-ytCBS) likely affects cofactor binding. This is exemplified by the aggregration and insolubility of the G245R-ytCBS variant. Furthermore, the G245L variant showed a 16-fold increase in K_m of L-Ser suggesting that access of serine substrate to the active site is blocked by the substitution of glycine to bulkier leucine or arginine residues. Patients carrying the G305R mutation are responsive to vitamin B_6 doses. However, since L-Ser binding is impaired, supplementation with B_6, would likely be accompanied by administration of folic acid and vitamin B_{12}. This would decrease the buildup of accumulated homocysteine by increasing the flux through the remethyation pathway.

The potential of the four tryptophan residues of yCBS as probes of conformational change and domain interactions was explored in chapter 4. Single and triple phenylalanine-substitution variants of the four tryptophan residues (W132, W263, W333 and W340) of yCBS were characterized in the truncated and full-length enzyme forms. Residues W132 and W263 are located in the active site, while W333 and W340 are located in the linker region and are useful probes to understand the interaction between the catalytic and regulatory domain. The effect of W132F and W340F on stability was minimal, while the W263F and W333 substitutions reduce the stability of yCBS. Residue W263 is the main contributor for FRET to the PLP cofactor, thereby providing a sensitive probe of active site conformation. The significant increase in the quenching constant of W333F and W340F-yfCBS implies that substitution of these residues causes a change in the microenvironment of the linker region. Residues W333

and W340 could be useful probes to investigate conformational changes associated with the regulatory domain and of the oligomeric status of yCBS, since the crystal structure of full-length yCBS enzyme has not been solved yet. The possibility of ligand-binding to the regulatory domain and potential conformational change in the yCBS enzyme was tested in chapter 5.

The regulatory domain of hCBS contains a tandem pair of CBS motifs that bind *S*-adenosylmethionine (SAM) and lead to enzyme activation. In contrast, drosophila dCBS and yeast yCBS are not activated by SAM. The results of this study using mass spectrometry show that the regulatory domain of yCBS does not bind SAM. In addition, mass spectrometric analysis shows that SAM-binding does not occur in full-length (yfCBS) enzyme and no change in specific activity is observed for yfCBS in the presence of SAM, MTA, ATP and AMP. This is similar to the mass spectrometry analysis of dCBS, which demonstrated that SAM-binding does not occur in the regulatory domain of dCBS. A recent study using ITC showed that yCBS have a low affinity binding for SAM, but no effect on activity, stability or conformational changes was observed. In conclusion, the role of the regulatory domain in yCBS remains unclear and awaits further studies.

7. REFERENCES.

Aitken S.M., and Kirsch J.F. Kinetics of the yeast cystathionine beta-synthase forward and reverse reactions: Continuous assays and the equilibrium constant for the reaction. *Biochemistry.* **42**, 571-578 (2003).

Aitken, S. M., and Kirsch, J. F. The enzymology of cystathionine biosynthesis: Strategies for the control of substrate and reaction specificity. *Arch. Biochem. Biophys.* **433**, 166-175 (2005).

Aitken, S. M., and Kirsch, J. F. Role of Active-Site Residues Thr81, Ser82, Thr85, Gln157, and Tyr158 in Yeast Cystathionine β-Synthase Catalysis and Reaction Specificity. *Biochemistry*. **43**, 1963–1971 (2004).

Amodeo G.A., Rudolph M.J., Tong L. Crystal structure of the heterotrimer core of *Saccharomyces cerevisiae* AMPK homologue SNF1. *Nat. Genet.* **449**, 492–495 (2007).

Arad M, Benson D.W., Perez-Atayde A.R., McKenna W.J., Sparks E.A., Kanter R.J., McGarry K., Seidman J.G., and Seidman C.E. Constitutively active AMP kinase mutations cause glycogen storage disease mimicking hypertrophic cardiomyopathy. *J. Clin. Invest.* **109**, 357–362 (2002).

Aral B., Coudé M., London J., Aupetit J., Chassé J-F, Zabot M-T, Chadefaux-Vekemans B., Kamoun P. Two novel mutations (K384E and L539S) in the C-terminal moiety of the cystathionine b-synthase protein in two French pyridoxine-responsive homocystinuria patients. *Hum. Mutat.* **9**, 81–82 (1997).

Bateman A. The structure of a domain common to archaebacteria and the homocystinuria disease protein. *Trends Biochem. Sci.* **22**, 12-13 (1997).

Belew M.S., Quazi F.I., Willmore W.G., and Aitken S.M. Kinetic characterization of recombinant human cystathionine beta-synthase. *Protein expression and purification.* **64**, 139-145 (2009).

Bella D.L., Hirschberger L.L., Kwon Y.H., Stipanuk M.H. Cysteine metabolism in periportal and perivenous hepatocytes: perivenous cells have greater capacity for glutathione production and taurine synthesis but not for cysteine catabolism. *Amino Acids.* **23**,454–58 (2002).

Berg J., Tymoczko J., and Stryer L. *Biochemistry,* 5th ed. New York:W. H. Freeman (2001).

Bettati, S., Campanini, B., Vaccari, S., Mozzarelli, A., Schianchi, G., Hazlett, T. L., Gratton, E., and Benci, S. Unfolding of pyridoxal 5'-phosphate-dependent O-acetylserine sulfhydrylase probed by time-resolved tryptophan fluorescence. *Biochim. Biophys. Acta* **1596,** 47–54 (2002).

Blackstone E., Morrison M., Roth M.B. H_2S induces a suspended animation-like state in mice. *Science.* **308**, (5721):518 (2005).

Burkhard P., Tai C.-H., Ristroph C.M., Cook P.F. and Jansonius J.N. Ligand binding induces a large conformational change in O-acetylserine sulfhydrylase from *Salmonella typhimurium. J. Mol. Biol.* **291,** 941–953 (1999).

Burkhard P., Rao G.S.J., Hohenester E., Schanckers K.D., Cook P.F. and Jansonius J.N. Three dimensional structure of O-acetylserine sulfhydrylase from *Salmonella typhimurium. J. Mol. Biol.* **283,** 121–133 (1998).

Butz L., and du Vigneaud V. The formation of a homologue of cystine by the decomposition of methionine with sulfuric acid. *J. Biol. Chem*. **99**, 135–42 (1932).

Campanini B., Raboni S., Vaccari S., Zhang L., Cook P.F., Hazlett T.L., Mozzarelli A., and Bettati S. Surface-exposed tryptophan residues are essential for O-acetylserine sulfhydrylase structure, function, and stability. *J. Biol. Chem.* **278**, 37511-37519 (2003).

Caudill M.A., Wang J.C., Melnyk S., Pogribny I.P., Jernigan S., Collins M.D., Santos-Guzman J., Swendseid M.E., Cogger E.A. and James S.J. Intracellular S-Adenosylhomocysteine Concentrations Predict Global DNA. Hypomethylation in Tissues of Methyl-Deficient Cystathionine β-Synthase Heterozygous Mice. *J. Nutr.* **131,** 2811–2818 (2001).

Cherney, M.M., Pazicni, S., Frank, N., Marvin, K.A., Kraus, J.P., and Burstyn, J.N. Ferrous human cystathionine β-synthase loses activity during enzyme assay due to a ligand switch process. *Biochemistry.* **46**, 13199-13210 (2007).

Curien G., Job D., Douce R., and Dumas R. Allosteric activation of arabidopsis threonine synthase by S-adenosylmethionine. *Biochemistry* **37**, 13212-13221 (1998).

D'Angelo A., and Selhub J. Homocysteine and thrombotic diseases. *The American Society of Hematology*. **90,** 1–11 (1997).

Dunathan H.C. Conformation and reaction specifity in pyridoxal phosphate enzymes. *Proc. Natl. Acad. Sci USA* **55,** 712–716 (1966).

Denninger J. W., and Marletta M. A. Guanylate cyclase and the NO/cGMP signaling pathway, *Biochim. Biophys. Acta: Bioenergetics.* **1411**, 334-350 (1999).

Eftnik M.R. and Ghiron C.A. Fluroescence quenching studies with proteins. *Anal. Biochem.* **114**, 199-227 (1981).

Elliot A.C., and Kirsch J.F. Pyridoxal phosphate enzyme: Mechanistic, structural, and evolutionary considerations. *Annu. Rev. Biochem.* **73**, 383–415 (2004).

Ereño-Orbea J., Majtan T., Oyenarte I., Kraus J.P., and Martínez-Cruz L.A. Structural basis of regulation and oligomerization of human cystathionine β-synthase, the central enzyme of transsulfuration. *Proc. Natl. Acad. Sci* **40**, E3790-3799 (2013).

Ereño-Orbea J., Majtan T., Oyenarte I., Kraus J.P, and Martínez-Cruz L.A. Structural insight into the molecular mechanism of allosteric activation of human cystathionine β-synthase by SAM. *Proc. Natl. Acad. Sci* **40**, E3845-3852 (2014).

Finkelstein J. D., Kyle W. E., Martin J. J., and Pick A.-M. Activation of cystathionine synthase by adenosylmethionine and adenosylethionine. *Biochem. Biophys. Res. Commun*. **66**, 81−87 (1975).

Frank N., Kery V., Maclean K. N., and Kraus J. P. Solvent-Accessible Cysteines in Human Cystathionine β-Synthase: Crucial Role of Cysteine 431 in S-Adenosyl-L-methionine Binding. *Biochemistry* **45**, 11021−11029 (2006).

Gallagher P.M., Ward P., Tan S., Naughten E., Kraus J.P., Sellar G.C., McConnell D.J., Graham I., and Whitehead A.S.. High frequency (71%) of cystathionine b-synthase mutation G307S in Irish homocystinuria patients. *Hum. Mutat.* **6**, 177–180 (1995).

Gaustadnes M., Ingerslev J., and Rutiger N. Prevalence of congenital homocystinuria in Denmark. *New England Journal of Medicine* **340**(19): 1513 (1999).

Ge Y., Konrad M.A., Matherly L.H., and Taub J.W. Transcriptional regulationof the human CBS -1b basal promoter: synergetic transactivation by transcription factors NF-Y and sp1/sp3. *Biochem. J.* **357**, 97–105 (2001).

Gilles-Gonzalez, M. A., Gonzalez, G., Perutz, M. F., Kiger, L., Marden, M. C., and Poyart, C. Heme-based sensors, exemplified by the kinase FixL, are a new class of heme protein with distinctive ligand binding and autoxidation, *Biochemistry*. **33**, 8067-8073 (1994).

Giovanelli J., Veluthambi K., Thompson G.A., Mudd S.H., and Datko A.H. *Plant Physiology.* **76,** 285–292 (1984).

Grompe M. The pathophysiology and treatment of hereditary tyrosinemia type 1. *Semin. Liver Dis.* **4**, 563-71 (2001).

Gupta S., Wang L., Anderl J., Slifker M.J., Kirk C., and Kruger W.D. Correction of cystathionine β-synthase deficiency in mice by treatment with proteasome inhibitors. *Hum. Mutat*. **34**,1085–1093 (2013).

Hayashi H. Pyridoxal enzymes: Mechanistic diversity and uniformity. *J. Biochem.* **118**, 463–473 (1995).

Higuchi R. Recombinant PCR. In: Innis MA, Gelfand DH, Sninsky JJ and White TJ (eds) PCR Protocols—A Guide to Methods and Applications, San Diego: *Academic Press*. pp. 177–183 (1990).

Hnizda A., Majitan T., Liu L., Pey A.L., Carpenter J.F., Kodicek M. Kozich V., and Kraus J.P. Conformational Properties of Nine Purified Cystathionine β-Synthase Mutants. *Biochemistry.* **51**, 4755-4763 (2012a).

Hnizda A., Spiwok V., Jurga V., Kozich V., Kodicek M., and Kraus J.P. Cross-talk between the catalytic core and the regulatory domain in cystathionine β-synthase: Study by differential covalent labeling and computational modeling. *Biochemistry.* **49**, 10526-10534 (2010).

Hnizda A., Jurga V., Raková K. and Kozich, V. Cystathionine beta-synthase mutants exhibit changes in protein unfolding: conformational analysis of misfolded variants in crude cell extracts. *J. Inherit. Metab. Dis.* **35**, 1-9 (2012b).

Hoffman G.F., Zschocke J., and Nyhan W.L. *Inherited metabolic diseases: A clinical approach.* Springer N.Y. (2010).

Ho C.S., Lam C.W.K., Chan M.H.M., and Tai H.L. Electrospray ionization mass spectrometry: Principles and clinical applications. *Clin. Biochem. Rev.* **24**, 3-12 (2003).

Ichinohe A., Kanaumi T., Takashima S., Enokido Y., Nagai Y., and Kimura H. Cystathionine beta-synthase is enriched in the brains of down's patients. *Biochem. Biophys. Reasearch. Comm.* **338**, 1547-1550 (2005).

Ignoul S., and Eggermont J. CBS domains: structure, function and pathology in human proteins. *Am J Physiol Cell Physiol.* **289**, 1369–1378 (2005).

Janosik, M., Kery, V., Gaustadnes, M., Maclean, K. N. & Kraus, J.P. Regulation of human cystathionine β-synthase by S-adenosyl-L-methionine: Evidence for two catalytically active conformations involving an autoinhibitory domain in the C-terminal region. *Biochemistry.* **40**, 10625–10633 (2001).

Janosik, M., Oliveriusova, J., Janosikova, B., Sokolova, J., Kraus, E., Kraus, J. P., and Kozich, V. Impaired heme binding and aggregation of mutant cystathionine β-synthase subunits in homocystinuria. *Am. J. Hum. Genet.* **68**, 1506−1513 (2001).

Janosik M, Sokolova J, Janosikova B *et al.,* Birth prevalence of homocystinuria in Central Europe: frequency and pathogenicity of mutation c.1105C>T (p.R369C) in the cystathionine beta-synthase gene. *Journal of Pediatrics* **154**(3): 431–437 (2009).

Jaworski A.F., and Aitken S.M. Exploration of the six tryptophan residues of *Escherichia Coli* cystathionine β-synthase as probes of enzyme conformational change. *Arch. Biochem. Biophys.* **538,** 138–144 (2013).

Jhee, K-H., McPhie, P., and Miles, E.W. Yeast cystathionine β-synthase is a pyridoxal phosphate enzyme but, unlike the human enzyme, is not a heme protein. *J. Biol. Chem.* **275**, 11541-11544 (2000a).

Jhee, K-H., McPhie, P., and Miles, E.W. Domain architecture of the heme-independent yeast cystathionine β-synthase provides insights into mechanisms of catalysis and regulation. *Biochemistry*. **39**, 10548-10556 (2000b).

Jhee, K-H., Niks, D., McPhie, P., Dunn, M. F. and Miles, E. W. The reaction of yeast cystathionine β-synthase is rate-limited by the conversion of aminoacrylate to cystathionine. *Biochemistry.* **40**, 10873-10880 (2001).

Kemp B.E. Bateman domains and adenosine derivatives form a binding contract. *J Clin Invest.* **113**, 182–184 (2004).

Kennan A., Aherne A., Palfi A., Humphries M., McKee A., Stitt A., Simpson D.A., Demtroder K., Orntoft T., Ayuso C., Kenna P.F., Farrar G.J., and Humphries P. Identification of an IMPDH1 mutation in autosomal dominant retinitis pigmentosa (RP10) revealed following comparative microarray analysis of transcripts derived from retinas of wild-type and Rho(-/-) mice. *Hum Mol Genet* **11**, 547–557 (2002).

Kery V., Bukovska G., and Kraus J. P. Transsulfuration Depends on Heme in Addition to Pyridoxal 5'-Phosphate. *J. Biol. Chem.* **269,** 25283–25288 (1994).

Kery, V., Poneleit, L. and Kraus, J. P. Trypsin cleavage of human cystathionine β-synthase into an evolutionarily conserved active core: Structural and functional consequences. *Arch. Biochem. Biophys.* **355**, 222-232 (1998).

Kluijtmans L.A., Boers G.H., Kraus J.P., van den Heuvel L.P., Cruysberg J.R., and Trijbels F.J. The molecular basis of cystathionine beta-synthase deficiency in Dutch patients with homocystinuria: effect of CBS genotype on biochemical and clinical phenotype and on response to treatment. *Am J Hum Genet*. **65**, 59–67 (1999).

Koutmos, M., Kabil, O., Smith, J. L., and Banerjee, R. Structural basis for substrate activation and regulation by cystathionine beta-synthase (CBS) domains in cystathionine β-synthase. *Proc. Natl. Acad. Sci. U. S. A.* **107**, 20958-20963 (2010).

Kozich V., Janosik M., Sokolova J., Oliveriusova J., Orendac M., Kraus J.P., and Elleder D. Analysis of CBS alleles in Czech and Slovak patients with homocystinuria: report on three novel mutations E176K, W409X and 1223 + 37 del99. *J. Inher. Met. Dis.* **20**, 363-366 (1997).

Kozich V., Sokolova J., Klatovska V., Krijt J., Janosik M., Jelinek K., and Kraus J.P. Cystathionine β-synthase Mutations: Effect of Mutation Topology on Folding and Activity. *Human Mutation.* **7**, 809–819 (2010).

Kraus J. P., Oliveriusova J., Sokolova J., Kraus E., Vlcek C., de Franchis R., Maclean K. N., Bao L., Bukovska G., Patterson D. *et al.,* The human cystathionine b-synthase (CBS) gene: complete sequence, alternative splicing, and polymorphisms. *Genomics.* **52**, 312-324 (1998).

Kraus, J. P., Janosík M., Kozich V., Mandell R., Shih V., Sperandeo M.P., Sebastio G., de Franchis R., Andria G., Kluijtmans L.A., Blom H., Boers G.H., Gordon R.B., Kamoun P., Tsai MY, Kruger WD, Koch HG, Ohura T and Gaustadnes M. Cystathionine β-synthase mutations in homocystinuria. *Hum. Mutat.* **13**, 362-375 (1999).

Kutzbach C., and Stokstad E.L.R. Mammalian methylene tetrahydrofolate reductase: partial purification, properties, and inhibition by *S*-adenosylmethionine. *Biochim. Biophys. Acta* **250**,459–77 (1971).

Lehrer S.S. Solute perturbation of protein fluorescence. The quenching of the tryptophyl fluorescence of model compounds and of lysozyme by iodide ion. *BioPhys. J.* **11**, 72a (1971).

Lodha, P. H., Hopwood, E. M. S., Manders, A. L. and Aitken, S. M. Residue N84 of Yeast Cystathionine β-Synthase is a Determinant of Reaction Specificity. *Biochimica et Biophysica Acta - Proteins and Proteomics.* **1804**, 1424-1431 (2010).

Lodha, P. H., Shadnia, H., Woodhouse, C. M., Wright, J. S. and Aitken, S. M. Investigation of residues Lys112, Glu136, His138, Gly247, Tyr248, and Asp249 in the active site of yeast cystathionine β-synthase. *Biochemistry and Cell Biology.* **87**, 531-540 (2009).

Lonn Eva. Homocysteine lowering with folic acids and B vitamins in vascular disease. *New Eng. Jour. Med.* **354**, 1567-1577 (2006).

Loo J.A. Electrospray ionization mass spectrometry: A technology for studying noncovalent macromolecular complexes. *Int. Jour. Mass Spec.* **200**, 175-186 (2000).

Lucas M., Ecinar J.A., Arribas E.A., and Martinez-Cruz L.A. Binding of S-methyl-5'-thioadenosine and S-adenosyl-L-methionine to protein MJ0100 triggers an open-to-closed conformational change in its CBS motif pair. *J.Mol.Biol.* **396**, 800-820 (2010).

Maclean K.N., Kraus E., and Kraus J.P. The dominant role of sp1 in regulating the CBS -1a and -1b promoters facilitates potential tissue-specific regulation by kruppel-like factors. *J. Biol. Chem.* **279**, 8558–8566 (2004).

Maclean, K. N., Gaustadnes, M., Oliveriusova, J., Janosik, M., Kraus, E., Kozich, V., Kery, V., Skovby, F., Ru diger, N., Ingerslev, J., Stabler, S. P., Allen, R. H., and Kraus, J. P. *Hum. Mutat.* **19**, 641–655 (2002).

MacLean, K. N., Janošík, M., Oliveriusová, J., Kery, V. and Kraus, J. P. Transsulfuration in *Saccharomyces cerevisiae* is not dependent on heme: Purification and characterization of recombinant yeast cystathionine β-synthase. *J. Inorg. Biochem.* **81**, 161-171 (2000).

Majitan T., Pey A.L., Fernandez R., Fernandez J.A., Martinez-Cruz L.A., and Kraus J.P. Domain organization, catalysis and regulation of eukaryotic cytathionine β-synthases. *PLOS*. **9**, e105290 (2014).

Maruthamuthu M., and Selvakumar G. Selective quenching of tryptophanyl fluorescence in bovine serum albumin by the iodide ion. *Chem. Sci*. **107**, 79–86 (1995).

Mayer F.V., Heath R., Underwood E., Sanders M.J., Carmena D., McCartney R.R. ADP Regulates SNF1, the *Saccharomyces cerevisiae* Homolog of AMP-Activated Protein Kinase. *Cell Metab.* **14**, 707–714 (2011).

McCorvie T.J., Kopec J. and Yue W.W. Inter-Domain communication of human cystathionine beta-synthase: Structural basis of s-adenosyl-L-methionine activation. *J. Biol. Chem.* **289**, 36018-36030 (2014).

McCully K.S. Vascular pathology of homocysteinemia: implications for the pathogenesis of arteriosclerosis. *Am. J. Pathol*. **56**, 111–28 (1969).

Meier, M., Janosik, M., Kery, V., Kraus, J. P., and Burkhard, P. Structure of human cystathionine beta-synthase: a unique pyridoxal 5'-phosphate-dependent heme protein. *EMBO J.* **20**, 3910-3916 (2001).

Meier, M., Oliveriusova, J., Kraus, J.P. and Burkhard, P. Structural insights into mutations of cystathionine β-synthase. *Biochim. Biophys. Acta.* **1647**, 206-213 (2003).

Miles W.M., and Kraus J.P. Cystathionine β-synthase: Structure, Function, Regulation, and Location of Homocystinuria causing Mutations. *Jour. Biol. Chem*. **279**, 29871–29874 (2004).

Mudd S.H., Levy H.L., Skovby F. *Disorders of transsulfuration. The metabolic and molecular bases of inherited disease.* New York: McGraw-Hill. p 1279–1327 (1995).

Mudd S.H., Finkelstein J.D., Refsum H., Ueland P.M., Malinow M.R., Lentz S.R. Homocysteine and its disulfide derivatives: a suggested consensus terminology. *Arterioscler. Thromb. Vasc. Biol*. **20**, 1704–1706 (2000).

Mudd S.H., Levy H.L., Skovby F. Disorders of transsulfuration. In: Scriver C.R., Beaudet A.L., Sly W.S., Valle D., Childs B., Kinzler K.W., Vogelstein B, editors. *The Metabolic & Molecular Bases of Inherited Disease.* pp. 2007–2056 (2001).

Naughten E.R., Yap S., and Mayne P.D. Newborn screening for homocystinuria: Irish and world experience. *Eur J Pediatr*. **157**(Suppl 2):S84–S87 (1998).

Ogier de Baulny H., Gerard M., Saudubray J.M., and Zittoun J. Remethylation defects: guidelines for clinical diagnosis and treatment. *Eur. J. Pediatr.* **157**, 2:S77–83 (1998).

Ojha S., Wu J., LoBrutto R., and Banerjee R. Effects of heme ligand mutations including a pathogenic variant, h65r, on the properties of human cystathionine beta synthase. *Biochemistry.* **41,** 4649–4654 (2002).

Oyenarte I., Majtan T., Ereno J., Corral-Rodriguez M.A., Kraus J.P., and Martinez-Cruz L.A. Purification and crystallization and preliminary crystallographic analysis of human cystathionine beta-synthase. *Acta Cryst.* **68**, 1318-1322 (2012).

Pace CN., and Scholtz JM. Measuring the conformational stability of a protein. In: Creighton, TE., editor. *Protein Structure: A Practical Approach.* Oxford University Press; New York: p. 299-321 (1997).

Pazicni, S., Cherney, M. M., Lukat-Rodgers, G. S., Oliveriusova, J., Rodgers, K. R., Kraus, J. P., and Burstyn, J. N. The heme of cystathionine beta-synthase likely undergoes a thermally induced redox-mediated ligand switch, *Biochemistry.* **44**, 16785-16795 (2005).

Pey A.L, Majitan T, SanchezRuiz M.J and Kraus J.P. Human cystathionine *β*-synthase (CBS) contains two classes of binding sites for S-adenosylmethionine (SAM): complex regulation of CBS activity and stability by SAM. *Biochem. J.* **449**, 109–121 (2013).

Pogribna M., Melnyk S., Pogribny I., Chango A., Yi P., and James S.J. Homocysteine Metabolism in Children with Down Syndrome: In Vitro Modulation. *Am. J. Hum. Genet.* **69**, 88–95 (2001).

Quazi, F., and Aitken, S. M. Characterization of the S289A,D mutants of yeast cystathionine β-synthase. *Biochimica et Biophysica Acta - Proteins and Proteomics.* **1794**, 892-897 (2009).

Refsum H., and Ueland P.M. Homocysteine and cardiovascular disease. *Annual Review of Medecine.* **49**, 31-62 (1998).

Refsum H., Fredriksen A., Meyer K., Ueland P.M., and Kase B.F. Birth prevalence of homocystinuria. *Pediatrics* **144**, 830–832 (2004).

Saposnik Gustavo. Homocysteine-lowering therapy and stroke risk, severity and disability: additional findings from the HOPE 2 trial. *Stroke.* **40**, 1365-1372 (2009).

Scott, J. W., Hawley S.A., and Hardie D.G. CBS domains form energy-sensing modules whose binding of adenosine ligands is disrupted by disease mutations. *J. Clin. Invest.* **113**, 274-284 (2004).

Selhub J. Homocysteine metabolism. *Ann. Rev. Nutr*. **19**, 217-246 (1999).

Sen S., Yu J., and Banerjee R. Mapping peptides correlated with transmission of intrasteric inhibition and allosteric activation in cystathionine β-synthase. *Biochemistry.* **44**, 14210-14216 (2005).

Shelver, D., Kerby, R. L., He, Y., and Roberts, G. P. CooA, a CO-sensing transcription factor from *Rhodospirillum rubrum*, is a CO-binding heme protein, *Proc. Natl. Acad. Sci. U.S.A.* **94**, 11216-11220 (1997).

Shibuya N., Tanaka M., Yoshida M., Ogasawara Y., Togawa T., Ishii K., and Kimura H. 3-Mercaptopyruvate sulfur transferase produces hydrogen sulfide and bound sulfane sulfur in the brain. *Antioxid. Redox. Signal.* **11**, 703–714 (2009).

Sim W.C. , Yin H-Q., ChoicH.S., Choi Y.J., Kwak H.C., Kim S.K., and Lee B.H. L-Serine supplementation attenuates alcoholic fatty Liver by enhancing homocysteine metabolism in mice and rats. *Jour. Nutr.* 145, 260–267 (2015).

Singh R.H., Kruger W.D., Wang L., Pasquali M., and Elsas L.J. Cystathionine beta-synthase deficiency: effects of betaine supplementation after methionine restriction in B6-nonresponsive homocystinuria, *Genet. Med*. **6,** 90–95 (2004).

Singh L.R., Gupta S., Honig N.H., Kraus J.P., Kruger W.D. Activation of mutant enzyme function in vivo by proteasome inhibitors and treatments that induce Hsp70. *PLoS Genet.* 6:e1000807 (2010).

Singh, S., Ballou D.P., and Banerjee R. Pre-Steady-State Kinetic Analysis of Enzyme-Monitored Turnover during Cystathionine β-Synthase-Catalyzed H2S Generation *Biochemistry* **50**, 419–425 (2011).

Singh, S., Padovani, D., Leslie, R. A., Chiku, T., and Banerjee, R. Relative contributions of cystathionine β-synthase and γ-cystathionase to H2S biogenesis via alternative trans-sulfuration reactions. *J. Biol. Chem.* **284**, 22457–22466 (2009).

Street T.O., Courtemanche N., and Barrick D. Protein folding and stability using denaturants. *Methods in Cell. Biology.* **84**, 295-325 (2008).

Su Y., Majtan T., Freeman K.M., Linck R., Ponter S., Kraus J.P., and Burstyn J.N. Comparative study of enzyme activity and heme reactivity in Drosophila melanogaster and Homo sapiens cystathionine β-synthases. *Biochemistry* **52**, 741−751 (2013).

Taoka, S., and Banerjee, R. Stopped-flow kinetic analysis of the reaction catalyzed by the full-length yeast cystathionine β-synthase. *J. Biol. Chem.* **277**, 22421–22425 (2002).

Taoka, S., Lepore, B.W., Kabil, O. Ojha, S., Ringe, D., and Banerjee, R. Human Cystathionine *β*-Synthase Is a Heme Sensor Protein. Evidence That the Redox Sensor Is Heme and Not the Vicinal Cysteines in the CXXC Motif Seen in the Crystal Structure of the Truncated Enzyme. *Biochemistry.* **41**, 10454-10461 (2002).

Tate S., and Elborn S. Progress towards gene therapy for cystic fibrosis. *Expert Opin Drug Deliv* **2**, 269–80 (2005).

Tauger S.A., Webb W., and Siuzdak G. Peptide and protein analysis with mass spectrometry. *Spectroscopy.* **16**, 15-28 (2002).

Thorson M.K., Majtan T., Kraus J.P. and Barrios A.M. Identification of Cystathionine b-Synthase Inhibitors Using a HydrogenSulfide Selective Probe. *Angew. Chem. Int. Ed.* **52**, 4641 –4644 (2013).

Ubbink JB, Becker PJ, Vermaak WJ. Results of B-vitamin supplementation study used in a prediction model to define a reference range for plasma homocysteine. *Clin. Chem.* **41**,1033–7 (1995).

Vozdek, R., Hnizda, A., Krijt, J., Kostrouchova, M. and Kozich, V. Novel structural arrangement of nematode cystathionine β-synthases: characterization of *Caenorhabditis elegans*CBS-1. *Biochem. J.* **443**, 535–547 (2012).

Walters J., Milam S.L. and Clarck A.C. Practical approaches to protein folding and assembly. *Methods Enzymol*. **455**, 1-39 (2009).

Wasslen K.V., Canez C.R., Lee H., Manthorpe J.M. and Smith J.C. Trimethylation Enhancement Using Diazomethane (TrEnDi) II: Rapid In-Solution Concomitant Quaternization of Glycerophospholipid Amino Groups and Methylation of Phosphate Groups via Reaction with Diazomethane Significantly Enhances Sensitivity in Mass Spectrometry Analyses via a Fixed, Permanent Positive Charge. *Anal. Chem.* **86**, 9523−9532 (2014).

Watanabe, H., Kragh-Hansen, U., Tanase, S., Nakajou, K., Mitarai, M., Iwao,Y., Maruyama, T., and Otagiri, M. Conformational stability and warfarin-binding properties of human serum albumin studied by recombinant mutants. *Biochem. J.* **357,** 269–274 (2001).

Weeks, C.L., Singh, S., Madzelan, P., Banerjee, R., and Spiro, T.G. Heme regulation of human cystathionine β-synthase activity: insights from fluorescence and raman spectroscopy. *J. Am. Chem. Soc.* **131**, 12809-12816 (2009).

Welch G.N., and Loscalzo J. Homocysteine and atherothrombosis. *N Engl J Med.* **338**,1042-50 (1998).

Wilcken D.E., and Wilcken B. The natural history of vascular disease in homocystinuria and the effects of treatment, *J. Inherit. Metab*. *Dis*. **20,** 295–300 (1997).

Yaghmai R., Kashani A.H., Geraghty M.T., Okoh J., Pomper M. Progressive cerebral edema associated with high methionine levels and betaine therapy in a patient with cystathionine *β*-synthase (CBS) deficiency. *Am. J. Med. Genet.***108**, 57–63 (2002).

Yap, S., Rushe, H., Howard, P. M., and Naughten, E. R. The intellectual abilities of early-treated individuals with pyridoxine-nonresponsive homocystinuria due to cystathionine beta-synthase deficiency. *J. Inherit. Metab. Dis.* **24**, 437-447 (2001).

Zhang C., Chi F.L., Xie T.H. and Zhou Y.H. Effect of B-vitamin supplementation on stroke: a meta analysis of randomized controlled trials. *Plos One.* **8**(11), e81577 (2013).

Zhao, W., Zhang, J., Lu, Y., and Wang, R. The vasorelaxant effect of H_2S as a novel endogenous gaseous K_{ATP} channel opener. *EMBO J.* **20,** 6008–6016 (2001).

APPENDICES

Appendix A: Site-directed variants of ytCBS (Chapter 3)

Table A1-1: Sequence of mutagenic primers used to introduce single point mutations in ytCBS.

Primers	Sequence (mutated codons in bold)
E111K	GAAAAAATGTCTAAC**AAA**AAAGTTTCTGCCT
E111V	GAAAAAATGTCTAAC**GTG**AAAGTTTCTGTCC
E244D	CTGACTACAAAGTT**GAT**GGTATTGGTATG
E244V	CTGACTACAAAGTT**GTG**GGTATTGGTATG
E244Q	CTGACTACAAAGTT**CAG**GGTATTGGTATG
T326A	AGGTCGTACCTA**GCG**AAATCGTCGATGAC
K327E	TCGTACCTAACC**GAA**TTCGTCGATGACGAA
K327N	TCGTACCTAACC**AAC**TTCGTCGATGACGAA
K327L	TCGTACCTAACC**CTG**TTCGTCGATGACGAA
T197A	GCTGGTGCTGGT**GCG**GGTGGGACTATTAGCG
T197S	GCTGGTGCTGGT**AGC**GGTGGGACTATTAGCG
G245A	GACTACAAAGTTGAG**GCG**ATTGGTTATGATTTTG
G245L	GACTACAAAGTTGAG**GTG**ATTGGTTATGATTTTG
G245R	GACTACAAAGTTGAG**CGT**ATTGGTTATGATTTTG
I246G	GACTACAAAGTTGAGGGTGGTG**GTT**ATGATTTTG
I246A	GACTACAAAGTTGAGGGTGGTG**GCG**ATGATTTTG
G247A	GTTGAGGGTATT**GCG**TATGATTTTGTTCC
G247S	GTTGAGGGTATT**AGC**TATGATTTTGTTCC
Y241F	CTGATATCACTGAC**TTC**AAAGTTGAGGGTATTG

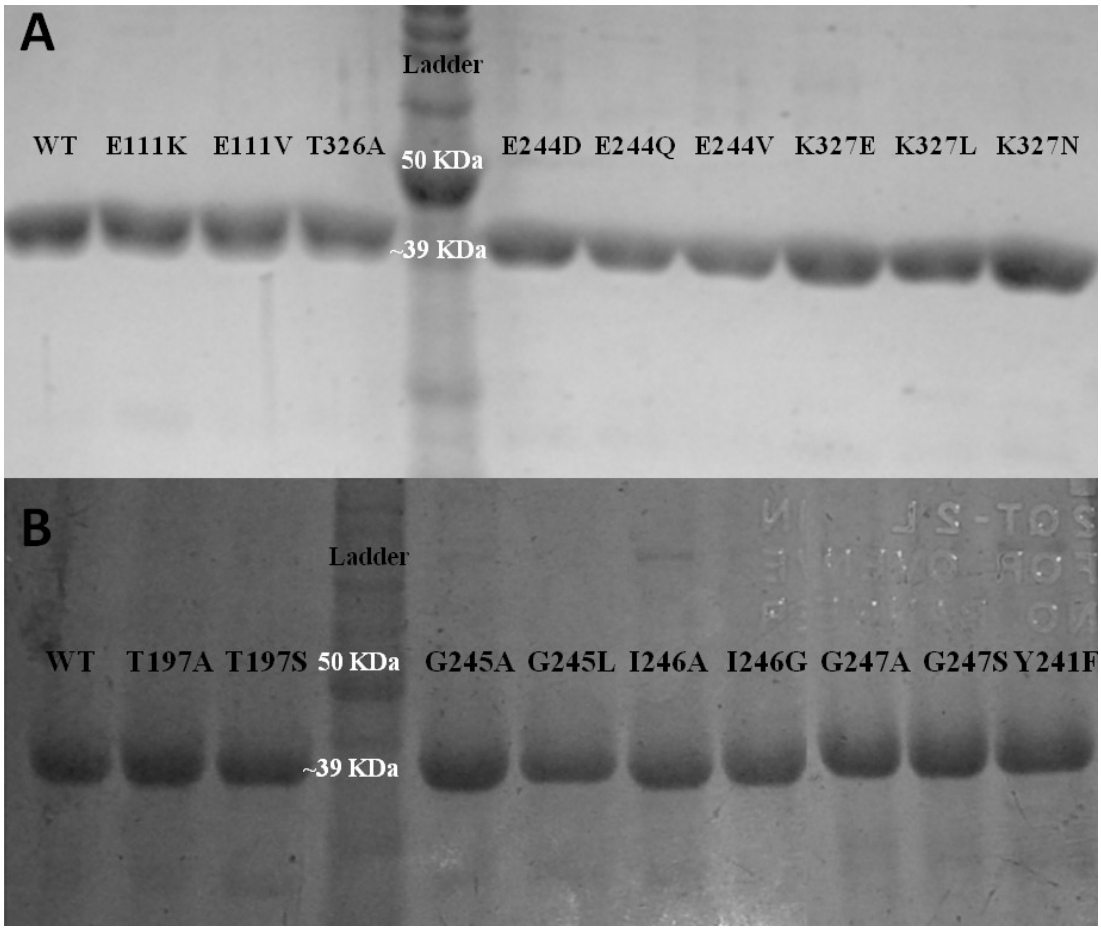

Figure A1-1: SDS-PAGE of 4 μg of each of the wild-type and site-directed variants of ytCBS demonstrating the purity of the recombinant enzymes. A) K112 hydrogen-bonding network and B) G247 site-directed variants.

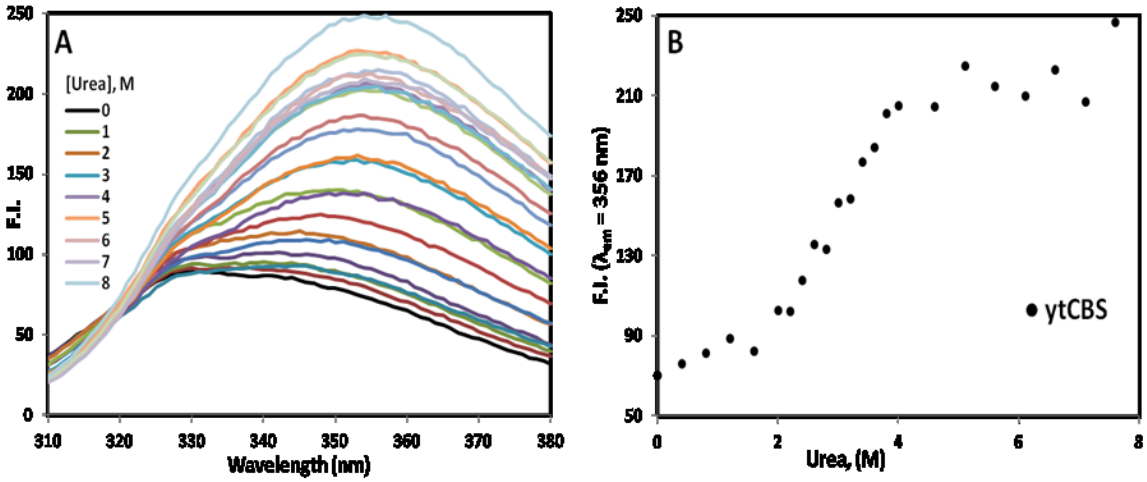

Figure A1-2: Urea denaturation of ytCBS. A) Fluorescence emission spectra of ytCBS, in the presence of 0 – 8 M urea, following excitation at 295 nm. B) Denaturation curve of ytCBS at emission wavelength of 356 nm at which unfolding was monitored, due to the largest difference in signal between the native and unfolded protein. Spectra were recorded between 300 and 380 nm (λ_{ex} = 295 nm and λ_{em} = 356 nm, excitation, emission slit = 5 nm).

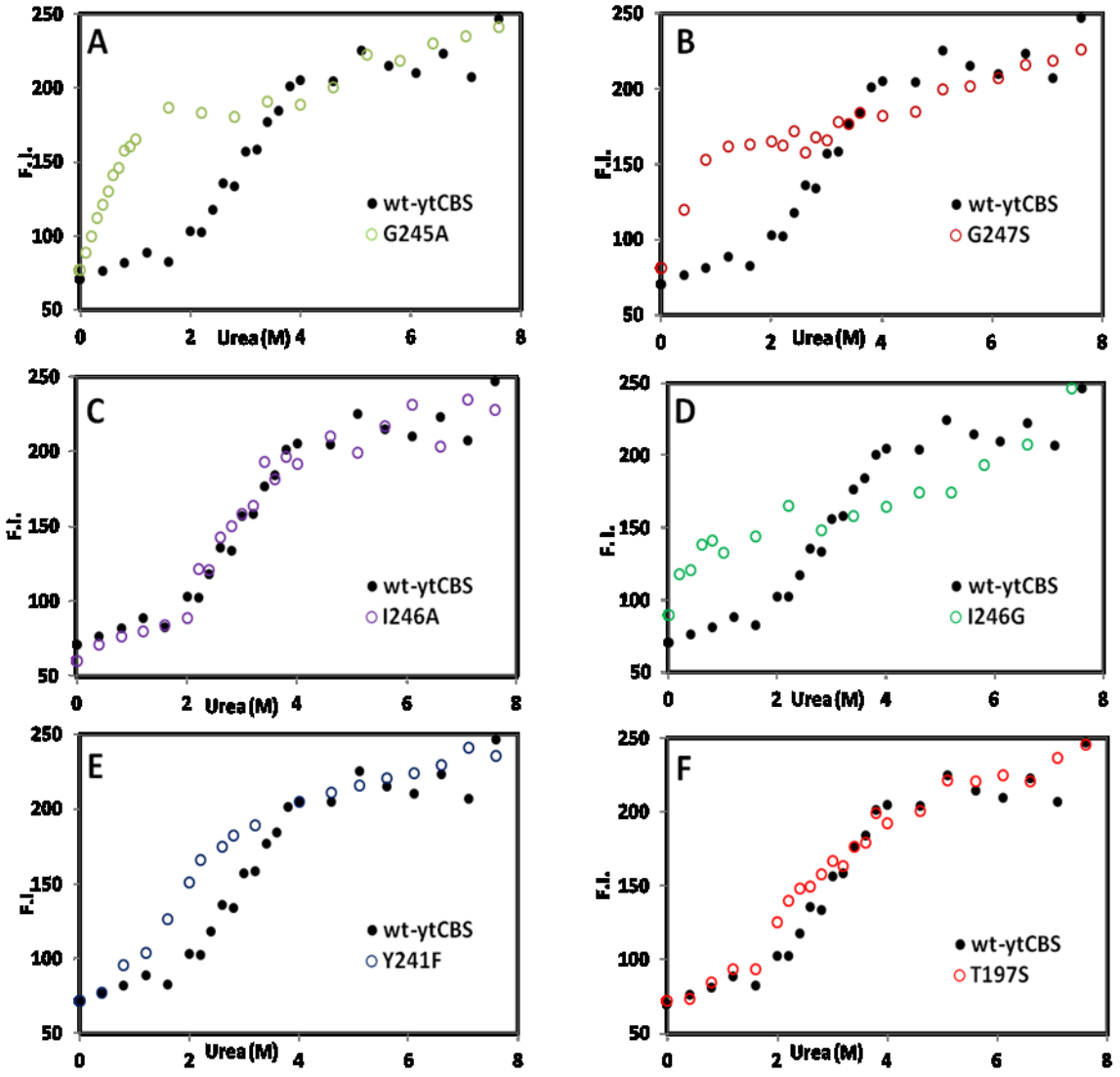

Figure A1-3: Fluorescence-monitored urea denaturation of wild-type and site-directed variants of truncated yCBS enzyme. Dependence of fluorescence emission on urea concentration for 1 μM monomer wt-ytCBS (●) and A) G245A, B) G247S, C) I246A, D) I246G, E) Y241F and F) T197S variants (○). Spectra were recorded between 300 and 380 nm (λ_{ex} = 295 nm and λ_{em} = 356 nm).

Appendix B: tryptophan residues of ytCBS and yfCBS (Chapter 4)

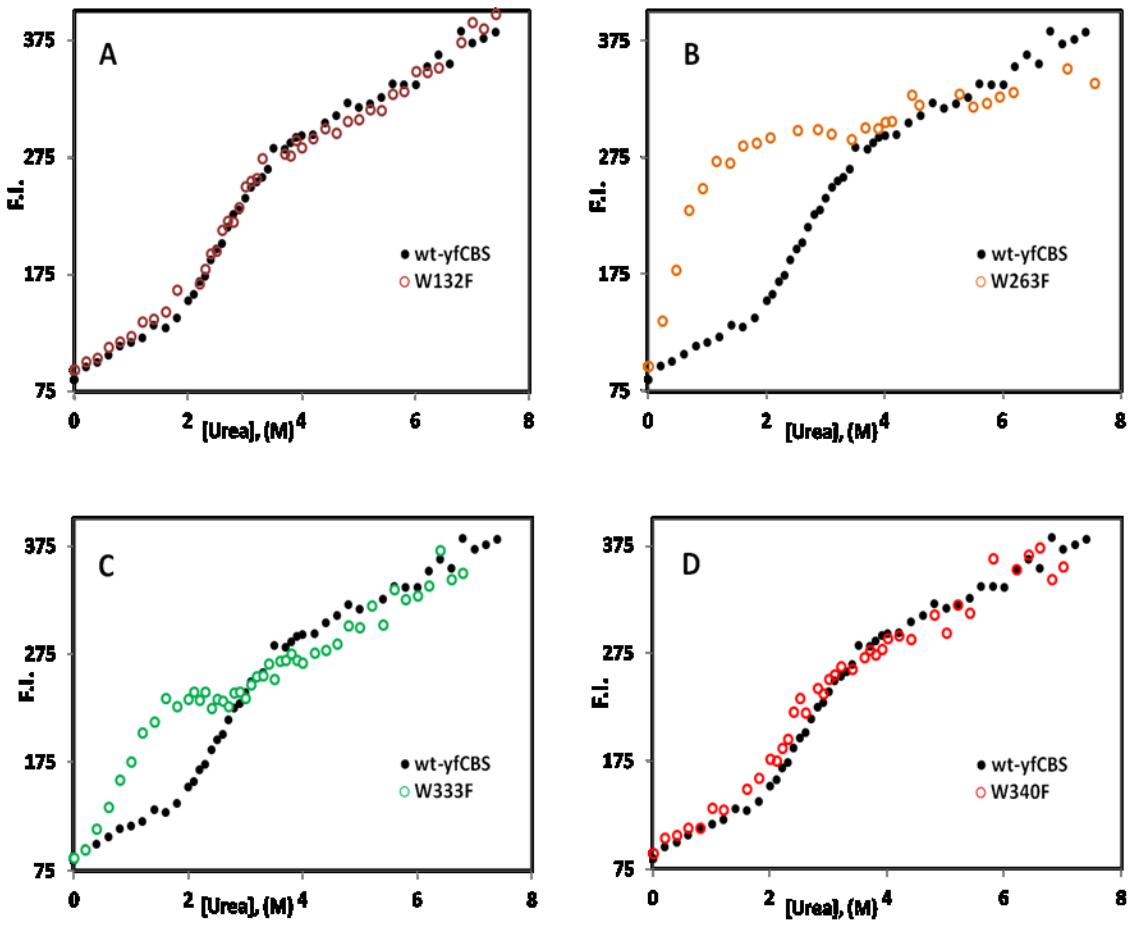

Figure B1-1: Fluorescence-monitored urea denaturation of wild-type and single W→F variants of full-length yfCBS enzyme. Dependence on denaturant concentration of the fluorescence emission of wild-type yfCBS and the single tryptophan substitution variants A) W132F, B) W263F, C) W333F and D) W340F. Solutions containing 1.0 µM of monomer yfCBS enzyme were incubated 16 hours at 25˚C in urea concentrations between 0 - 7.6 M. Samples were excited at 295 nm and the emission spectra were recorded between 320 - 380 nm (emission, excitation slit = 5 nm). The fluorescence intensity at 356 nm was plotted versus urea concentration.

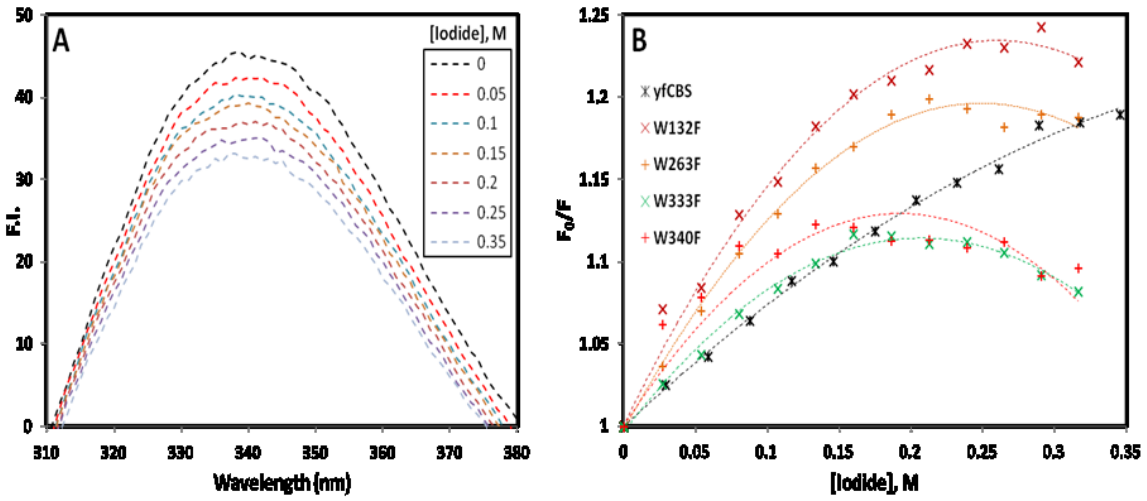

Figure B1-2: Quenching of yCBS *via* iodide. A) Fluorescence emission spectrum of 10 μM monomer wild-type yCBS, in the presence of 0 – 0.35 M iodide. B) Stern-Volmer plots of yfCBS and single W→F variants. Spectra were recorded between 300 and 380 nm (λ_{ex} = 295 nm).

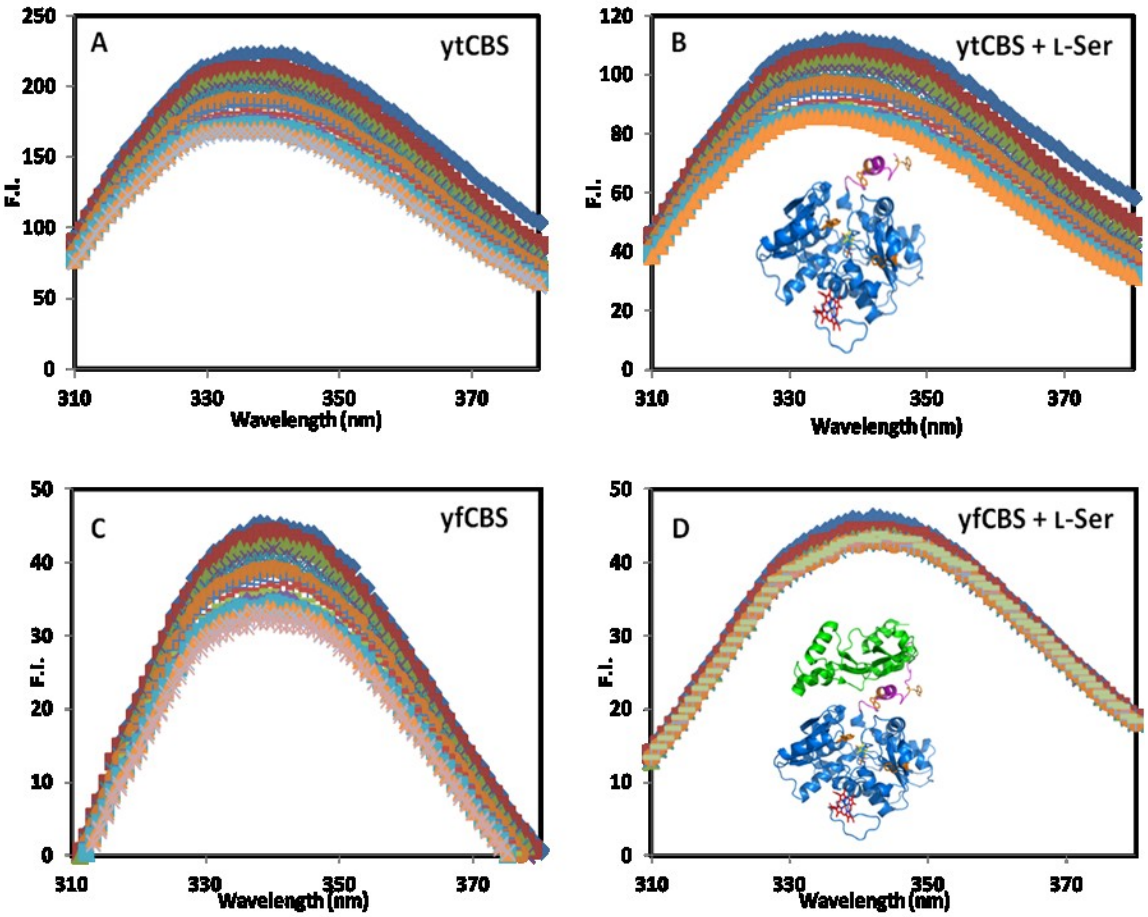

Figure B1-3: Quenching with iodide, in the open and closed conformation, of ytCBS and yfCBS. A) & B) Fluoresence emission spectrum of ytCBS in the absence and presence of 10 mM L-Ser substrate, respectively. Inset shows the truncated form of CBS monomer lacking the regulatory domain. C) & D) Fluoresence emission spectrum of yfCBS in the absence and presence of 10 mM L-Ser substrate, respectively. Inset shows the full-length monomer form of the CBS enzyme. Spectra were recorded for 10 μM monomer ytCBS or yfCBS between 300 and 380 nm (λ_{ex} = 295 nm), varying iodide concentration 0 – 0.35 M (excitation, emission slit = 5 nm).

Appendix C: SAM-binding in yCBS (Chapter 5)

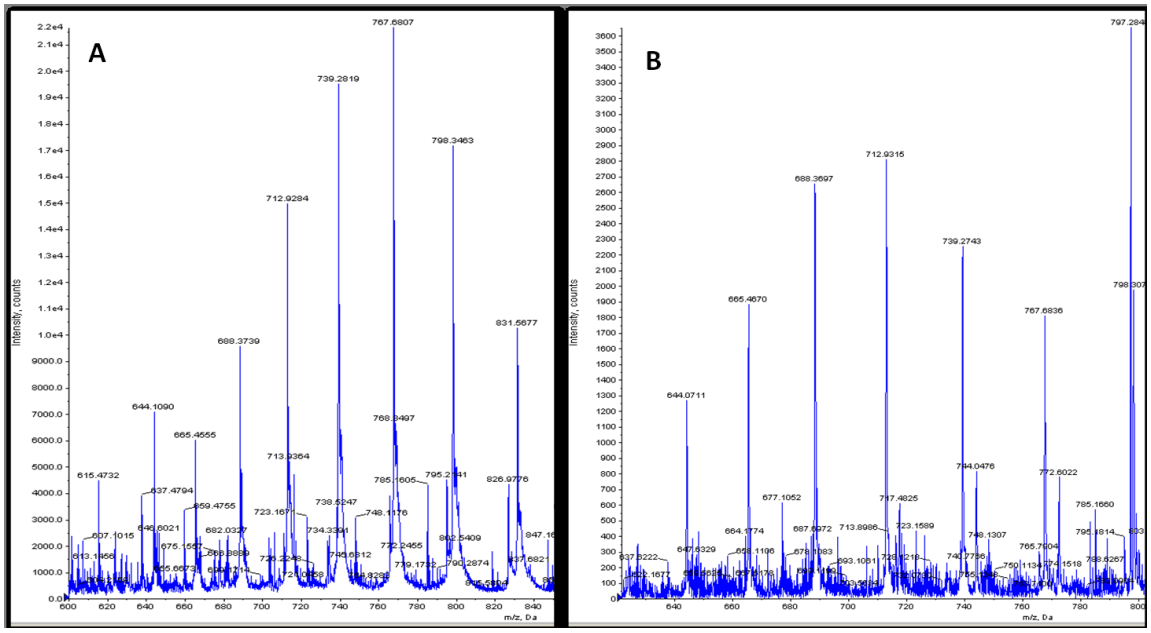

Figure C1-1: Deconvoluted mass spectra of yCBS regulatory domain. Multiple charge states were used to determine the experimental mass of A) As-isolated (MW = 19933 Da) and B) SAM-treated (MW = 19333 Da) yCBS regulatory domain.